

Further Studies on Radioactive Fallout

Project Leader:
Elmar R. Reiter

Progress Report No. 2
September 1965
Under Contract AT (11-1) – 1340
With
U. S. Atomic Energy Commission

Colorado State University
Department of Atmospheric Science
Technical Paper No. 70



**Department of
Atmospheric Science**

Paper No. 70

TABLE OF CONTENTS

	Pages
Heavy Iodine-131 Fallout Over the Midwestern United States, May 1962; by E. R. Reiter and J. D. Mahlman	1-53
A Case Study of Mass Transport from Stratosphere to Troposphere, Not Associated with Surface Fallout; by E. R. Reiter and J. D. Mahlman	54-83
Relation of Tropopause-Level Index Changes to Radioactive Fallout Fluctuations; by J. D. Mahlman	84-109
The Behavior of Jet Streams in Potential Fallout Situations; by E. R. Reiter	110-121
Development of Computer Programs for Computation of Montgomery Stream Functions and Plotting of Thermo- dynamic Diagrams; by J. D. Mahlman and W. Kamm	122-145

HEAVY IODINE - 131 FALLOUT OVER THE MIDWESTERN
UNITED STATES, MAY 1962

by

E. R. Reiter and J. D. Mahlman

ABSTRACT

Heavy I-131 fallout observed in milk from the Wichita milkshed on 13 May 1962 raised a controversy on whether the debris originated from a vented underground test in Nevada (Martell, 1964, 1965) or from the U. S. atmospheric test series over Christmas Island (List, Telegadas, and Ferber, 1964). Careful meteorological analysis excludes the 8 May 1962 Nevada Paca shot as a debris source for this Wichita fallout case. There is a possibility, however, that some fractionated radioactive material from this Paca shot may have drifted into the Colorado region, causing slight increases in radioactivity and significant debris age shifts on 11 May 1962.

I. THE CONTROVERSY:

Several statements have appeared recently in scientific journals and in published transcripts of congressional hearings, on the possible sources of I-131 fallout over the United States (Martell, 1962, 1964, 1965; Martell, Shedlovsky, and Watkins, 1965; Minx, 1962; Penn and Martell, 1963; List, Telegadas, and Ferber, 1964; Machta, 1962, 1963; Machta, List, and Telegadas, 1962; Reiter, 1963 a, b).

Martell and his co-investigators contend that in cases of high I-131 concentrations in radioactive fallout over the contiguous United States, vented nuclear shots at the Nevada test site constituted the major--or at least an important--debris source. Their argument is mainly based on radiochemical evidence. I-131 (half life 8 days) is expected to occur in high concentrations only in very young debris clouds. Because of the volatile nature of I-131, fractionation of radioactive material escaping from an underground test would tend to increase the relative concentration of this constituent of the debris. Although this reasoning favors recent Nevada tests as source of the observed radioactive fallout, it does not exclude the possibility of advection of debris from regions outside the United States by strong jet-stream winds aloft.

The other investigators oppose Martell's conclusion on the grounds of meteorological and conflicting radiochemical evidence. Preliminary analyses of trajectories at tropopause level or in the lower stratosphere indicate that nuclear tests outside the United States territory caused the observed fallout increases (Machta, 1962, 1963; List, Telegadas, and Ferber, 1964). As long as these conclusions are based on approximate trajectory analyses, there is still room for Martell's argument. Quasi-isentropic trajectories-- although they involve time consuming computations--offer a much higher degree of reliability (Danielsen, 1961). They may be applied

successfully if contaminated air masses move dry-adiabatically within a stable layer in which turbulent diffusion processes are of only small consequence. Under such conditions, large debris concentrations may travel over great distances under the influence of a jet stream. They may reach the turbulent mixing layer near the ground by dry-adiabatic descent from the stratosphere (Reed, 1955; Danielsen, 1959, 1964 a, b; Staley, 1960, 1962; Reiter, 1963 a, b; Mahlman, 1964, 1965 a), by washout processes (List, Telegadas, and Ferber, 1964), or by a combination of both (Reiter and Mahlman, 1964, 1965).

At the present there are two fallout cases on record over which considerable controversy has developed. One pertains to high radioactivity counts over the eastern United States during the second half of September 1961 (Machta, 1963; Machta, List, and Telegadas, 1962, 1964; Reiter, 1963 a, b, 1964; Penn and Martell, 1963, 1964 a, b, c; Martell, 1964, 1965; Martell, Shedlovsky, and Watkins, 1965; Lockhart, 1964). The other occurred in May 1962 over the central United States and showed especially in the high I-131 level in pasteurized milk from several milksheds supplying metropolitan regions. This report is concerned with a re-evaluation of the latter case.

The argument which developed from these observations of radioactive fallout could be considered purely academic if it were only a question of weighing radiochemical against meteorological evidence, or vice versa. Even a discussion of the health hazards associated with the consumption of contaminated milk could not have led to the existing controversy, because the ratification of the test ban treaty has revealed almost global unanimity on this subject. Unfortunately, more fundamental considerations have heated the discussion, and it is in the light of these issues that observational evidence will have to be weighed.

In both instances, September 1961 and May 1962, underground tests in Nevada have been blamed by Martell and his associates to be responsible to a large degree for the observed fallout increase. The Antler shot of 15 September 1961 produced a radioactive cloud observed by aircraft to be less than 9000 ft high (Allen, 1962). Some fallout, therefore, could be expected from this underground experiment because it was not claimed to have been "contained". The Paca shot of 7 May 1962 was contained, i. e. no radioactive gases were observed escaping the test site at detonation time (Hardy, Rivera, and Collins, 1964). However, post-shot drilling operations were conducted within 24 hours of shot time. Measurable amounts of radioactivity may have been produced near the test site, although no accounts of these have been made available at this time.

The uncertainties resulting from this withheld information have provided fuel for the following arguments presented by Martell (1965): If underground nuclear tests, originally reported as "contained", nevertheless introduced radioactive debris into the atmosphere, how efficient and effective are present containment measures? If containment cannot be achieved satisfactorily, what potential danger of test ban treaty violation is involved in underground testing? If underground tests, originally pronounced as "safe", were capable of producing unpredicted "hot spots" of fallout in dairy regions, how great a health hazard would a continuation of such "legal" testing constitute for part or all of the population of the United States? Even if fallout from such underground tests did not exceed human tolerance levels, what amount of dilution of nuclear debris would be required before the debris clouds crossed the U. S. borders in order not to be regarded as a treaty violation?

Instead of taking issue with these questions--justified as they may be--this study attempts to evaluate the available evidence on neutral grounds, and to weigh it with reference to the conflicting statements issued by Martell (1964, 1965) and by List, Telegadas, and Ferber (1964).

II. THE EVIDENCE:

(1) Radioactivity in Milk: Milk samples taken from several dairy regions in the Midwest revealed a striking increase in iodine-131 near the middle of May 1962. Data provided by the U. S. Public Health Service (1962) and the U. S. Public Health Service Pasteurized Milk Network (1962) show radiation levels rising from less than 60 picocuries/liter to over 600 near Wichita between 6 and 13 May 1962. Slightly smaller, but still very strong increases, are observed in samples from the St. Louis milkshed. These data are shown in Fig. 1 and Table 1; they also have been used by Martell (1964) in his reasoning. The heavy fallout of iodine-131 continued in the Wichita, Kansas, and in the Kansas City, Missouri, region until early June. Table 2 after List, Telegadas, and Ferber (1964) gives values in pc/liter observed in pasteurized milk from these two milksheds beyond the observation dates shown in Table 1.

(2) Radioactivity of Dry Air: Measurements of radioactivity in dry air and precipitation by the U. S. Department of Health, Education, and Welfare Radiation Surveillance Network gives only a small-almost negligible--increase of radioactivity in air on 9 May in the general area where the heavy iodine fallout was observed. Fig. 2 shows a sequence of analyses of radioactivity analyzed in 24 hour air and precipitation samples. Collection time of these samples was approximately 09 local time or 15 GMT in the midwestern United States.

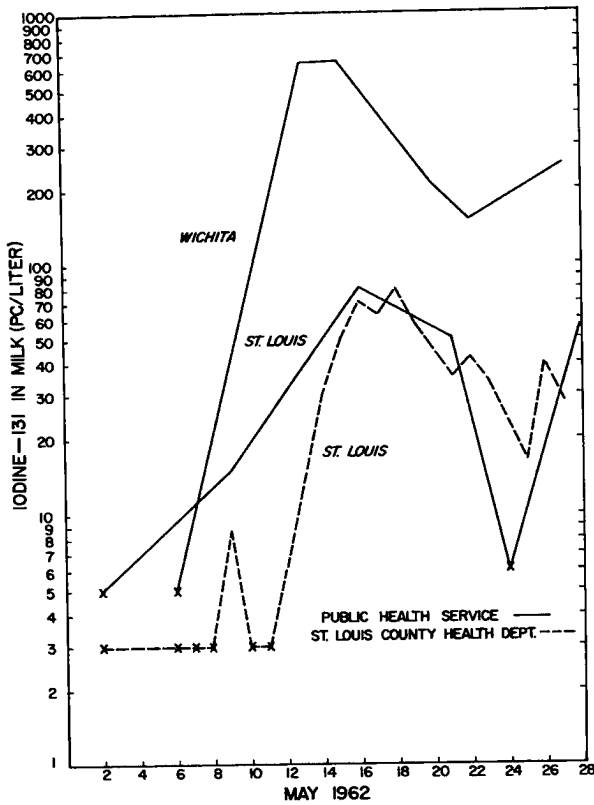


Fig. 1: Concentrations of Iodine-131 in pasteurized milk from Wichita, Kansas, and St. Louis, Missouri, milkshed areas during May 1962 (after Martell, 1964).

Table 1: Iodine-131 concentrations in pasteurized milk (pc/liter) for indicated stations (after U. S. Public Health Service, 1962 b).

Milk sampling station	Date May 1962	8	9	10	11	12	13	14	15	16	17	18	19	20	21	22	23	24	25	26	27	28
Little Rock, Ark.								30									<10	40				
Denver, Colo.				<10							45							<10				75
Des Moines, Iowa				<10							300							60				
Wichita, Kans.							670		660					215		165					250	
Louisville, Ky.		<10							20													
Minneapolis, Minn.					<10							290										
Kansas City, Mo.				45								605							150			
St. Louis, Mo.			15							80												75
Syracuse, N. Y.						<10												<10				
Cincinnati, Ohio				<10							50											
Chattanooga, Tenn.				<10					30								<10		20			
Charleston, W. Va.					<10													50				

Wichita		Kansas City	
Date	Amount	Date	Amount
6 May	< 10	4 May	< 10
13 May	670	11 May	40
15 May	660	18 May	600
20 May	215	25 May	150
23 May	160	29 May	590
27 May	250	1 June	780
29 May	340	5 June	450
3 June	160		

Table 2: Iodine-131 (pc/liter) in samples of pasteurized milk from Wichita, Kansas, and St. Louis, Missouri, milkshed areas (after List, Telegadas, and Ferber, 1964).

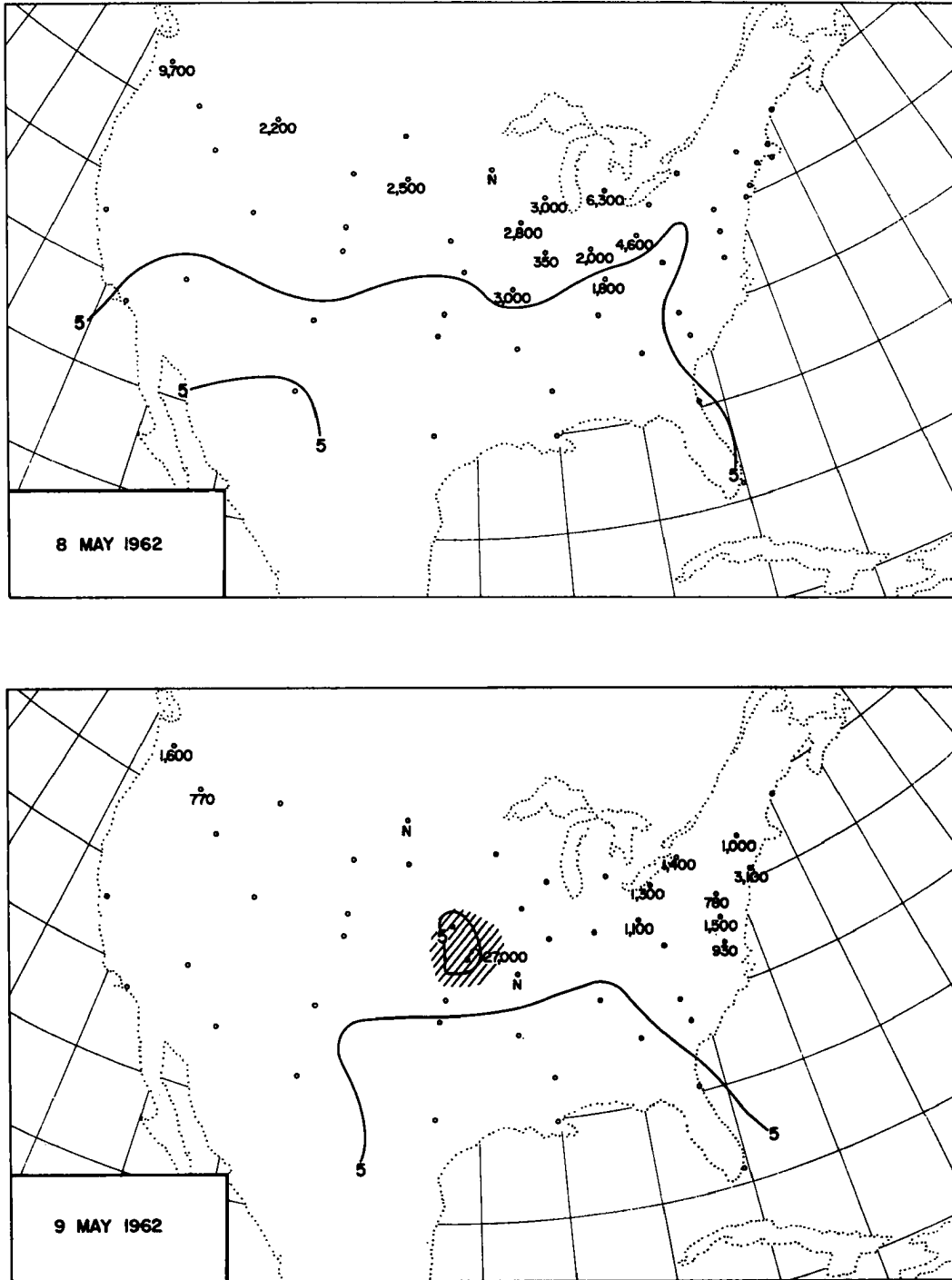


Fig. 2: Gross beta radioactivity in dry air (pc/m³) and numerical values of radioactivity in precipitation (pc/liter) from 8-13 May 1962. Areas of debris age < 100 days, diagonal hatching; areas of age < 30 days, vertical hatching.

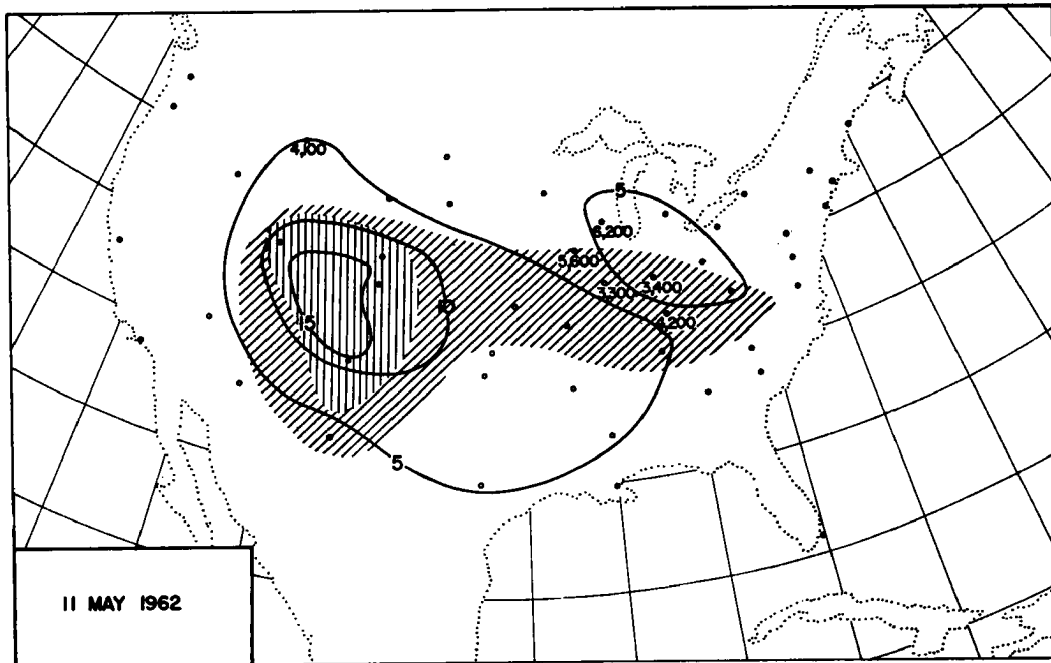
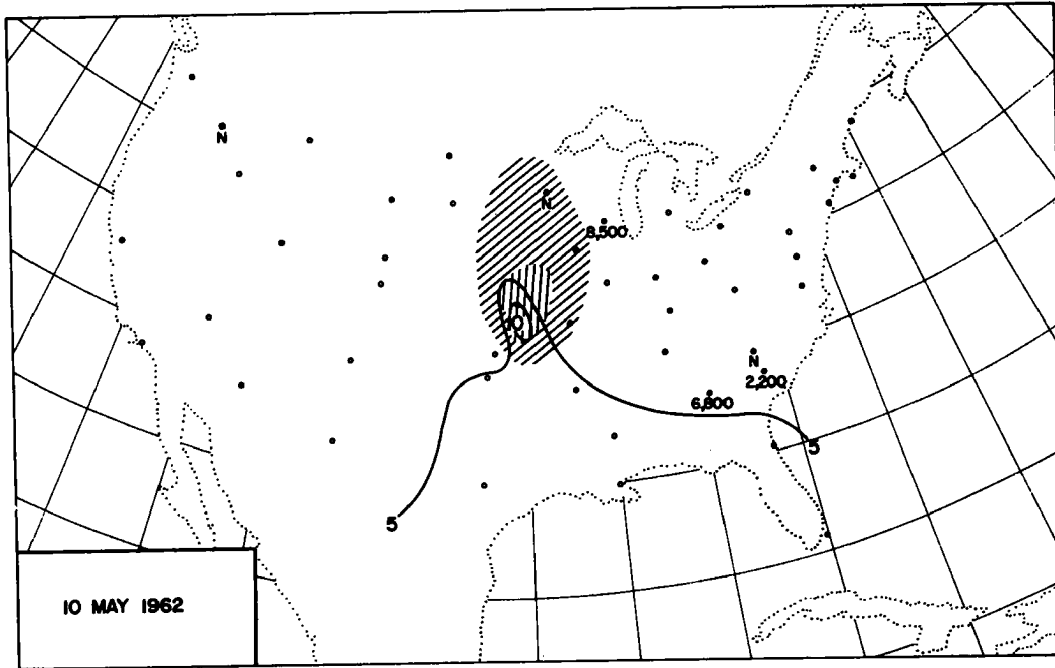


Fig. 2: Continued.

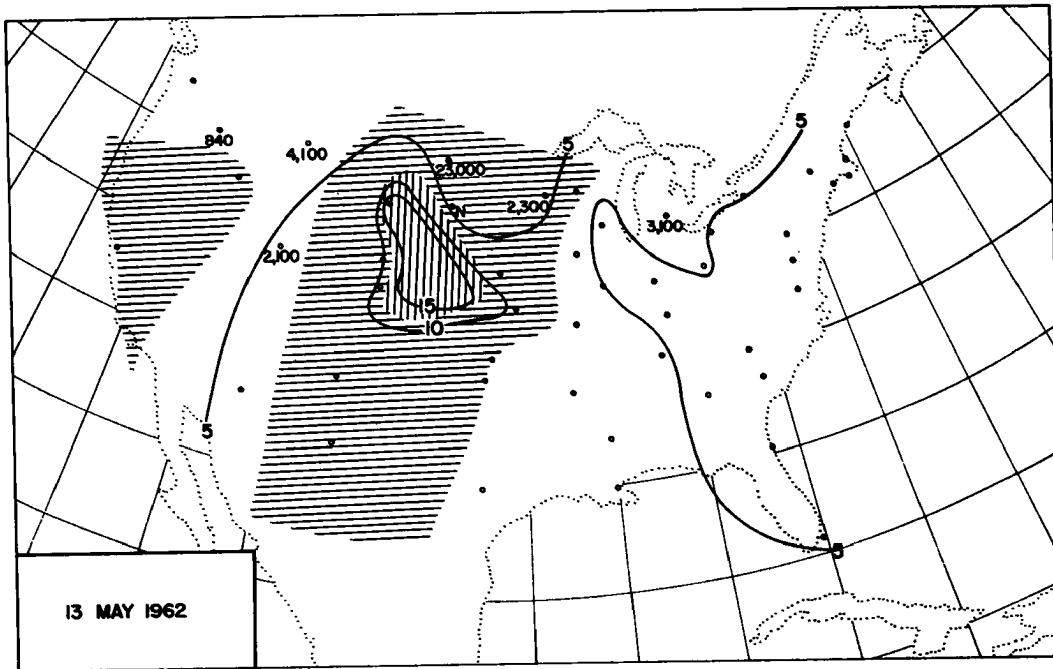
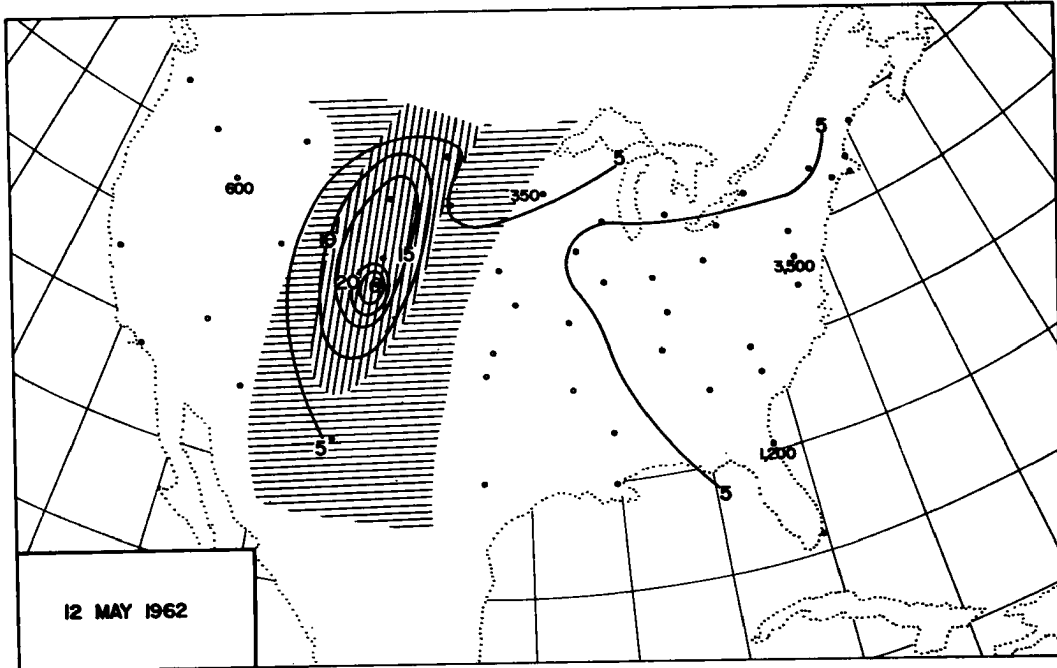


Fig. 2: Continued.

If there is anything striking at all about the data presented in these analyses, it is the high concentrations in precipitation, and the shift in debris age from >100 to only 34-40 days in the general area where the milk contamination was observed.

How may one explain the large discrepancies between contamination amounts in precipitation and milk samples as compared with those in dry air? There are two possible explanations:

(a) The two sets of measurements are obtained by different collection and analysis techniques, which may be totally incompatible. Although Martell (1965) bears some justified grievance against the milk sampling techniques (excessive weighing of samples with no detectable radioactivity against those with contamination above threshold value, in arriving at monthly mean values), these data should not be held at fault in the present case. The inadequate techniques criticized by Martell would tend to decrease, rather than to exaggerate radiation levels. Furthermore, the reliability of the dry air data of the Radiation Surveillance Network must be determined. They have produced reliable data in the past (e. g. Reiter, 1963 a, b; Mahlman, 1964, 1965 a; Reiter and Mahlman, 1964, 1965 a, b) upon which Penn and Martell (1963) and also Machta, List, and Telegadas, (1962) hinged some pertinent conclusions. Although contamination magnitudes from both measurements should not be expected to be identical (for one reason, because dry-air filter techniques measure other contaminants besides I-131), differences should not amount to as much as the observed discrepancies. Indeed, if we were to doubt the quality of these measurements, we may as well not attempt to resolve the argument at this point, because no one could tell that any radioactivity to be concerned about had been adequately measured at all.

(b) A more plausible explanation is that the two seemingly discrepant sets of data carry different statistical meaning and require different physical interpretation. Martell (1964), as well as List, Telegadas, and Ferber (1964), maintain that it takes the I-131 fallout in the order of two to four days from the time it reaches the ground to complete the transfer from vegetation to dairy milk. As may be seen from Fig. 2, even on 9 May no sizeable fallout intensities have been measured by the dry-air filter measurements.

The analyzed milk samples are assumed to be representative for conditions integrated over the whole milkshed (the approximate boundaries of the Wichita milkshed are shown in Fig. 3). Following the argument of List, Telegadas, and Ferber, individual dairy farms may very well have shown much higher concentrations of I-131 than those given in Tables 1 and 2.

The dry air filter samples are collected from a very wide-meshed network. They represent a 24 hour time integration for each individual observation station. The volume of air processed during one day amounts roughly to $L^3 \cdot \Delta t = 2300 \text{ m}^3$, if L^3 is the sampling volume per second, and $\Delta t = 86,400 \text{ sec}$. With a mean surface wind speed of 7 mps at Topeka, Kansas, where the air sample was taken, a scale-length $\bar{V} \cdot \Delta t = 600 \text{ km}$ was covered by the measurements during the 24 hour period.

Although the filter size F used in the air sampler was not available from literature, it appears that even with a small filter the flow rate $\frac{L^3}{F}$ through the filter must have been considerably less than the mean wind speed, since $L^3 = 0.027 \frac{\text{m}^3}{\text{sec}}$. Thus, the filter device samples within 24 hours an air space of the approximate magnitude $V \cdot F \cdot \Delta t = 6 \times 10^5 \times F \text{ m}^3$, whereby not the whole amount of air contained in this space has actually passed through the filter, because $V > \frac{L^3}{F}$. Nevertheless, a continuous sample is extracted from

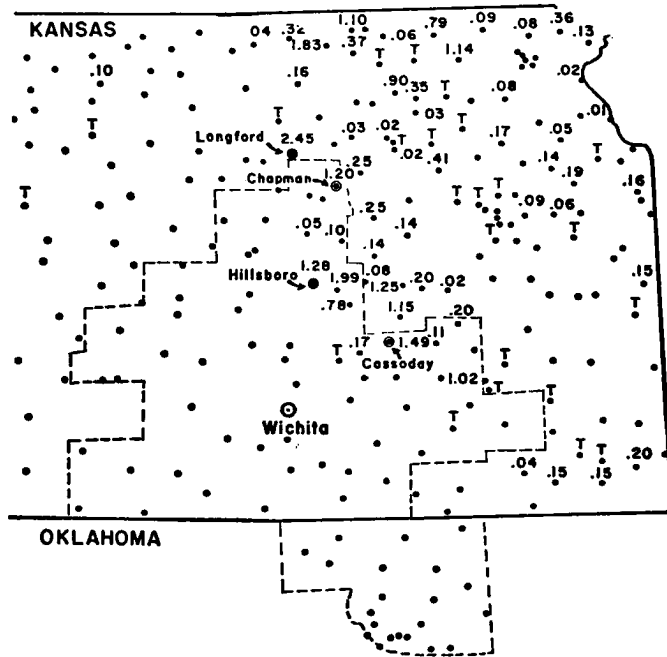


Fig. 3: Precipitation (inches) during 24-hour period ending 9 May 1962, 7 a. m. C. S. T. The Wichita milkshed is outlined by a dashed line. Dots indicate locations of reporting stations; where no numerical value is given, no rain occurred. T denotes trace of precipitation (after List, Telegadas, and Ferber, 1964).

this volume; therefore, we have to consider it as the representative sampling space. Assuming $F \sim 0.1 \text{ m}^2$ (which, in all probability is an over estimate), we arrive at a sampling space $V \cdot F \cdot \Delta t$ of ca. $6 \times 10^4 \text{ m}^3$, or at a sampling area $V \cdot \sqrt{F} \cdot \Delta t$ of $2 \times 10^5 \text{ m}^2$ or 0.2 km^2 .

The characteristic distance between filter-sampling stations over the contiguous United States is approximately 500 km. The area for which measurements from one station are tacitly assumed to be representative, therefore, is of the order of $250,000 \text{ km}^2$. It appears that only a fraction of less than $1:10^6$ of the total area has effectively been sampled by measurements over one station. Thus, these measurements truly constitute only spot samples.

The Wichita milkshed is roughly $6 \times 10^4 \text{ km}^2$ in area. Foraging livestock naturally will not sample this area continuously but selectively. Assuming that the transport mechanisms had a characteristic scale length considerably larger than the average distance between dairy farms and their pastures in this region (order of magnitude, say, 10 km), the milk samples analyzed for radioactivity will not have been affected seriously by the "filtering-effect" of the sampling technique (Pasquill, 1962). They will constitute a highly representative sample of radioactive fallout averaged over an area of roughly $6 \times 10^4 \text{ km}^2$, or a scale length of approximately 250 km.

Even if the fallout phenomenon were of the same scale length as the sampling distance (i. e., the average distance between dairy pastures), the random nature of both the fallout phenomenon and sampling technique would lead us to expect that a representative amount of I-131 will have been caught in the milk sample. Characteristic magnitudes of fallout would, however, be difficult to estimate in this case, even more so after the output from the whole milkshed had been mixed.

Thus, we have the following statistical problem to consider in comparing the two sets of measurements:

Milkshed: Scale length of sample ~ 10 km

Scale length of averaging ~ 250 km

Dry-air filters: Scale length between stations (or spot sample) ~ 500 km

Since the heavy I-131 fallout was essentially, although not completely (see Fig. 2) missed by the dry-filter sampling stations, and yet showed quite predominantly over several milksheds, we may draw the following statistical conclusions:

The characteristic length scale of the fallout phenomenon producing the observed increase in I-131 concentrations must have been considerably less than 500 km, yet of the order of, or larger than 10 km, if both methods of measurement had been equally sensitive to the physical fallout mechanism.

This condition, however, was quite definitely not realized in the present case because the filter data are representative of dry air radioactivity, whereas milk contamination may be caused by dry and/or washout deposits. The Wichita and Kansas City milksheds experienced considerable precipitation during the time period when I-131 could have been consumed by foraging livestock. Fig. 3 shows the precipitation map for 8-9 May (List, Telegadas, and Ferber, 1964).

In view of this fact we have to consider that the observed I-131 deposition results from washout by precipitation. It must be noted that none of the Radiation Surveillance Network Stations in the area experienced precipitation during the period 8-9 May except for Topeka, Kansas, which reported 0.25 cm (with fallout intensity 27,000 pc per liter) (Fig. 2).

This adds new significance to the statistical considerations made above. Had one estimated mean area precipitation from measurements taken only at the Radiation Surveillance Network stations, one would have arrived at the conclusion that the weather regime over the whole area in question was relatively dry. The map shown in

Fig. 3 reveals, however, that considerable precipitation fell in the Wichita-Kansas City region on 8 and 9 May. Even though part of the Wichita milkshed remained dry, heavy rain and hail along its northeastern border still produced appreciable mean area precipitation. This is in line with the well-known fact that as long as the grid distance between precipitation stations is considerably larger than the average diameter of the rain-producing convective cloud systems, an increase in observation density will simulate an "increase" in computed mean area rainfall.

Considering the precipitation amounts shown in Fig. 3, it is quite obvious that well-developed convective cloud systems accounted for most of the precipitation over the Wichita milkshed. Average horizontal dimensions of approximately 20 km measured along a direction from SW to NE appear reasonable for individual convective systems, judging from the distance between stations reporting excessively large precipitation amounts, and adjacent stations with rather small amounts. Axes of high precipitation amounts seem to be oriented from NW to SE, parallel to the winds near tropopause level. The longest of these axes stretches about 150 km along the line Hillsboro-Cassoday. Both scale lengths, 20 km and 150 km, lie well within the range established by statistical reasoning.

We, therefore, may conclude that I-131 fallout patterns and precipitation patterns over and near the Wichita milkshed show very similar--possibly the same--scale characteristics.

(3) Air Samples in the Stratosphere: The Defense Atomic Support Agency, Project Star Dust, conducted a number of sampling flights during the month of May over the western United States along a flight corridor from approximately $31^{\circ}08'N$, $101^{\circ}24'W$ to $48^{\circ}34'N$, $112^{\circ}21'W$. Fig. 4 shows a cross-section along the sampling

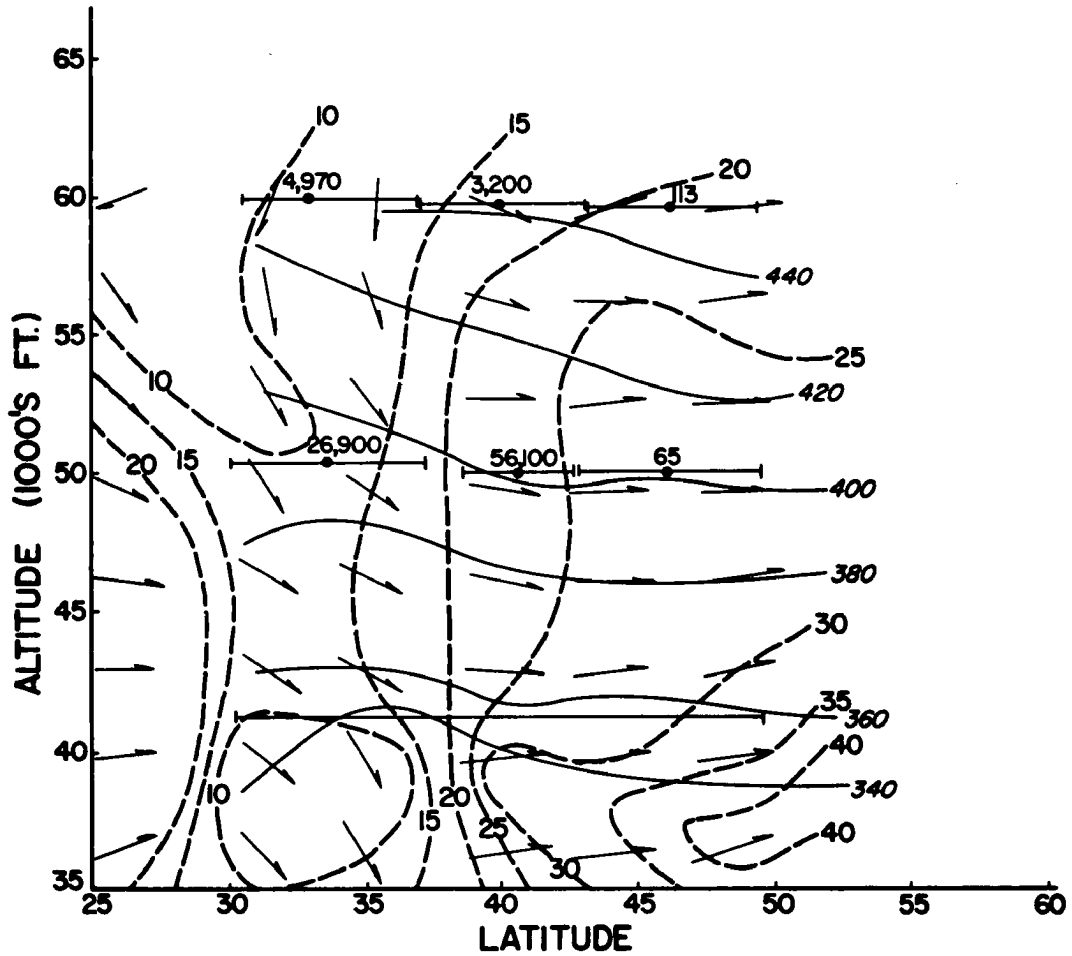


Fig. 4: Cross-section through the atmosphere along Project Star Dust flight track, 8 May 1962. Potential temperatures ($^{\circ}$ K, solid lines) and isotachs (mps, dashed lines) analyzed from 8 May 12 GMT data of Brownsville, San Antonio, Amarillo (Texas), Denver (Colorado), Lander (Wyoming), and Great Falls (Montana). Radioactivity data are given in disintegrations per minute per standard cubic foot, as measured by Project Star Dust Flight, 8 May, approximately 15 to 18 GMT. Values are averaged over flight legs indicated by horizontal lines.

track, indicating radioactive intensities for the flight on 8 May 1962. Data from radio-chemical analyses are also included in this diagram. Radiation counts were quite high (exceeding 10,000 disintegrations per minute per standard cubic foot of air) on 8 May at 50,000 ft between 31° and 43° N, on 10 May at approximately the same level at 30° N, and on 18 May at 55,200 ft between 31° and 35° N. On 8 May the air sample taken between 38° and 43° N at 50,000 ft showed I-131 concentrations of 5,300 disintegrations / min ft³, the largest iodine concentration of all research flights in May. Fig. 5 shows successive data arranged in the form of time sections. From this diagram it becomes obvious that atmospheric layers were not contaminated uniformly. Periods of higher and lower radioactivity concentrations may be observed, indicating the drift of debris clouds across the sampling path.

Main attention shall be given to the high concentrations of I-131 observed on 8 May near the 50,000 ft level, which is close to the 400 K isentropic surface. Hardly any debris is observed at 41,000 ft (potential temperature ca. 340 K) in the same latitudinal belt. The layered structure of radioactive debris clouds in the stratosphere clearly suggests that horizontal advection over relatively large distances was the main transport mechanism which imported this debris over the United States.

(4) Schedule of Nuclear Explosions: List, Telegadas, and Ferber (1964) and Martell (1964, 1965) disagree in naming the possible source of debris that caused the heavy fallout over the Wichita and Kansas City milksheds. The former group of authors holds the atmospheric tests over Christmas Island, conducted by the United States, to be responsible for the fallout, whereas Martell contends that fractionated material from the Nevada test site played an important role. The schedule of nuclear testing given in Table 4 does not preclude either of the two sources.

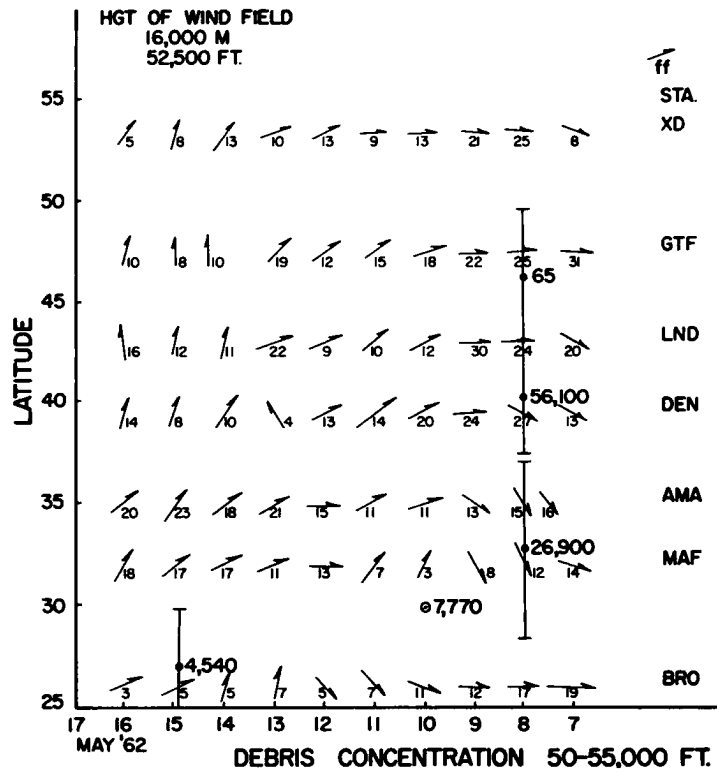
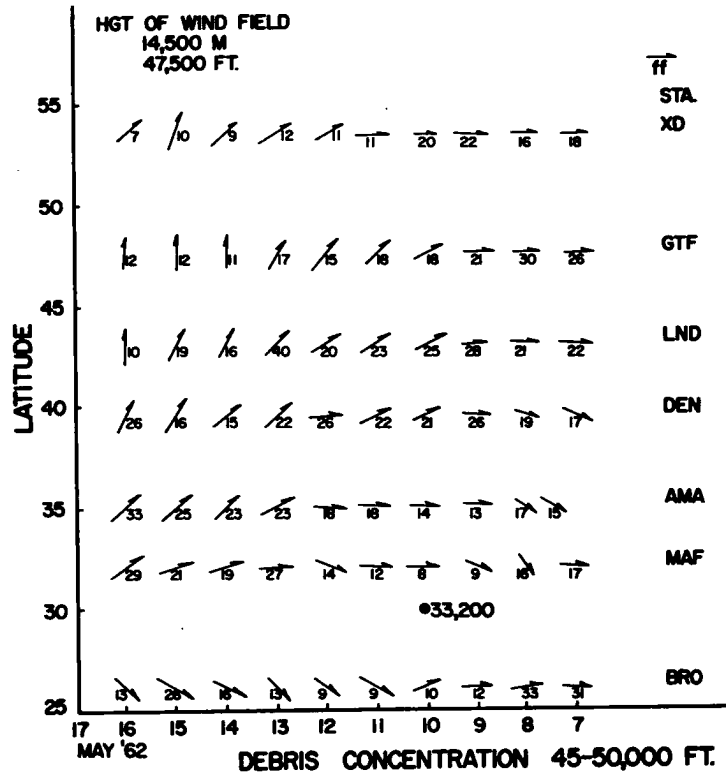


Fig. 5: Time section along Project Star Dust flight track for the period 7 to 17 May 1962 of winds (speeds given numerically in mps) and radioactive debris concentrations (disintegrations per minute per standard cubic foot) at levels and within layers as indicated. Winds have been obtained from radiosonde stations XD = Edmonton, Alberta; GTF = Great Falls, Montana; LND = Lander, Wyoming; DEN = Denver, Colorado; AMA = Amarillo, Texas; MAF = Midland, Texas; BRO = Brownsville, Texas.

Table 3:

U. S. NUCLEAR DETONATIONS

<u>No.</u>	<u>Date</u>	<u>Time (GMT)</u>	<u>Name</u>	<u>Type of Burst</u>	<u>Yield</u>	<u>Location</u>
1962: OPERATION DOMINIC						
1	25 Apr	1545	Adobe	Air	Intermediate	Christmas Is. Area
2	27 Apr	1602	Aztec	Air	Intermediate	Christmas Is. Area
3	2 May	1802	Arkansas	Air	Low Megaton	Christmas Is. Area
4	4 May	1904	Questa	Air	Intermediate	Christmas Is. Area
5	6 May	2330	Frigate Bird	Missile		Christmas Is. Area
6	8 May	1801	Yukon	Air	Intermediate	Christmas Is. Area
7	9 May	1701	Mesilla	Air	Intermediate	Christmas Is. Area
8	11 May	1537	Muskegon	Air	Intermediate	Christmas Is. Area
9	11 May	2000	Swordfish	Underwater	Low	Eastern Pacific Ocean
10	12 May	1703	Encino	Air	Intermediate	Christmas Is. Area
11	14 May	1522	Swanee	Air	Intermediate	Christmas Is. Area
12	19 May	1537	Chetco	Air	Intermediate	Christmas Is. Area
13	25 May	1609	Tanana	Air	Low	Christmas Is. Area
14	27 May	1703	Nambe	Air	Intermediate	Christmas Is. Area
<u>No.</u>	<u>Date</u>	<u>Time (GMT)</u>	<u>Name</u>	<u>Type of Burst (ft.)</u>	<u>Yield</u>	<u>Remarks*</u>
1962: CONTINENTAL TEST						
17	5 Apr		Dormouse Prime	Underground	9.7 KT	1, 8
18	6 Apr		Passaic	Underground	Low	1, 8
19	12 Apr		Hudson	Underground	Low	1, 8
20	14 Apr		Platte	Underground	1.7 KT	4, 6, 7
21	21 Apr		Dead	Underground	Low	1, 8
22	27 Apr		Black	Underground	Low	1, 8
23	7 May	1933	Paca	Underground	Low	1, 8
24	12 May	1900	Aardvark	Underground	37 KT	2, 8
25	19 May		Eel	Underground	Low	4, 5, 7
26	25 May		White	Underground	Low	1, 8

* Categories of Release of Radioactivity

1. No radiation levels detected above background on or off the Nevada Test Site from radioactivity released by this detonation.
2. Radiation levels detected near surface zero above normal background from radioactivity released by this detonation. No other radiation levels detected on or off the Nevada Test Site from radioactivity released by this detonation.
3. Radiation detected on-site from radioactivity released by this detonation. No radiation levels above background detected off the Nevada Test Site in populated areas from radioactivity released by this detonation. ("On-site" as used above includes the Las Vegas Bombing and Gunnery Range.)
4. Some radioactivity detected in off-site areas. For details see subsequent tabulations.
5. Event released small visible quantities of radioactive steam and/or gases.
6. A persistent cloud was produced containing appreciable quantities of radioactivity associated with particulates.
7. No radiation detected at the work site or any other location from releases of gaseous radioactivity during post-shot drilling or tunnel re-entry operations.
8. Some radiation detected in the area surrounding surface zero from gaseous radioactivity released during post-shot drilling or tunnel re-entry operating. No radioactivity detected off the Nevada Test Site from post-shot operations.
9. Although a cloud was formed, the U. S. Public Health Service off-site monitoring network did not identify any radioactivity in the off-site area, as defined in category 3, which could be attributed to this event.

(5) Precipitation Regime: It has been mentioned earlier that statistical evidence indicates that I-131 was transported to the ground by precipitation over the Wichita and Kansas City milksheds. Fig. 3 shows hourly precipitation data for this region. Severe thunderstorm activity was reported over the milkshed area, and heavy hail was observed in eight counties between Longford (slightly north of the Wichita milkshed) and Cassoday (List, Telegadas, and Ferber, 1964). The Wichita WSR-57 radar reports that a number of cloud tops exceeded the 50,000 ft level between 7 p. m. CST on 8 May, and 2 a. m. CST on 9 May (01-08, GMT) (Fig. 6). Most of these cloud-top observations are well within range of accuracy of the radar (List, Telegadas, and Ferber, 1964). In fact, the possibility of error is minimized in this case because the U. S. Weather Bureau WSR-57 radar echo tops are routinely corrected for beamwidth error as well as for height of antenna above sea level and curvature of the earth. It is not quite clear, therefore, why Martell (1965) questions the possibility that thunderstorm clouds may penetrate to such heights. Considerably deeper penetrations into the stratosphere have been observed on occasion (L. O. Grant, oral communication).

As may be seen from Fig. 7, a large amount of energy of convective instability was available in the region of thunderstorm occurrence. The Hourly Surface Observations [U. S. Weather Bureau, Local Climatological Data (Supplement)] indicate cloud bases of 6000 to 9000 ft at Wichita Municipal Airport between 8 May 21 GMT and 9 May 02 GMT. Assuming that similar cloud-base heights were observed in the precipitation region northeast of Wichita, and that moist-adiabatic stratification characterized the atmosphere within the convective clouds above cloud base, overshooting of the cloud tops to 50,000 ft and higher appears quite feasible from Fig. 7. Even if one took into account entrainment of, and mixing with, dryer air of the environment outside the cumulus towers, a large amount of free buoyant energy would still be present.

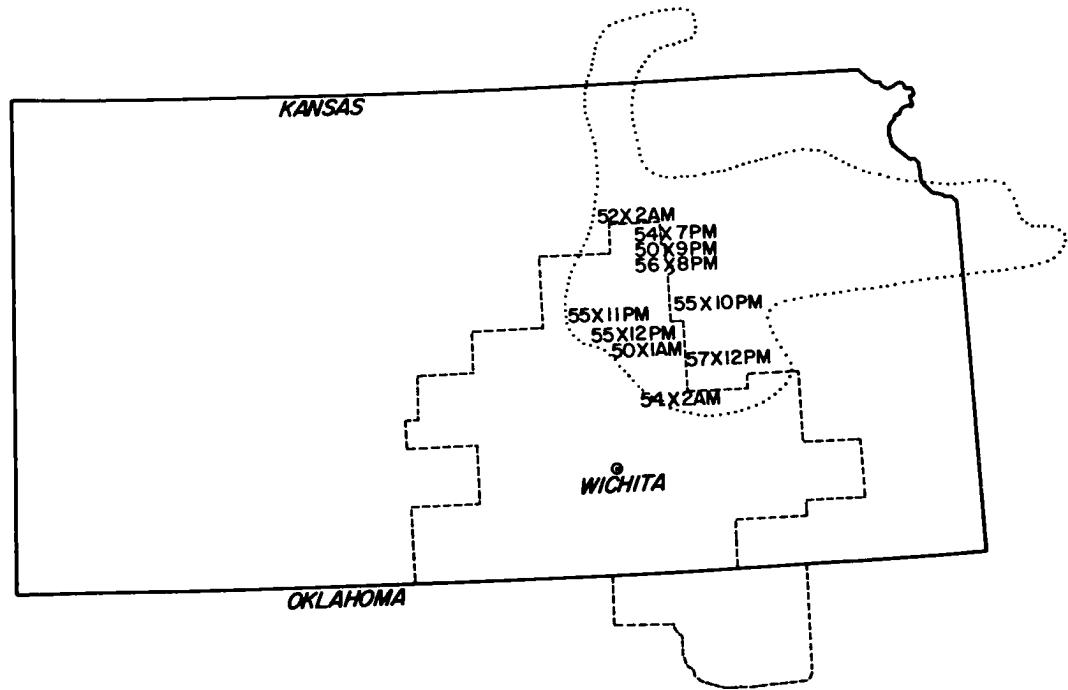


Fig. 6: Area of thunderstorm echoes (dotted line) reported by Wichita radar, 9 May 01 GMT (8 May 07 p. m. CST) to 9 May 08 GMT (9 May 02 a. m. CST). Location of each echo $\geq 50,000$ ft is shown by an X, altitude (thousands of ft) and time of occurrence (CST) are indicated (after List, Telegadas, and Ferber, 1964).

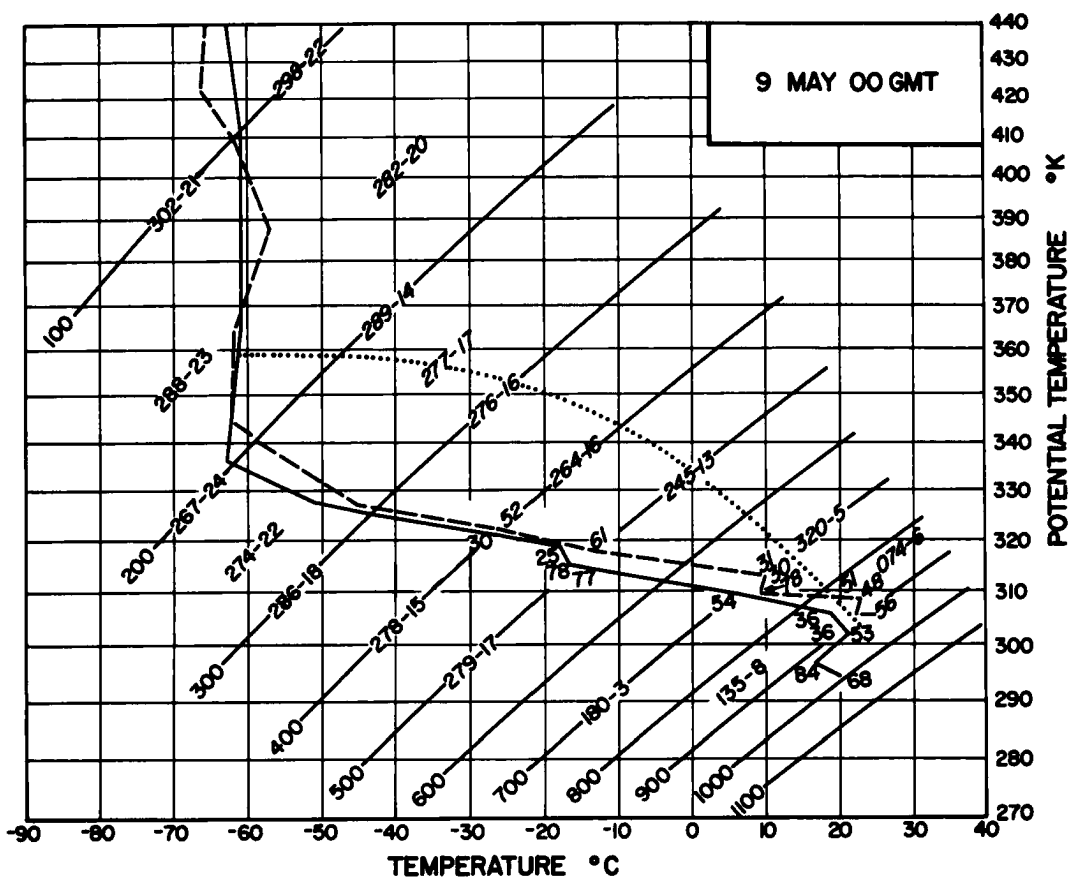


Fig. 7: Temperature sounding for Dodge City (DDC), Kansas, and Topeka (TOP), Kansas, on 9 May 1962, 00 GMT plotted on a tephigram. Relative humidities, wind directions, and wind speeds are given numerically along the sounding. Region of favorable convective activity for two soundings is given by dotted line.

Even though the precipitation regime over the central United States appears to be conducive to radioactive fallout, meteorological analysis will have to prove the levels at which I-131 may have been present in the atmosphere when removal of debris occurred by washout. Such proof will be offered in the subsequent chapter.

III. TRANSPORT OF DEBRIS IN THE ATMOSPHERE:

(A) Dry Transport Processes

Although the radioactive debris was deposited in the Wichita and Kansas City milkshed regions during a period of excessive precipitation and hailfall, the transport of this debris into these areas was accomplished by quasi-horizontal advection. No precipitation was reported between the Nevada test site and Wichita during the possible travel time of the debris. No high reaching "tapping" mechanism, penetrating into the stratosphere, was observed west of Wichita along the presumable path of Christmas Island fallout. We may, therefore, assume that these transport processes were essentially isentropic, except for those trajectories in the lower troposphere which may have been subject to frictionally induced mixing near the ground.

In order to check the hypothesis of List, Telegadas, and Ferber (1964) that stratospheric tapping provides the source of the Wichita I-131 increase, trajectories were calculated starting from the region where high values of radioactivity were measured by the Project Star Dust Flight of 8 May 1962 at 50,000 ft. From chemical analysis it was determined that this debris was due to a nuclear shot over Christmas Island on 4 May 1962. Trajectories were computed isobarically at 100 mb and isentropically at $\theta = 400$ K. Both sets produced essentially the same results as given by List, Telegadas, and Ferber for assumed horizontal air motion at the 50,000 foot level (Fig. 10 b). These results show that the heavily contaminated stratospheric air previously encountered by aircraft was over the

Wichita milkshed close to the 50,000 ft level from 9 May 00 GMT to 06 GMT. This corresponds exactly to the period of most violent convective activity as reported by the Wichita and Kansas City WSR-57 radar facilities (see Fig. 6). The 700 mb charts for 8-9 May 1962 show that the area of intense storm activity coincides with, and was accentuated by, the presence of a well-defined meso-scale cyclonic system propagating eastward from its point of origin to the lee of the Rocky Mountains (Fig. 8). The storm region was characterized by small areas of high local precipitation amounts with intense hail storms also reported.

The possibility that the Christmas Island shot provided the observed contamination at 50,000 ft was checked by estimating approximate trajectories over the data sparse Pacific Ocean. Because of the lack of data in this region, it is not possible to show explicitly that the trajectories from the 4 May Christmas Island shot trace to the region where the Project Star Dust flight intercepted nuclear contamination. However, considerations of energy and potential vorticity conservation show that this possibility definitely exists. The lower stratospheric flow at this time was, in fact, characterized by a large westerly wave reaching all the way to the equator (Fig. 9). It thus appears that a stratosphere equatorial debris injection may easily have reached temperate latitudes in a very short time with such a favorable long wave positions in the lower stratosphere.

Hence, the debris origin hypothesis of List, Telegadas, and Ferber is in all probability correct provided that two basic conditions are met: (1) that all other sources of debris may be excluded on the basis of disagreement between time of trajectory arrival and fallout increase in the Wichita area; and (2) that a plausible physical mechanism can be found which is capable of transporting radioactive particles from the lower stratosphere to the ground by convective and washout processes.

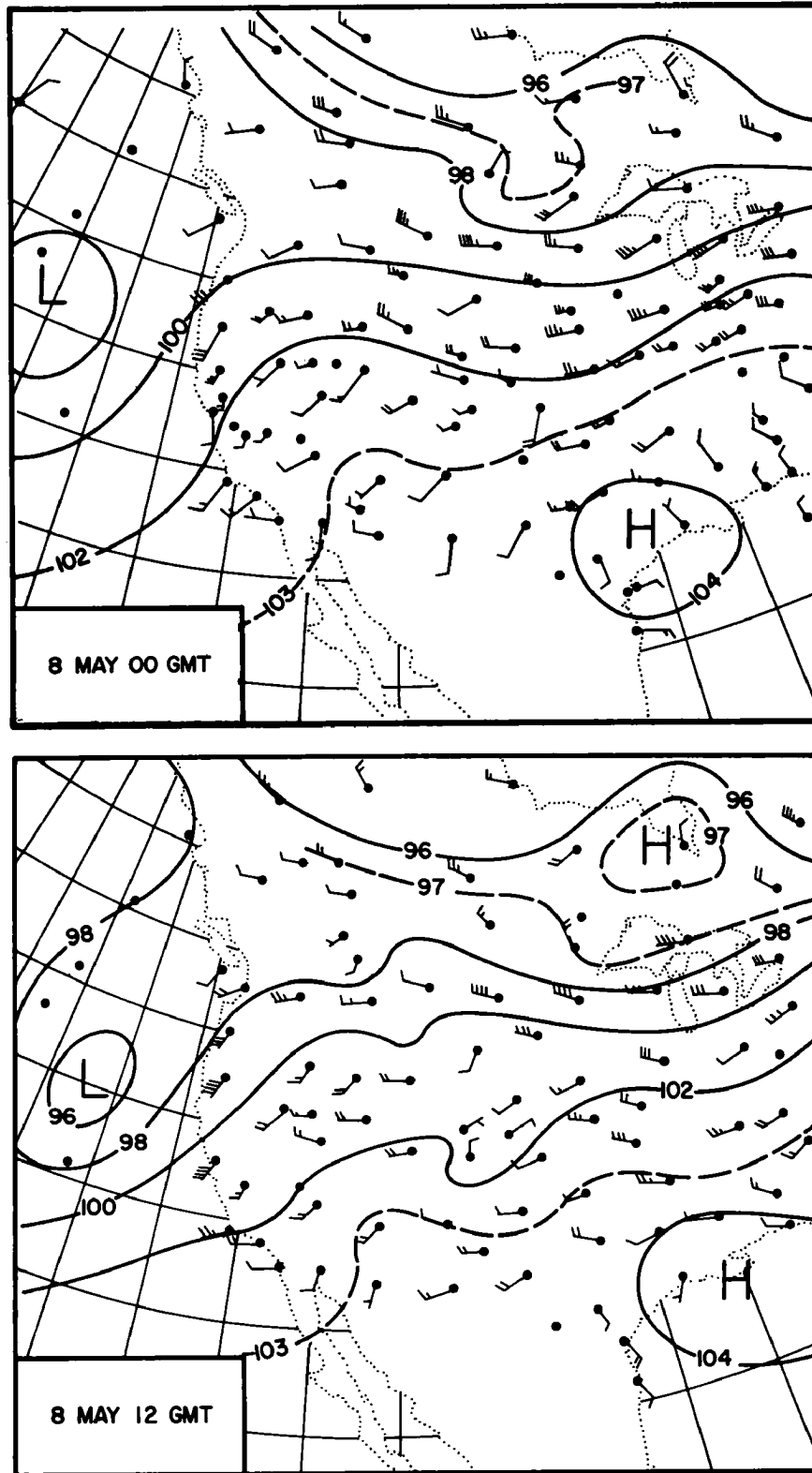


Fig. 8: 700 mb charts for 8 May 00 and 12 GMT and for 9 May 00 and 12 GMT. Solid lines are height contours (100's ft). Wind directions plotted with speeds given in knots.

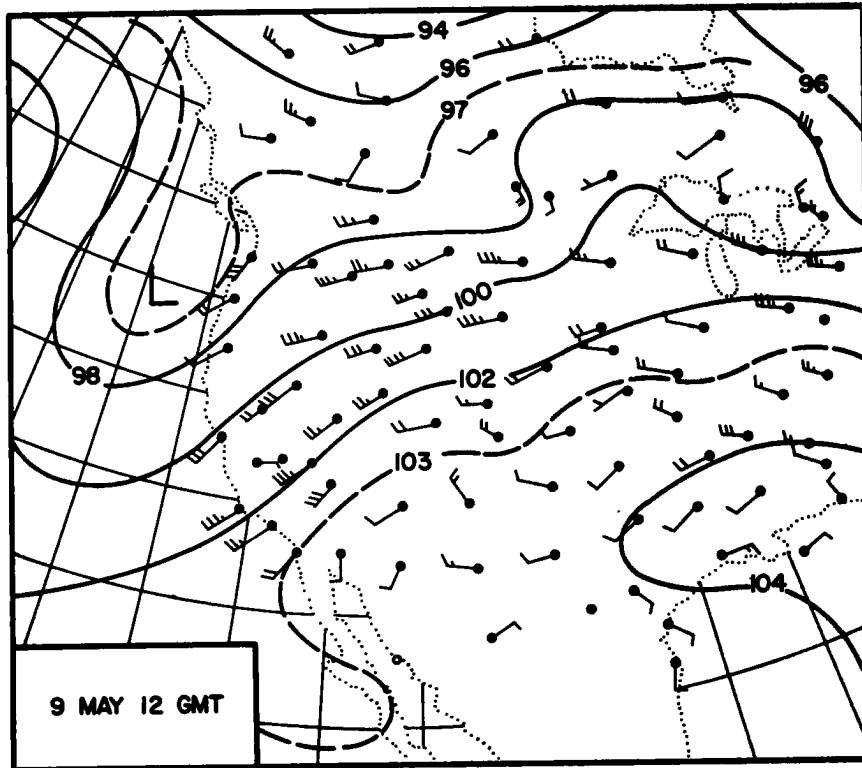
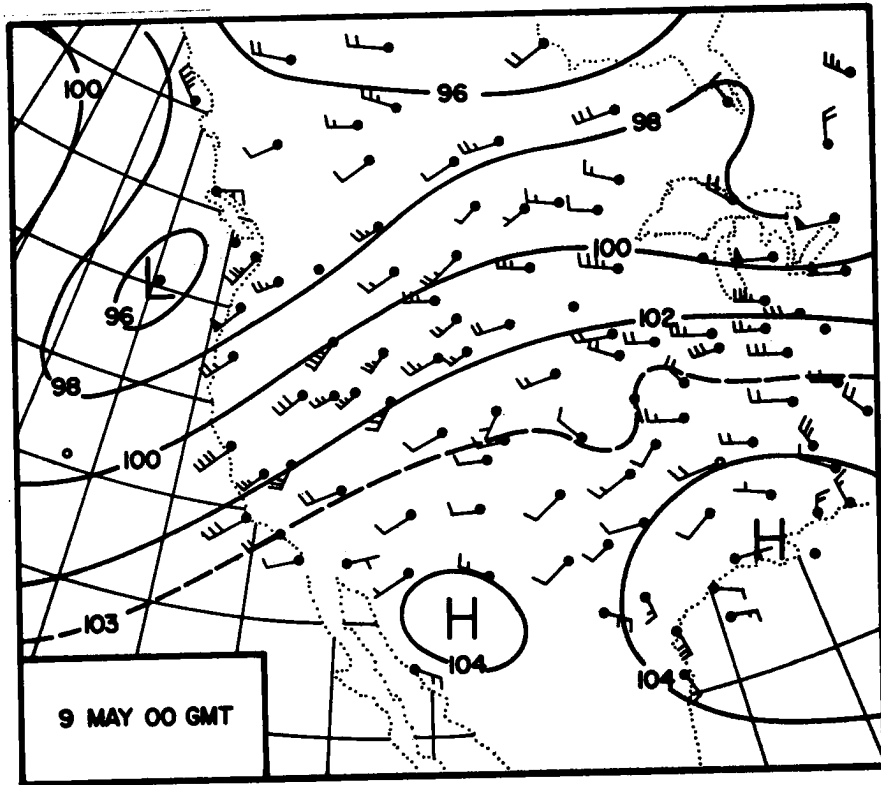


Fig. 8: Continued.

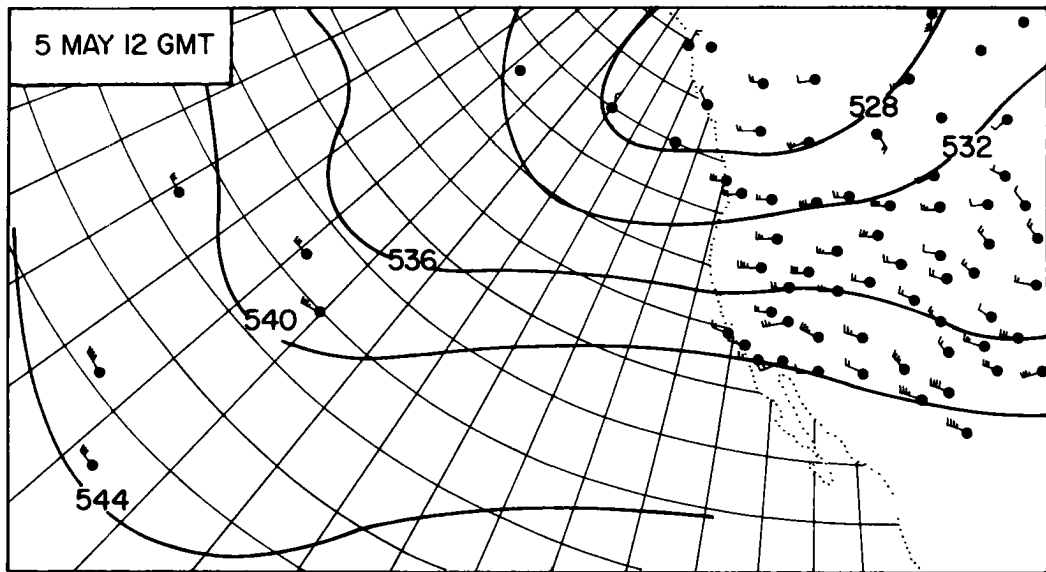
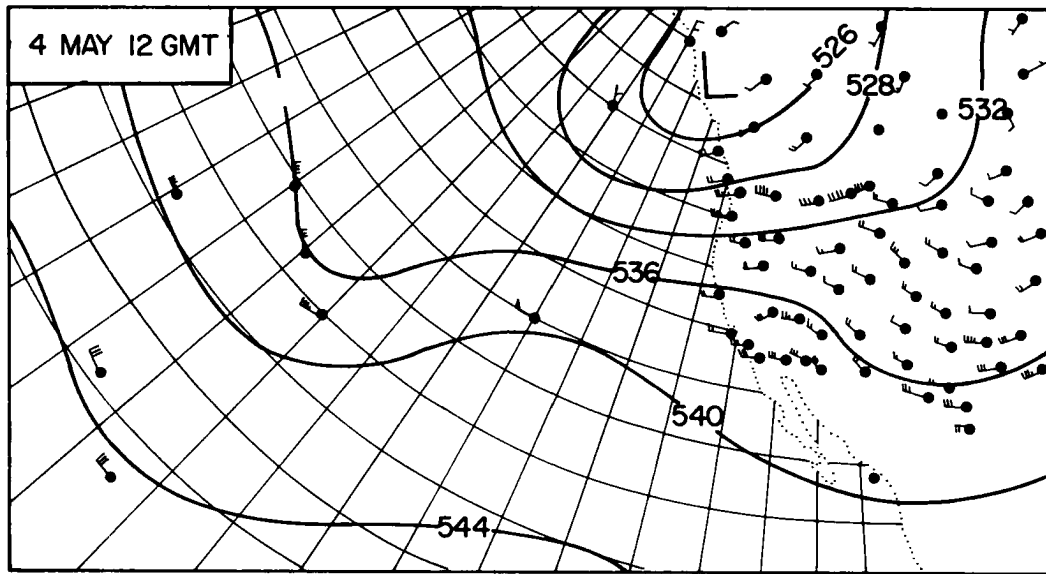


Fig. 9: 100-mb contour heights ($\text{ft} \times 10^2$) and winds (knots) for dates and observation times as indicated. Meridians and latitude circles are drawn for every 5 degrees. The Christmas Island test site is in the lower left corner of each map.

To check other possible sources (i. e. , the Paca shot mentioned by Martell) isentropic trajectoires were traced backward from Dodge City on 9 May 1962, 00 GMT at the isentropic levels $\theta = 310, 315, 320, 330,$ and 400 K. Of these, the upper levels 330 and 400 K show that the trajectories lead backward to a point over the Nevada test site by 8 May 06 GMT (Fig. 10. a).

However, debris released from post-Paca shot drilling could not have reached these higher levels, because the thermal energy of a debris cloud released during such drilling operations would have been totally insufficient to penetrate the surface inversion and the stable layers present at higher levels over the test site at that time. This implies that the vertical transport of debris for this type of release is completely dependent upon the static stability of the atmosphere in the test region. From Fig. 11 it is readily seen that vertical ascent of debris will be strongly inhibited above the 315 K potential temperature surface and definitely will not be permitted in the 330 -400 K layer. This consideration demands that any debris release from the Nevada site be transported entirely between the 310 and 320 K levels.

Computation of the trajectories at the 315 and 320 K levels shows rather strikingly that the air from Dodge City cannot be traced back to the Nevada region, but has a much more southerly origin (Fig. 10). Furthermore, the air at these isentropic levels moves much too slowly to be able to emanate from the Nevada region at the time of the nuclear experiment 7 May, 1933 GMT. Also, because debris was allegedly not released until within 24 hours after detonation time, the Nevada Paca shot could not have been involved in the Wichita fallout for irrefutable meteorological reasons.

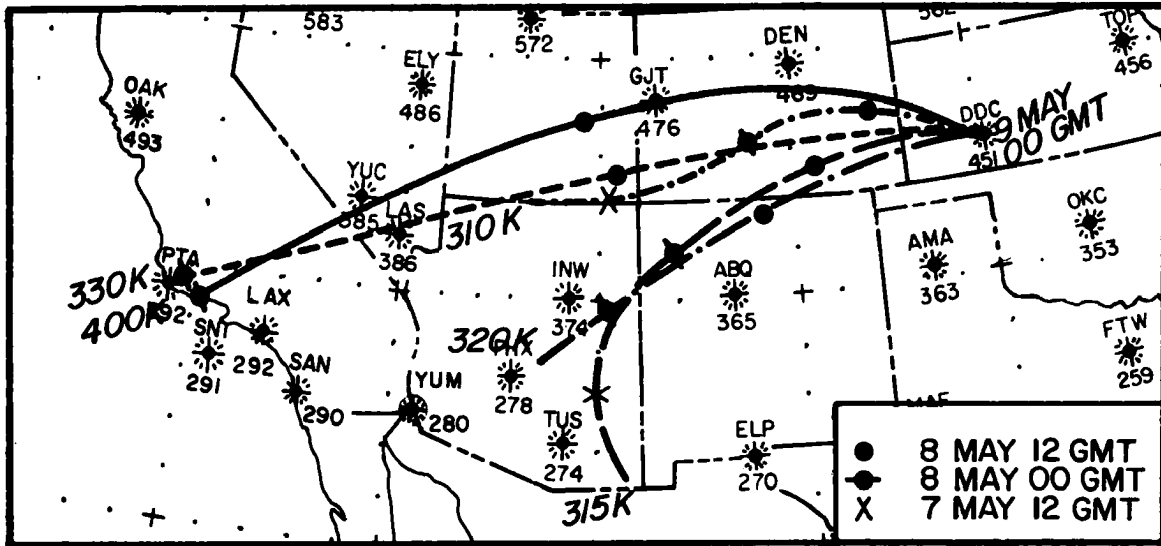


Fig. 10 a: Backward isentropic trajectories from Dodge City (DDC), Kansas, 9 May 00 GMT at levels $\theta = 310, 315, 320, 330,$ and 400 K. Time of trajectory position at various levels is indicated in legend. Extension of line past last symbol is additional 6-km trajectory.

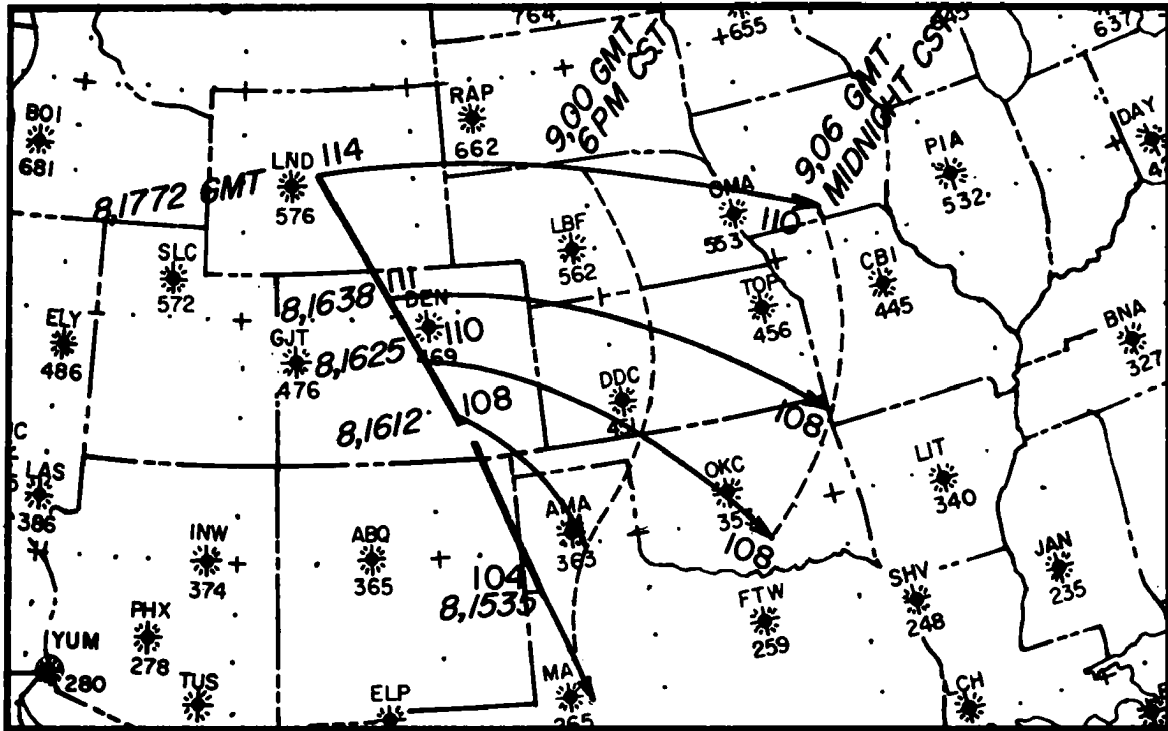


Fig. 10 b: Forward isentropic trajectories at $\theta = 400$ K from points and times of intersection by Project Star Dust flight of 8 May 1962. Time and pressures on the $\theta = 400$ K surface are indicated.

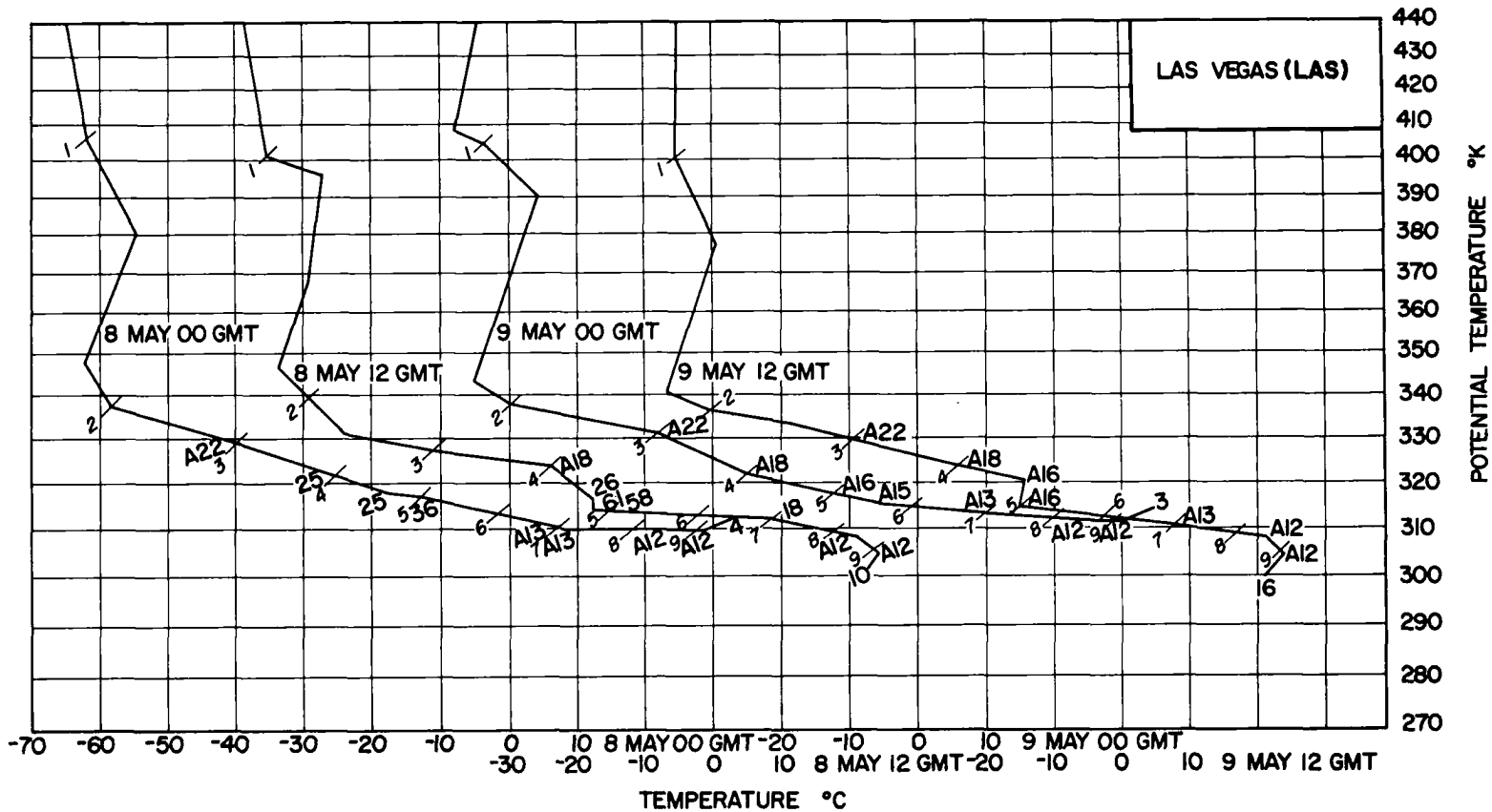


Fig. 11 a: Temperature soundings for Las Vegas (LAS), Nevada, from 8 May 00 GMT to 9 May 12 GMT plotted on a tephigram. Temperature coordinate is shifted 30°C to the right for each successive observation time. Vertical numbers along sounding: relative humidity (per cent, prefix "A" denotes a "motor-boating" report); slant numbers: pressures (100's of mb).

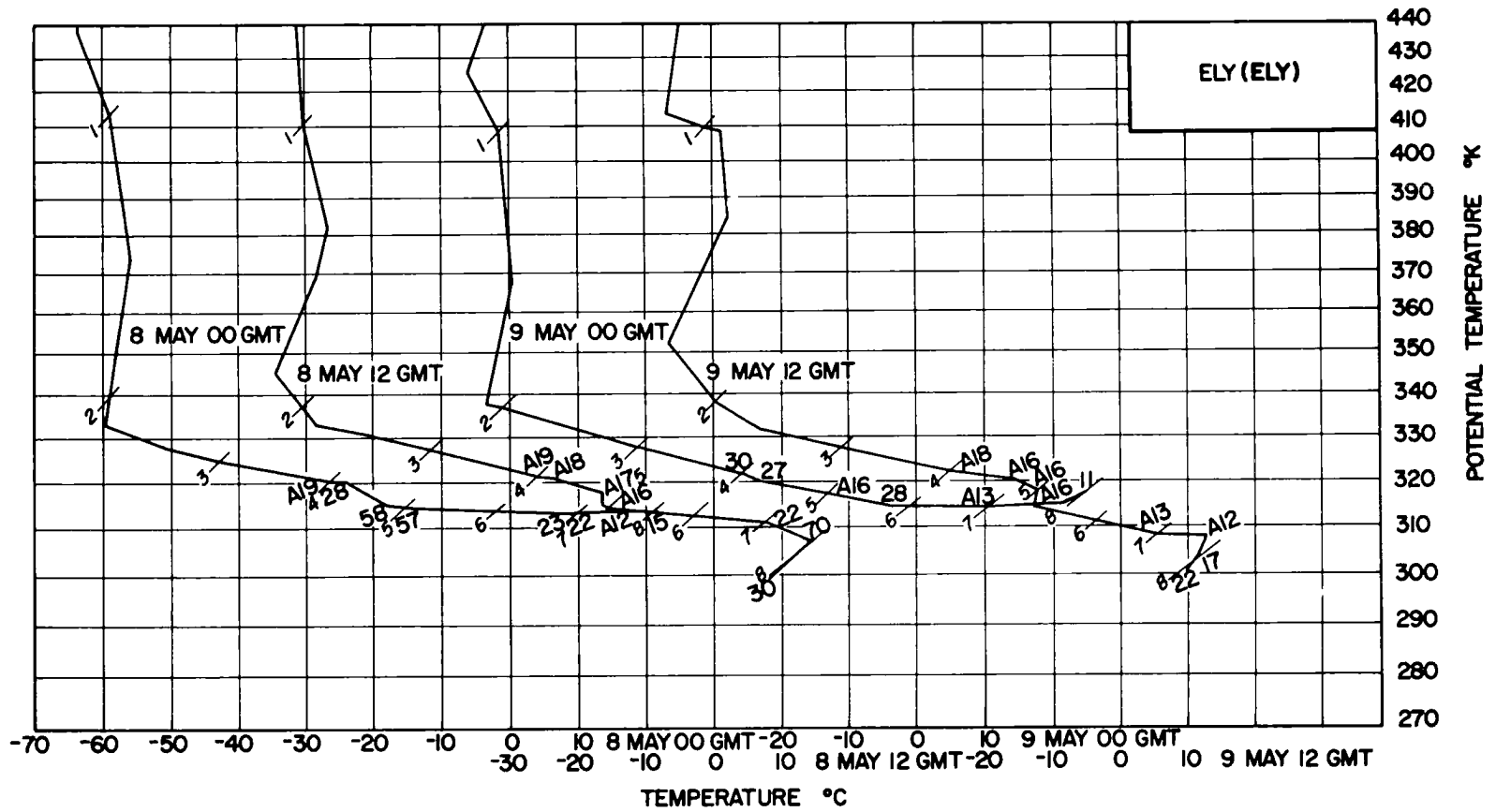


Fig. 11b: Temperature soundings for Ely (ELY), Nevada, from 8 May 00 GMT to 9 May 12 GMT. For explanation see legend to Fig. 11a.

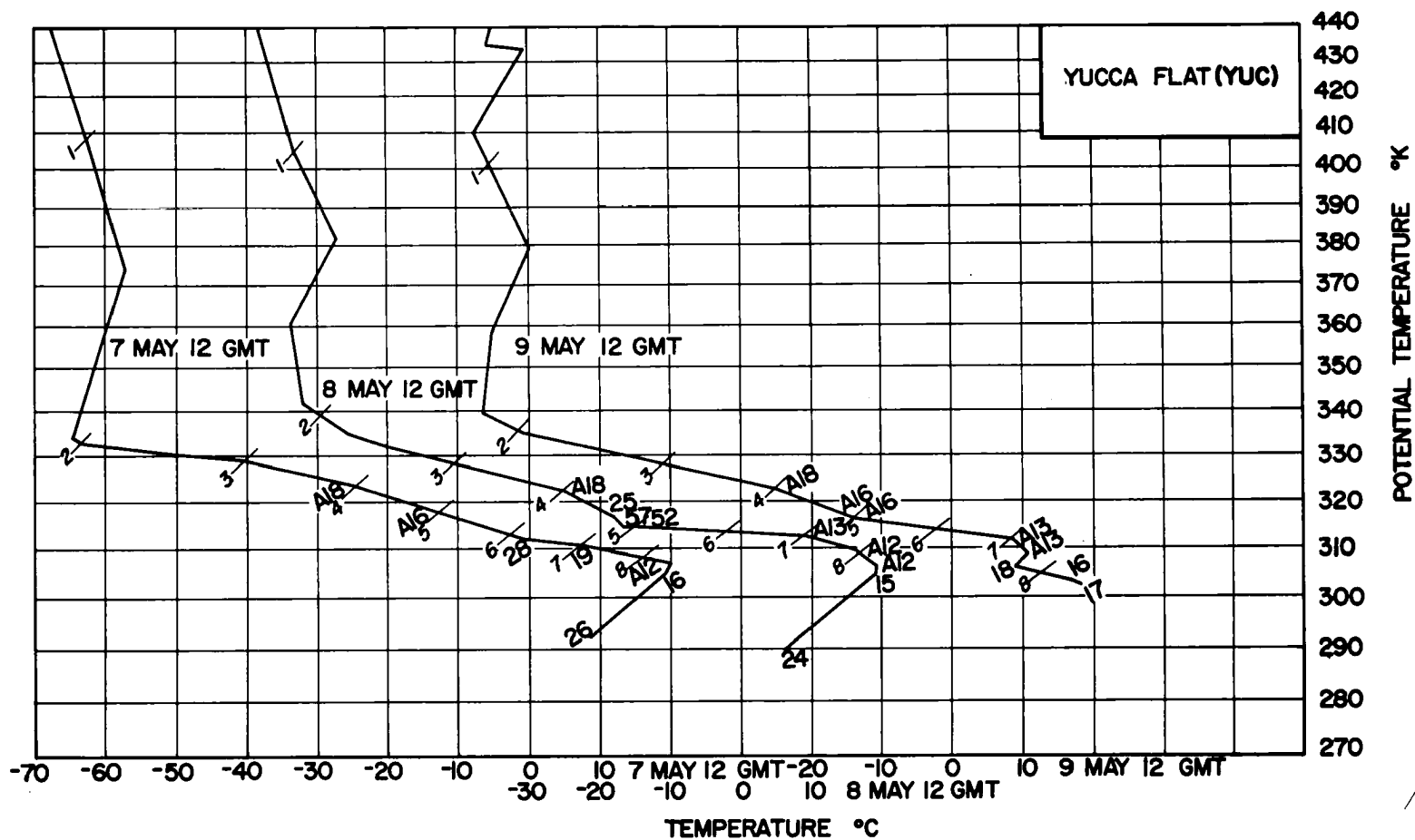


Fig. 11 c: Temperature soundings for Yucca Flat (YUC), Nevada, for 24 hr intervals from 7 May 12 GMT to 9 May 12 GMT. For explanation see legend to Fig. 11 a.

The attempt to follow the meteorological argument presented by Martell (1964) becomes difficult as a result of the following reasons:

(1) Trajectories shown in the paper are computed on constant height surfaces, thus make no attempt to trace vertical motions, nor do they satisfy basic energy considerations (Danielsen, 1961).

(2) The starting point of the trajectories is taken from the Nevada test region on 7 May 12 GMT, more than seven hours before the announced detonation time of 7 May 1933 GMT, and even longer before the drilling operations and the possible release of fractionated debris.

(3) At the starting time of Martell's trajectories, the low troposphere was characterized by a quite pronounced nocturnal inversion (Fig. 11). It thus is difficult to visualize a physical process which would result in contamination of the 4 and 6 km levels at which trajectories were presented in Martell's paper.

(4) Finally, even Martell's trajectories rule out Nevada as a possible source because they move considerably northward of the actual fallout region.

(B) Evaluation of the 11 May, Public Health Service Fallout Increase

From the Public Health Service Radiation Surveillance Network Data for radioactivity in air, a significant increase of intensity and a corresponding decrease in debris age was noted to occur in the 11 May collection over, and in the vicinity of, Colorado (Fig. 2). However, no precipitation occurred in the Colorado area from 9-12 May. Thus, dry transport processes must be held responsible for this increase.

Previously, Martell (1962) has correctly argued that the fallout from underground tests due to post shot drilling will produce debris of the most volatile and gaseous products, which

will be restricted to the lower layers below inversion level. He further states, "in cases where the activity is placed in the lowest layers of the troposphere below the weather layers, a quite different pattern of behavior can be expected. Debris below cloud level will drift in a complicated pattern of surface winds and be rapidly scavenged over a limited area."

This appears to be a reasonable hypothesis and could provide a possible explanation of the Colorado fallout measured on 11 May. To test this the most logical approach would be, of course, to find the exact time in which the debris was released by post shot drilling and then to evaluate carefully the transport of this debris in terms of all available meteorological data (including special measurements in the region of the test site). At the present time, this quantitative approach is not possible because the exact time of release of debris into the atmosphere from the 7 May Paca shot and also the accompanying meteorological data have not yet been made publically available.

In order to proceed in spite of this difficulty, the transport of (assumed) contaminated air was evaluated at 12 hour intervals for 48 hours beginning at actual shot time. The disadvantages of this procedure are quite obvious in view of possible large differences in final trajectory positions resulting from only a few hours difference in time of the trajectory beginning. A further difficulty arises because the movement of surface debris releases is highly dependent upon the surface topography, local wind systems, and static stability.

If the debris had been released on 8 May 00 GMT, the environmental lapse rate would have been dry adiabatic up to about 500 mb. Thus, the debris would have been redistributed quickly throughout this layer and transported with the wind at $\theta = 315$ K. The isentropic trajectory analysis at this level shows that the air travels considerably slower than required and arrives to the north of the Wichita area by

9 May 00-06 GMT (Fig. 12). It immediately follows that any trajectory traced some hours after 8 May 00 GMT could not have been in the Wichita area during the time of intense convective activity from 00-06 GMT on 9 May. The trajectory taken from 8 May 00 GMT also shows that a debris release at this time could not have been responsible for the dry fallout increase in the Colorado area on 11 May.

If the debris had been released on 8 May 12 GMT it would have remained "trapped" in the surface inversion layer (Fig. 11) until the stratification again became adiabatic as a result of solar heating. Fig. 12 shows the debris transport at the top of the mixing layer from this assumed starting date. Had the contamination been released at this time, an increase in radioactivity in dry air should have been observed at Salt Lake City by the 9th or 10th of May. Since there was no increase at that time, it may be assumed that no substantial amount of debris could have been released on or about 8 May 12 GMT.

This procedure was repeated for 9 May 00 GMT with the same general conclusions as given previously for an assumed 8 May 12 GMT release. At 8 May 12 GMT, of course, the assumed debris would have remained trapped within the surface inversion for a short time before mixing in the adiabatic layer.

By assuming a debris release on 9 May 12 GMT (41 hours after the shot time), it is possible that a fallout increase could have resulted in the Utah, Colorado, Wyoming area. However, from the trajectories (see Fig. 12) it is difficult to justify meteorologically the fallout increases and age shifts at Santa Fe and El Paso (Fig. 2) on the assumption that the source of contamination was due to the 7 May Paca underground shot.

From the catalogue of announced atmospheric weapons tests (see Table 3), it appears that this observed radioactivity increase may also be due to the Christmas Island test series of early May. Because of the dry nature of the measured surface fallout, the

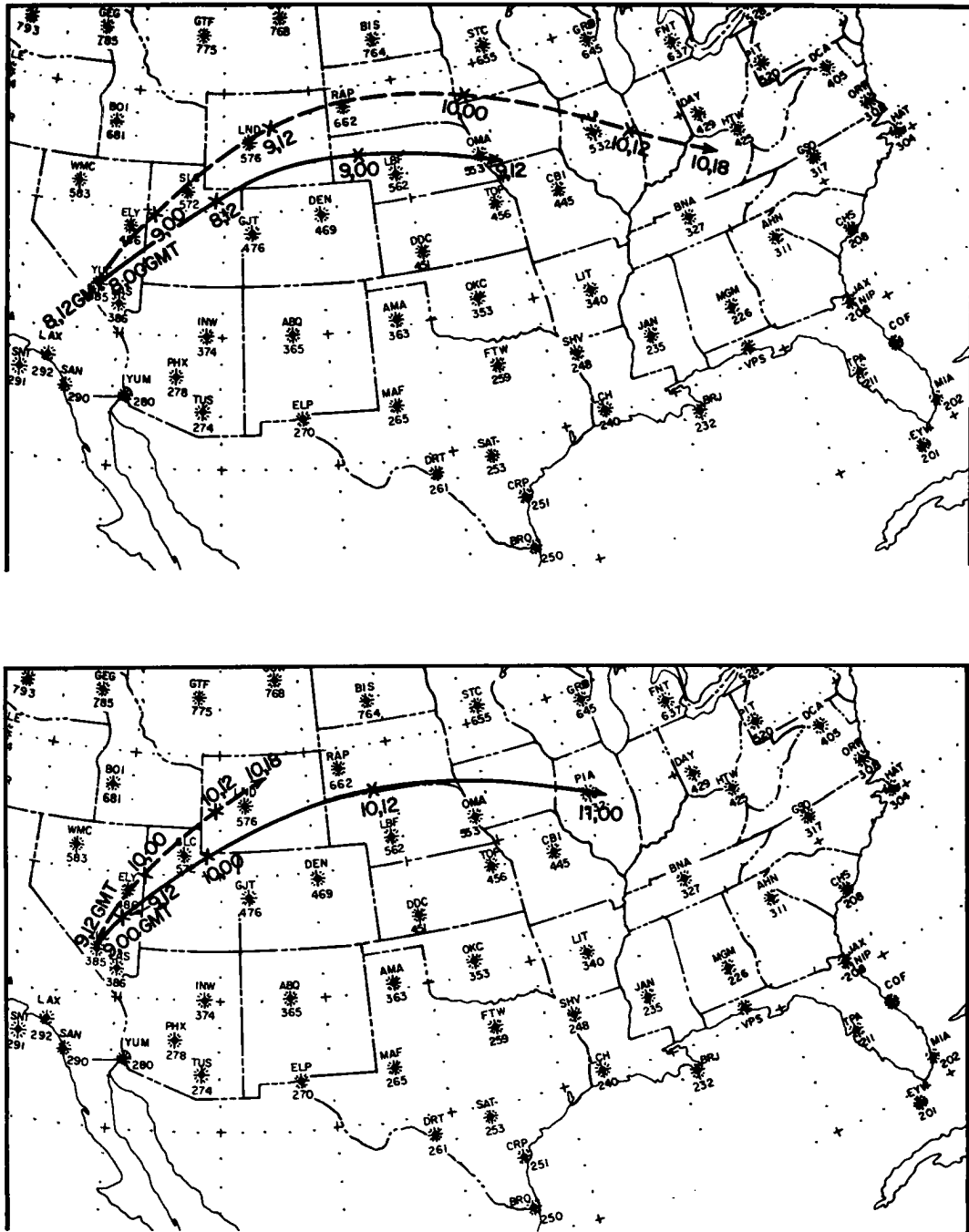


Fig. 12: Isentropic trajectories, starting from Yucca Flat (YUC), near the Nevada test site. 12-hour trajectory segments are marked by "X", with date and Greenwich time indicated. Trajectories starting on 8 May 1962, 00 and 12 GMT, and on 9 May, 00 GMT have been constructed on the 315 K isentropic surface; the trajectory starting on 9 May, 12 GMT has been traced on the 310 K isentropic surface.

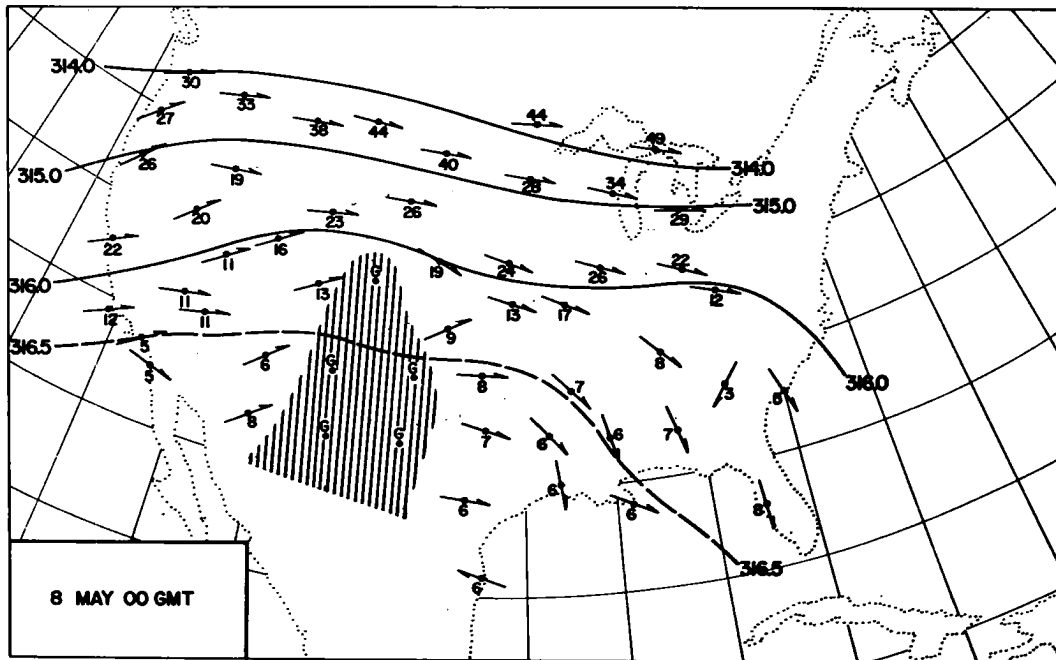
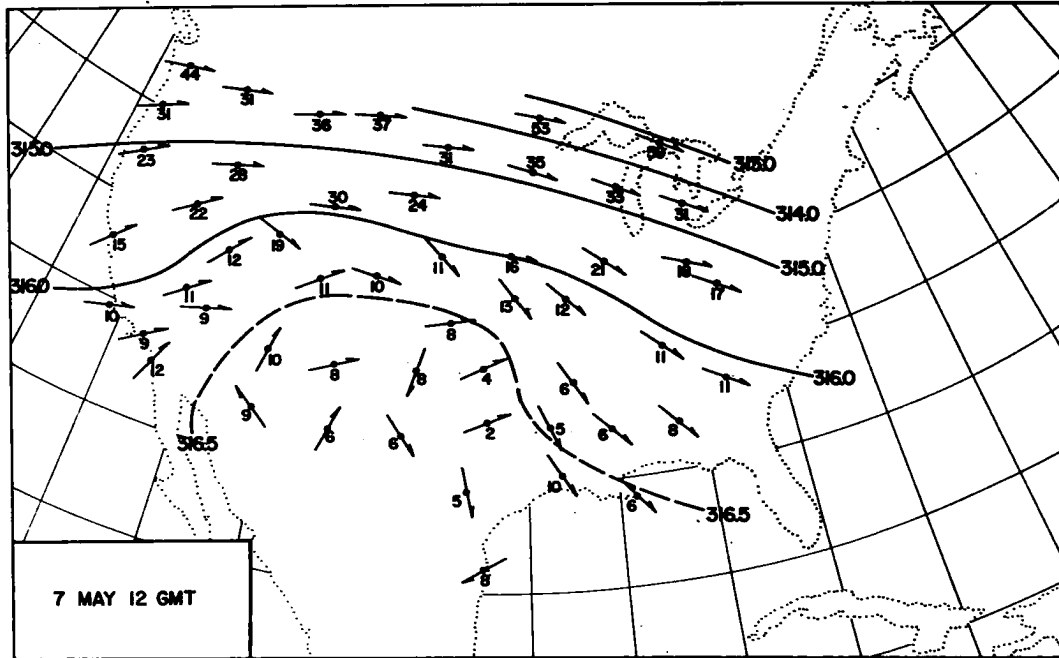


Fig. 13: Montgomery stream function (10^7 ergs/g) and winds (mps) on 315 isentropic surface for observation times as indicated. Shaded area and "G" on station locations indicate region in which this isentropic surface is below ground.

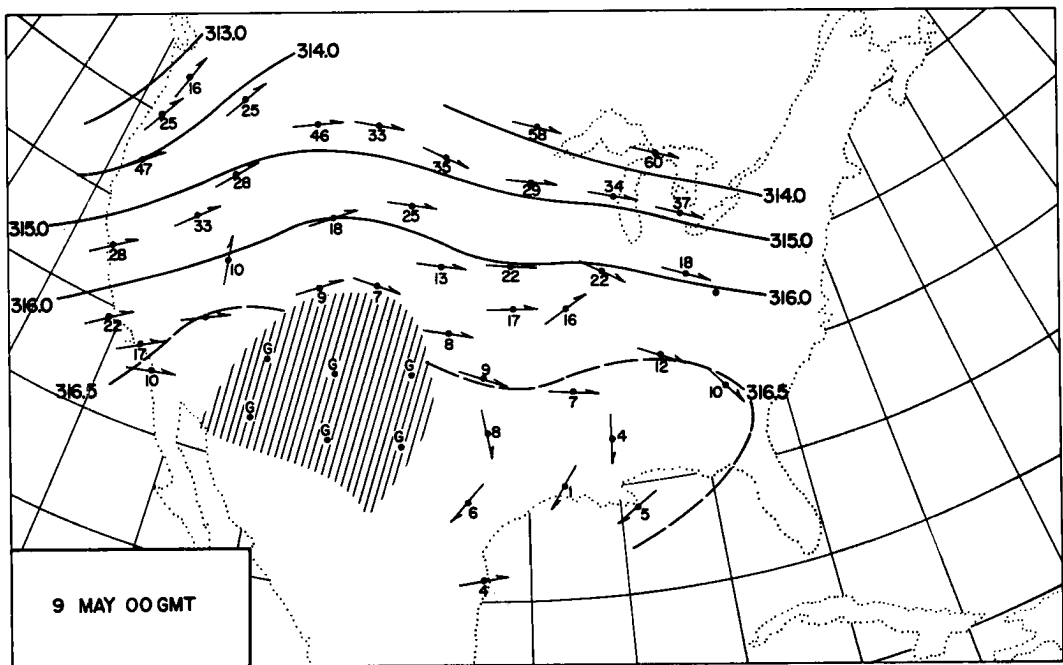
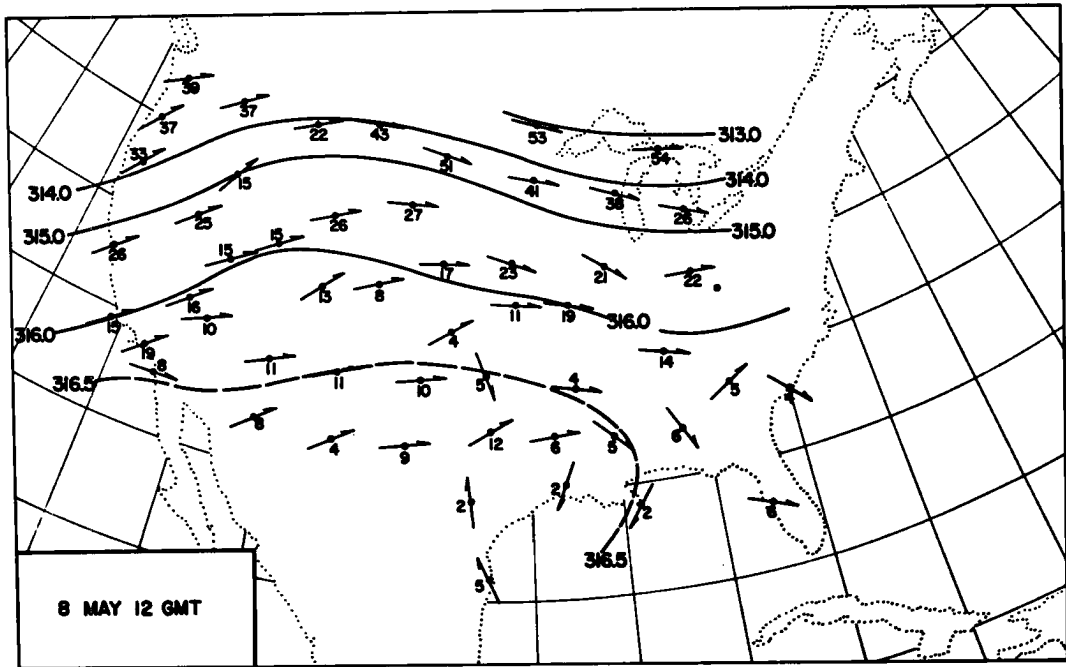


Fig. 13: Continued.

and radiochemical data in connection with the debris release time of the Nevada Paca underground shot. These data have not yet been made available. Without this pertinent information it is impossible to rule out either the Christmas Island or the Nevada shots as possible sources for the debris increase observed in the Colorado region.

(C) Washout by Precipitation

It has been reasoned from the foregoing analyses, that the only source of I-131 that could account for the milk contamination in the Wichita and Kansas City area was located in the stratosphere. Martell (1965) voiced criticism of the suggestion made by List, Telegadas, and Ferber (1964) that debris may have been removed from these stratospheric layers by washout processes. This argument is that "precipitation scavenging takes place at lower elevations and is hardly a quantitative process".

This statement is based on two untenable assumptions:

- (a) that there was a low-level debris source
- (b) that debris collection by precipitation is an ineffective removal mechanism at higher levels.

The first of the two assumptions already has been disproven. We still will have to contend with the second one.

A large number of studies--not considered in Martell's papers--have concerned themselves with the wet removal of debris from the atmosphere (Itagaki and Koenuma, 1962; Hall and Klehr, 1963; Booker, Hamada, and Kruger, 1964; Dingle, 1964; Hall and Nelson, 1964; Huff, 1965; Huff and Stout, 1964, 1965). Washout processes appear to be extremely complex and should not be summarized by the term "scavenging" because its use might lead to gross misinterpretation of the actual physical processes involved.

Facy (1962) has published a comprehensive summary on radioactive fallout. The flow diagram of Fig. 14, taken from his publication, indicates the complexity of the phenomenon.

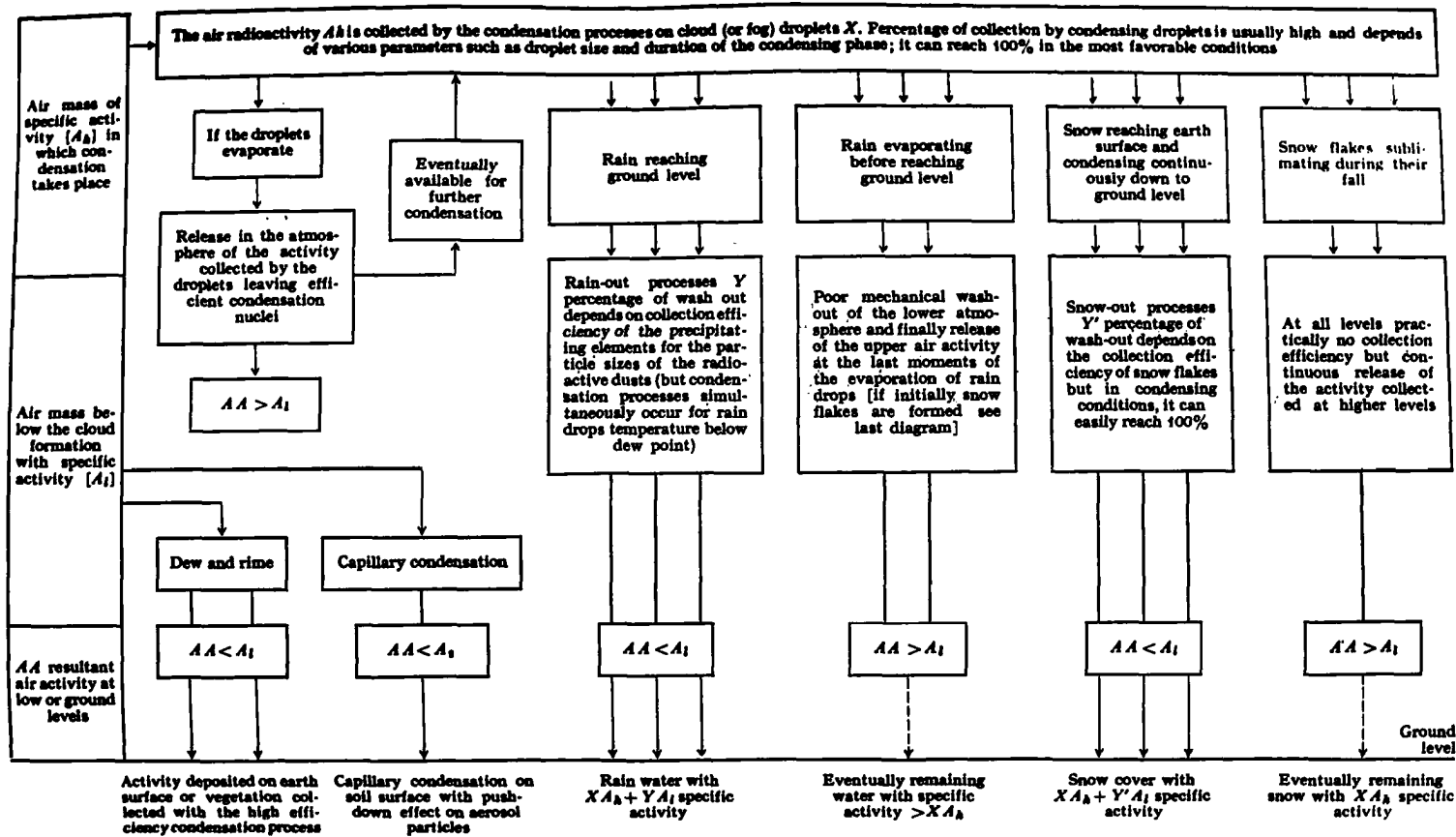


Fig. 14: Wet removal of radioactive debris by atmospheric condensation processes (after Facy, 1962).

It appears that "scavenging" of aerosols by cloud droplets is rather inefficient if these droplets are in a state of evaporation. They surround themselves with a thin shell of vapor, and the diffusion processes, acting in the direction of the vapor pressure gradient, tend to repel dust particles and other aerosols. Thus, a "dust-free" sphere seems to be generated around these droplets.

This rejection mechanism may be counteracted by collision processes, if the precipitation droplets are falling relative to the aerosol. The collection efficiency depends, among other things, upon the relative fall velocity of droplets, and on droplet and aerosol radii. Greenfield (1956) shows a simple nomograph (Fig. 15) from which collection efficiency may be computed in terms of per cent of particles of diameter "d" scavenged by rain "R" (in mm/hr) during the time "t".

If cloud particles are rising and in a state of condensation, their collection efficiency increases with the reversal of vapor-pressure gradient, which now is directed towards the droplet. This is shown in Fig. 16. In addition to the effect of the vapor-pressure gradient, relative velocities between the heavier (hence slower) cloud droplets and the rising, supersaturated (and radioactively contaminated) airstream within the clouds will help to increase the scavenging efficiency.

In the present case we have to assume that the radioactive aerosol was scavenged mainly by ice-nuclei. This is suggested by the low temperatures of ca. -60° at the 50,000 ft level measured over Topeka and Dodge City, Kansas, on 9 May 00 GMT (Fig. 7). The occurrence of heavy hailfall in the Wichita region also implies the involvement of the ice phase in the precipitation mechanism.

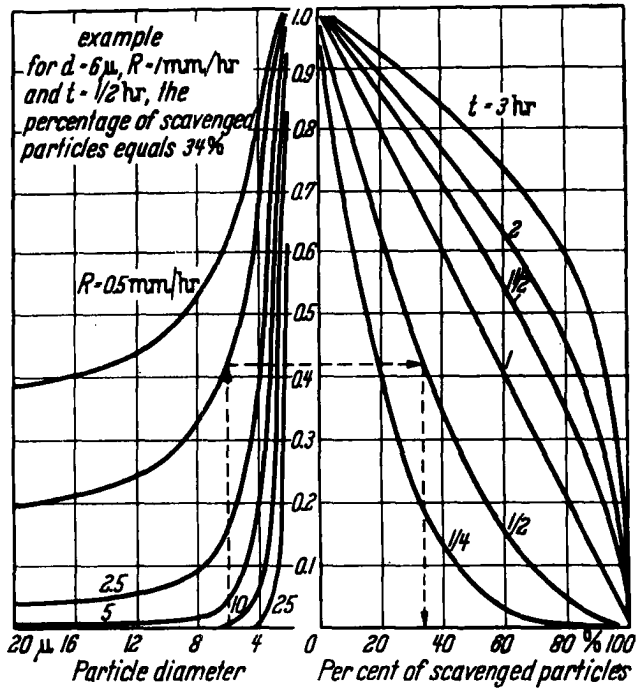


Fig. 16: Effect of vapor pressure gradient in the vicinity of a cloud droplet on the capture of aerosol particles (after Facy, 1962).

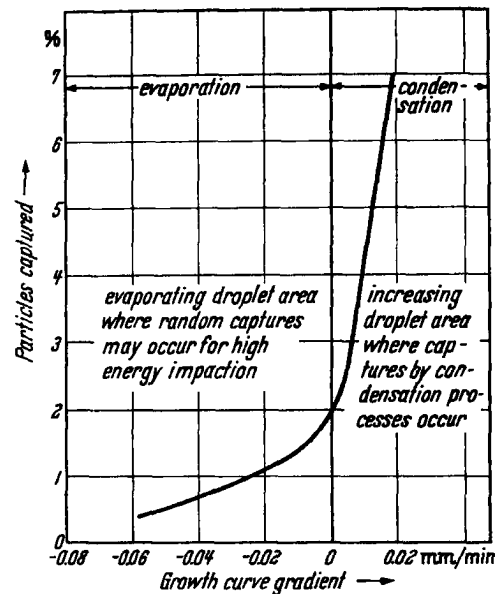


Fig. 15: Per cent of particles of a certain diameter, scavenged by rainfall of hourly rate R during time t (after Facy, 1962).

Since the saturation vapor pressure with respect to ice is lower than with respect to water, the vapor pressure gradient between ambient air and growing ice crystal should be larger, and therefore enhance the crystal's collection efficiency, than with supercooled water under similar conditions (Facy, 1962).

We, therefore, may assume that--as soon as the visible cloud tops penetrated the contaminated layer near 50,000 ft--turbulent mixing of cloud air with contaminated environmental air produced ideal scavenging conditions. That cloud tops actually penetrated to these heights--and into the contaminated layer--was firmly proven in the previous chapters. Thus, the conclusion of List, Telegadas, and Ferber (1964) as to the mechanism of the Wichita fallout stands uncorrected.

As indicated in the flow diagram of Fig. 14, evaporation from falling rain will release some of the radioactivity transported downward in precipitation. Hence the shift in age, and the almost unnoticeable increases in radioactivity observed by the Radiation Surveillance Network. Reiter and Mahlman (1964, 1965) have reported on a fallout case in November 1962 during which large increases of radioactive debris concentrations were observed in rainwater as well as in dry air. This case differed significantly from the one presented here, however. The November case was due to a wide-spread, low level debris source which had descended adiabatically from higher levels. Radioactivity was carried to the ground in part by dry mixing processes in the adiabatic surface layer, and only in part by precipitation.

In the present case precipitation was entirely responsible for the downward transport. Furthermore, only the tallest portions of the cumulo-nimbi, from which hail and excessively heavy rain was falling, had tapped the contaminated stratospheric layer. Only very little evaporation could have taken place while these heavy precipitation particles were falling through the lowest tropospheric layers.

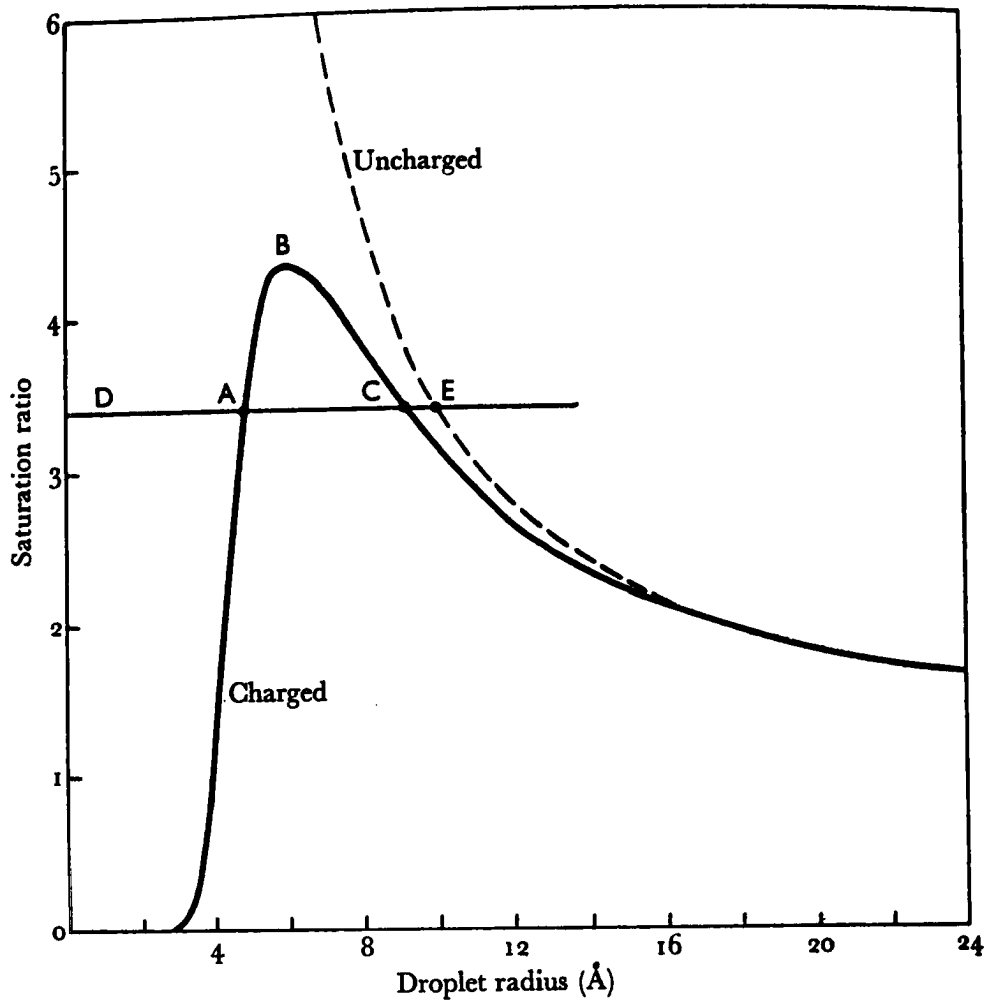


Fig. 17: Saturation ratio (i. e., supersaturation) as a function of radius for charged and uncharged water droplets (.after Fletcher, 1962).

observed in the Wichita and Kansas City milksheds around 13 May 1962. Tapping by cumulo-nimbi of a stratospheric debris cloud advected from Christmas Island not only presents a feasible explanation for the observed fallout, it also is the only mechanism which would satisfy the statistical peculiarities of the observations.

(2) This conclusion is in total agreement with meteorological conditions, such as the quasi-horizontal advection of contaminated air masses and cloud-physical requirements. It is not contradicted in any way by radiochemical evidence, as proven by the analyses of samples taken by Project Star Dust. However, as justly noted by Martell (1965), further evidence in this case has been recorded in the form of the U. S. Public Health Service gamma ray spectra on radioactive samples in Kansas and Missouri during May 1962. This information may have additional capability of determining whether or not the Wichita fallout was due to an unfractionated atmospheric shot or to a highly fractionated underground test. At the present time, these data have not been made available for use in analyzing this case. We strongly agree with Martell that the release of this data is certainly long overdue in view of the high degree of interest in this fallout case.

(3) Whereas this conclusion holds for the present case study, it should not be generalized in any way. There is a possibility that light increases in radioactivity of dry air and significant shifts in the age of this debris, observed in and around Colorado by the monitoring system of the U. S. Public Health Service Radiation Surveillance Network on 11 May, may have been caused by radioactive gases that escaped during the post-shot drilling operations subsequent to the Paca shot.

The present conclusions also do not include other fallout incidents that may have been linked with Nevada tests (Bostrom, 1963). Therefore, they do not supply a convenient answer to the argumentative questions raised in Chapter I.

V. ACKNOWLEDGEMENTS:

This study was carried out under the specific request of the U. S. Atomic Energy Commission. Certain data on post-shot drilling operations that might have been helpful in pin-pointing trajectory origins of Nevada debris, have not arrived in time to be included in this report. This, however, does not reflect in any way upon the validity of conclusions with respect to the Wichita fallout. It may have helped to construct a better case for or against the involvement of Nevada debris in the observed light increases of radioactivity in the Colorado region.

REFERENCES

- Allen, P. W. , 1962: Letter from P. W. Allen to E. A. Martell, June 19, 1962, Radiation Standards, Including Fallout, Part 2, Appendix, 775.
- Booker, R. D. , G. Hamada, and P. Kruger, 1963: Radioactive fallout from two severe storms in Oklahoma during May 1963, Hazleton-Nuclear Science Corporation, HNS-58, 52 pp.
- Bostrom, R. G. , 1963: Iodine-131 in milk and vegetables associated with July 1962 fallout in Utah, Fallout, Radiation Standards, and Countermeasures, Part I, 52-66.
- Chamberlain, A. C. , 1959: Deposition of iodine in northern England in October 1957, Quarterly Journal of the Royal Meteorological Society, 85, 350-361.
- _____, and R. C. Wiffin, 1959: Some observations on the behavior of radioiodine vapor in the atmosphere, Geofisica Pura e Applicata, 42, 42-48.
- Danielsen, E. F. , 1959: The laminar structure of the atmosphere and its relation to the concept of a tropopause, Archiv für Meteorologie, Geophysik und Bioklimatologie, A 11, 293-332.
- _____, 1961: Trajectories: isobaric, isentropic and actual, Journal of Meteorology, 18, 479-486.
- _____, 1964 a: Radioactivity transport from stratosphere to troposphere, Mineral Industries, Pennsylvania State University, 33 (6), 1-7.

- Danielsen, E. F. , 1964 b: Project Springfield Report, Defense Atomic Support Agency, 97 pp.
- Dingle, A. N. , 1964: Stratospheric tapping by intense convective storms and implications for public health in the United States, Department of Meteorology and Oceanography, University of Michigan, HNS-58, 1-6.
- Facy, L. , 1962: Radioactive precipitations and fallout, Nuclear Radiation in Geophysics, Berlin, Springer-Verlag, 202-240.
- Fletcher, N. H. , 1962: The Physics of Rainclouds, Cambridge, Cambridge University Press, 386 pp.
- Greenfield, S. M. , 1956: Ionization of radioactive particles in the free air, Journal of Geophysical Research, 61, 27-33.
- Hall, S. J. , and E. H. Klehr, 1963: Severe convective storms and the stratospheric scavenging of radioactive particles, First Progress Report, University of Oklahoma Research Institute, 67 pp.
- _____, and R. Y. Nelson, 1964: Severe convective storms and the stratospheric scavenging of radioactive particles, Second Progress Report, University of Oklahoma Research Institute, 37 pp.
- Hardy, E. P. , Jr. , J. Rivera, and W. R. Collins, Jr. , 1964: Fallout program quarterly summary report, Health and Safety Laboratory, U. S. Atomic Energy Commission, 336 pp.
- Huff, F. A. , 1965: Radioactive rainout relations on densely gauged sampling networks, Water Resources Research, 1, 97-108.
- _____, and G. E. Stout, 1964: Distribution of radioactive rainout in convective rainfall, Journal of Applied Meteorology, 3, 707-717.
- _____, and G. E. Stout, 1965: Study of Rainout of radioactivity in Illinois, Third Progress Report to Atomic Energy Commission, Illinois State Water Survey, 66 pp.
- Itagaki, K. , and S. Koenuma, 1962: Altitude distribution of fallout contained in rain and snow, Journal of Geophysical Research, 67, 3927-3934.
- Junge, C. E. , 1963: Air Chemistry and Radioactivity, New York and London, Academic Press, 382 pp.

- List, R. J., K. Telegadas, and G. J. Ferber, 1964: Meteorological evaluation of the sources of iodine-131 in pasteurized milk, Science, 146, 59-64.
- Lockhart, L. B., Jr., 1964 a: Behavior of airborne fission products, American Scientist, 52, 301-305.
- _____, 1964 b: Comments on paper by S. Penn and E. A. Martell, "An analysis of the radioactive fallout over North America in late September 1961", Journal of Geophysical Research, 69, 796-797.
- Machta, L., 1962: "Memorandum for the record, May 24, 1962", Hearings before the Subcommittee on Research, Development, and Radiation of the Joint Committee on Atomic Energy, Fallout Radiation Standards, and Countermeasures, Washington, D. C., Part 2, Appendix, 776-778.
- _____, R. J. List, and K. Telegadas, 1962: A survey of radioactive fallout from nuclear tests, Journal of Geophysical Research, 67, 763-774.
- _____, R. J. List, and K. Telegadas, 1964: Comments on paper by S. Penn and E. A. Martell, "An analysis of the radioactive fallout over North America in late September 1961", Journal of Geophysical Research, 69, 791-793.
- Mahlman, J. D., 1964: Relation of stratospheric-tropospheric mass exchange mechanisms to surface radioactivity peaks, Technical Paper No. 58, Department of Atmospheric Science, Colorado State University, 1-19.
- _____, 1965 a: Relation of stratospheric-tropospheric mass exchange mechanisms to surface radioactivity peaks, Archiv fur Meteorologie, Geophysik und Bioklimatologie, A 17, (to be published).
- _____, 1965 b: Relation of tropopause-level index changes to radioactive fallout fluctuations, Technical Paper No. 70, Department of Atmospheric Science, Colorado State University, 84 - 109.
- Martell, E. A., 1962: Possible contribution of underground nuclear explosions to recent fallout over the United States, Radiation Standards, Including Fallout, Part 2, Appendix, 748-752.
- _____, 1964: Iodine-131 fallout from underground tests, Science, 143, 126-129.
- _____, 1965: Iodine-131 fallout from underground tests II, Science, 148, 1756-1757.

- Martell, E. A., J. P. Shedlovsky, and C. A. Watkins, 1965: Radiochemical evidence for Antler shot contribution to the September 1961 fallout, Journal of Geophysical Research, 70, 1295-1302.
- Minx, R. P., 1962: "Memorandum for the record, July 25, 1962", Hearings before the Subcommittee on Research, Development, and Radiation of the Joint Committee on Atomic Energy, Fallout Radiation Standards, and Countermeasures, Washington, D. C., Part 2, Appendix, 783-787.
- Pasquill, F., 1962: Atmospheric Diffusion, London, Toronto, New York, D. Van Nostrand Company Ltd., 297 pp.
- Penn, S., and E. A. Martell, 1963: An analysis of the radioactive fallout over North America in late September 1961, Journal of Geophysical Research, 68, 4195-4207.
- _____, and E. A. Martell, 1964 a: Reply to "Comments on paper by S. Penn and E. A. Martell, 'An analysis of radioactive fallout over North America in late September 1961'", by E. R. Reiter, Journal of Geophysical Research, 69, 789-790.
- _____, and E. A. Martell, 1964 b: Reply to "Comments on paper by S. Penn and E. A. Martell, 'An analysis of the radioactive fallout over North America in late September 1961'", by L. Machta, R. J. List, and K. Telegadas, Journal of Geophysical Research, 69, 793-795.
- _____, and E. A. Martell, 1964 c: Reply to "Comments on paper by S. Penn and E. A. Martell, 'An analysis of the radioactive fallout over North America in late September 1961'", by L. B. Lockhart, Jr., Journal of Geophysical Research, 798-799.
- Reiter, E. R., 1963 a: A case study of radioactive fallout, Technical Paper No. 42, Department of Atmospheric Science, Colorado State University, 35 pp.
- _____, 1963 b: A case study of radioactive fallout, Journal of Applied Meteorology, 2, 691-705.
- _____, 1964: Comments on paper by S. Penn and E. A. Martell, "An analysis of the radioactive fallout over North America in late September 1961", Journal of Geophysical Research, 69, 786-788.

Reiter, E. R. and J. D. Mahlman, 1964: Heavy radioactive fallout over the southern United States, November 1962, Technical Paper No. 58, Department of Atmospheric Science, Colorado State University, 21-49.

_____, and J. D. Mahlman, 1965: Heavy radioactive fallout over the southern United States, November 1962, Journal of Geophysical Research, 70, (to be published).

U. S. Public Health Service, 1962 a: Radiation Surveillance Network, U. S. Department of Health, Education, and Welfare, May 1962.

U. S. Public Health Service, 1962 b: Pasteurized Milk Network, U. S. Department of Health, Education, and Welfare, May 1962.

A CASE STUDY OF MASS TRANSPORT FROM STRATOSPHERE
TO TROPOSPHERE, NOT ASSOCIATED WITH SURFACE FALLOUT

by

E. R. Reiter and J. D. Mahlman

ABSTRACT

On 18 and 19 April 1963 an intrusion of stratospheric air, descending into the troposphere within a stable layer, was observed east of the Rocky Mountains. No significant increases of radioactive fallout at the ground were measured in connection with this intrusion. Differences between this and earlier case studies, therefore, help to establish and confirm meteorological criteria for rapid transport of nuclear debris from the stratosphere to the low troposphere under quasi-adiabatic conditions.

I. INTRODUCTION:

In previous studies several intrusions of stratospheric air have been traced into the lower troposphere. These intrusions were observed to reach the ground within 2 or 3 days from the time they began descent from tropopause level (Reed, 1955; Danielsen, 1959 b, 1964 a, b; Staley, 1960, 1962; Reiter, 1963 a, b; Mahlman, 1964, 1965 a; Reiter and Mahlman, 1964, 1965). As the originally stratospheric air reached the ground, increases of the radioactivity level of dry air were observed when measurements were available.

Air contained within these intrusions is characterized by high values of potential vorticity

$$P = - \frac{\partial \theta}{\partial p} Q_z$$

where Q_z is the vertical component of absolute vorticity, and $-\frac{\partial \theta}{\partial p}$ is the vertical gradient of potential temperature in a pressure coordinate system. These high values of P are due to the stable stratification, to the strong cyclonic shears in the lower stratosphere north of the jet axis, and to the cyclonic streamline curvature within the forming upper troughs from which such intrusions originate.

Similar thermal stabilities and vorticity values, hence similar magnitudes of potential vorticity, are observed underneath the jet-stream core within the so-called "jet-stream front". Potential vorticities on either side of this high-tropospheric baroclinic zone are almost one order of magnitude less. The air within the jet-stream front, therefore, cannot have been produced by mixing of the two adjacent air masses, but constitutes the intrusion of stratospheric air mentioned before (Reed, 1955; Reed and Danielsen, 1959). High values of radioactivity (Staley, 1962; Danielsen, Bergman, and Paulson, 1962) and of ozone (Briggs and Roach, 1963) have actually been measured by aircraft in such

"jet-stream fronts".

Because of descending motions, air in these stable layers is quite dry. Thus, such intrusions are characterized by "motorboating" humidity reports even as they reach low-tropospheric levels (see e. g. Briggs and Roach, 1963; Mahlman, 1964, 1965 a; Reiter and Mahlman, 1964, 1965 a).

Case studies of stratospheric air intrusions, which produced dry radioactive fallout at the ground, revealed that a branch of the flow within the stable layer of high potential vorticity splits off and descends anticyclonically, while the rest of the (contaminated) stratospheric air continues to move in the middle troposphere. It appears that this splitting effect might be explained by the presence of a "cold dome" in the lower troposphere, over which a deep layer of air--including the stable layer under consideration--is forced to flow under conservation of potential vorticity (Reiter, 1965).

Reiter and Mahlman (1964, 1965) have concluded that rapid transport of stratospheric air to the ground within such high potential vorticity flow could be accomplished only if potential temperatures of this flow were approximately $295 \text{ K} < \theta < 305 \text{ K}$. The reasoning was that colder temperatures than those indicated by these limits characterize air of tropospheric origin in middle and higher latitudes. Air warmer than 305 K could be of stratospheric origin, but it could not reach the ground without diabatic effects acting over a number of days, and thus giving the contaminated stratospheric air a chance to diffuse.

Mahlman (1965 b) has derived correlations between a circulation index at the 300 mb level and radioactive fallout at the ground. The validity of such correlations hinges on the observation that occurrences of intense cyclogenetic activity at jet-stream levels control in a certain way the intrusions and descent of stratospheric air into the troposphere. Again, his calculations were corroborated by the previous case studies which traced contaminated stratospheric air to the ground.

In order to establish the validity of the limiting conditions of stratospheric flow reaching the lower troposphere which were derived from these previous studies, it was decided to make a detailed investigation of a case which, in certain ways, behaved similar to those studied previously, but which did not produce radioactive fallout. A characteristic example of stratospheric air intruding into the "jet stream front", and associated with a high-tropospheric trough development, was found on 18 and 19 April 1963 over and to the east of the Rocky Mountains.

II. THE SYNOPTIC WEATHER SITUATION:

Fig. 1 shows 250-mb isotachs and isotherms for 18 April 1963, 00 GMT and 19 April 00 GMT. A cut-off low is located over the Great Basin, with a strong jet stream flowing around its southeastern side. This jet shows a "fingery" structure which appears to be persistent with time (Reiter et al., 1965). Strong and gusty winds were observed by surface stations east of the Continental Divide. The low values of relative humidity, indicated by a large "dew point spread", suggests descending air motions along the eastern slopes of the Rocky Mountains in a strong chinook current. As may be seen from Fig. 2, this regime of dry and gusty air flow extends to considerable distance out into the Great Plains.

Fig. 3 shows a series of cross sections from Lander (LND), Wyoming, to Burrwood (BRJ), Louisiana, which lie approximately normal to the flow at jet-stream level. A stable layer is seen to emerge from the stratosphere before 18 April 00 GMT in association with the jet stream shown in Fig. 1. A potential temperature of 310 K appears to be characteristic of this layer. Strong winds and low humidities near the ground, as evident from the Denver sounding of 18 April 1962 (Fig. 4), indicate descending motions under foehn conditions in the lee of the mountains.

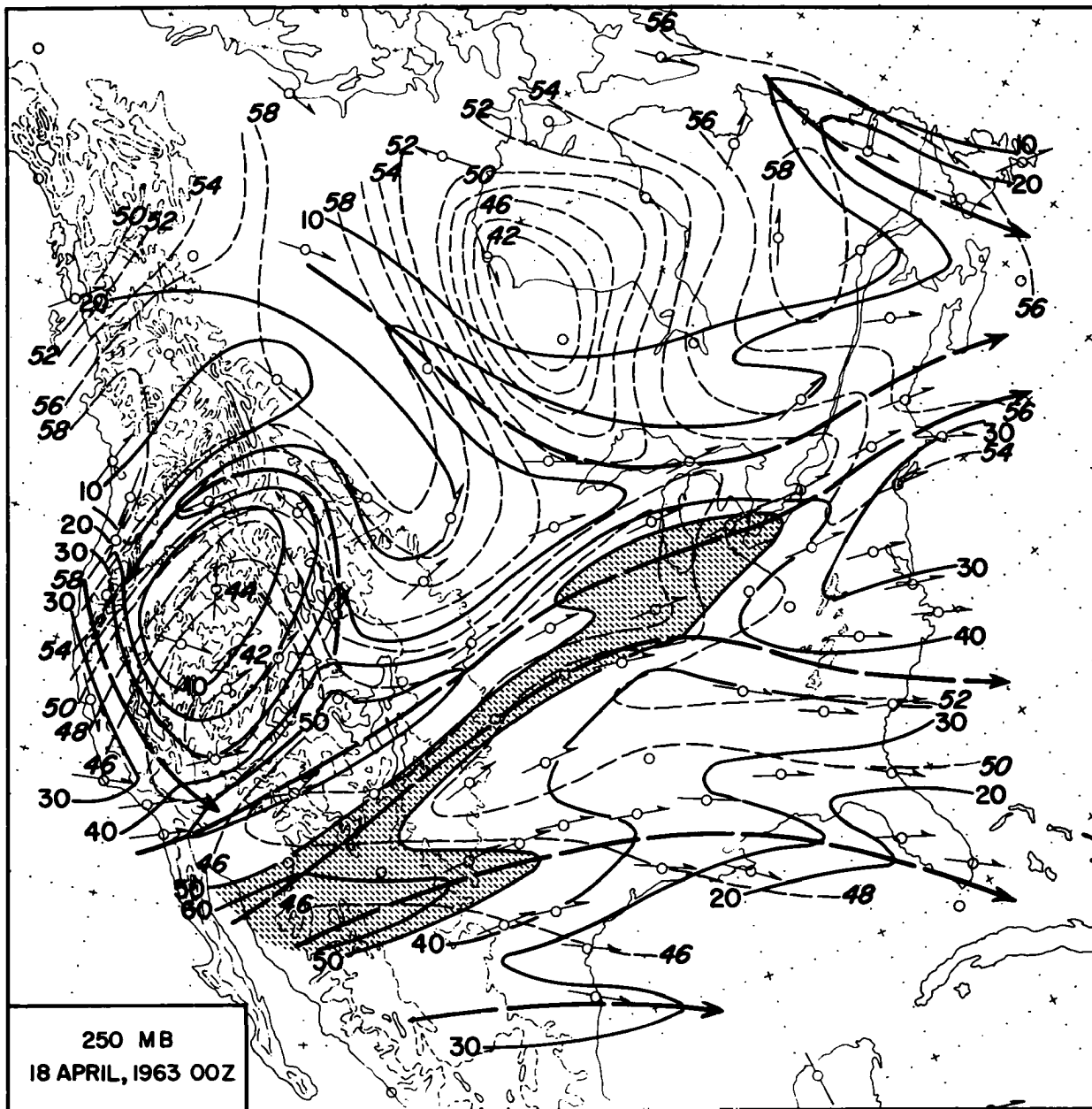


Fig. 1: 250-mb isotachs (solid lines, mps, vertical numbers, areas > 50 mps are shaded) and isotherms (thin dashed lines, °C, slanting numbers, minus signs omitted) for dates and observation times as indicated. Jet axes are marked by heavy dashed lines with arrows (after Reiter et al., 1965).

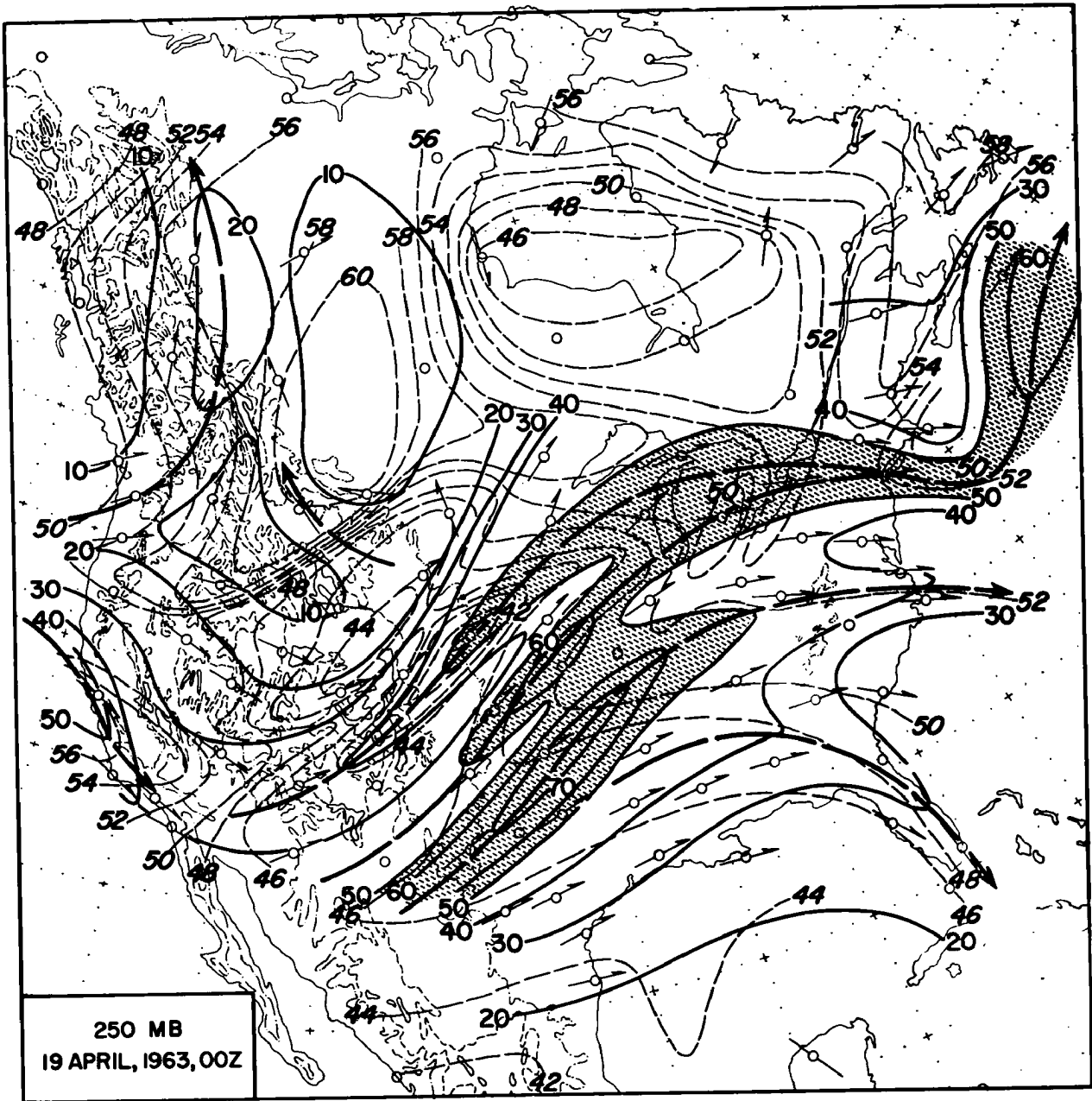


Fig. 1: Continued.

18 APRIL, 1963, 18Z

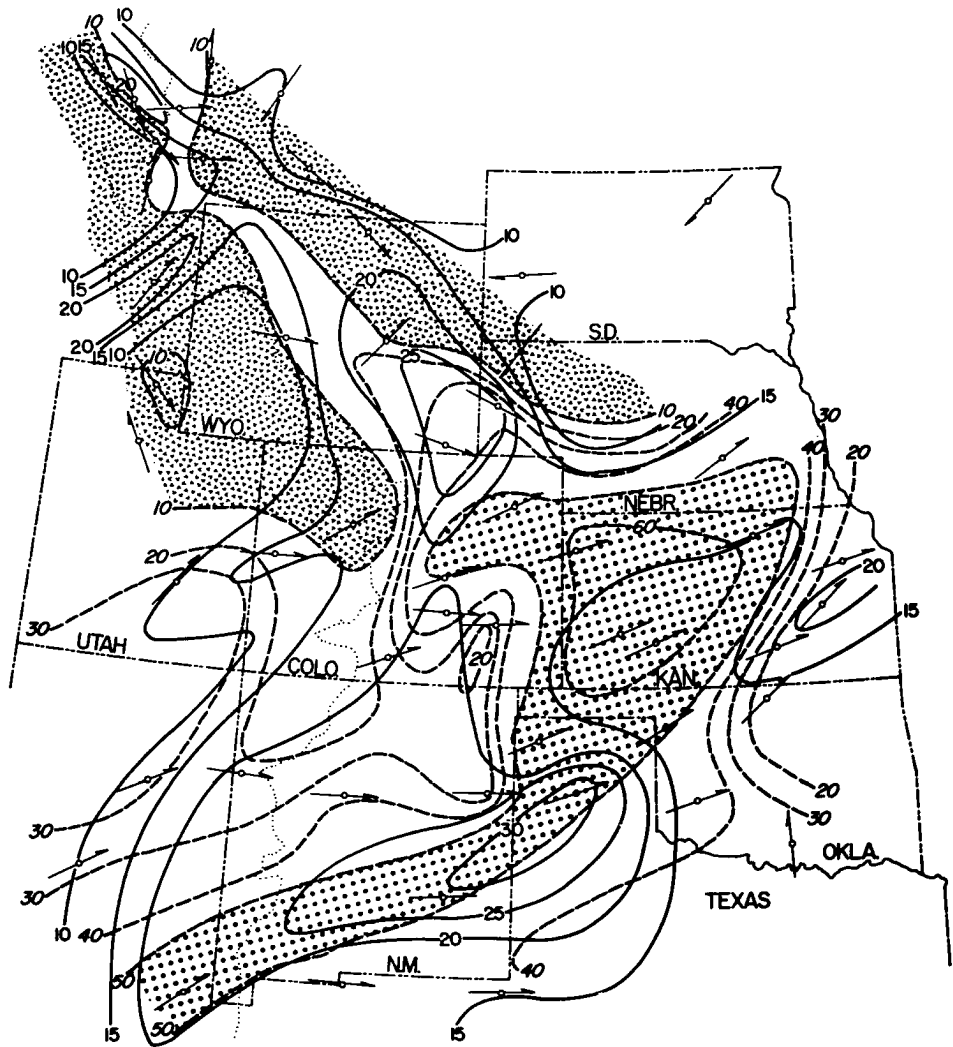


Fig. 2 a: Dew point spread (i. e., difference between dry- and wet-bulb thermometer, ° F, dashed lines, slanting numbers) and "steady" surface winds (averaged over 2 minutes at observation time, knots, solid lines, vertical numbers). Dry ($\Delta T \geq 50^\circ \text{F}$) and moist regions ($\Delta T \leq 10^\circ \text{F}$) indicated by different shading. Dates and observation times as indicated (after Reiter et al., 1965).

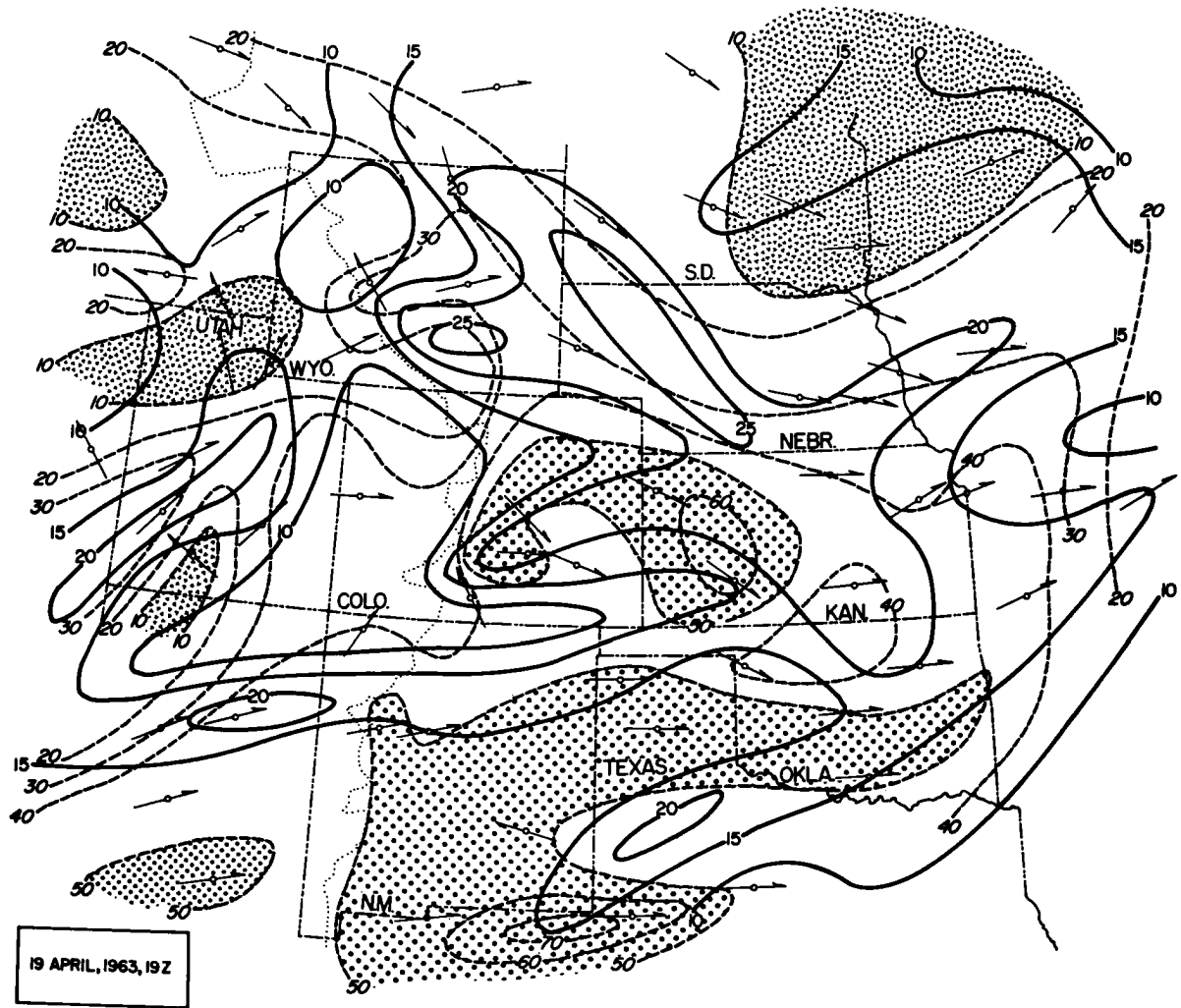


Fig. 2 a: Continued.

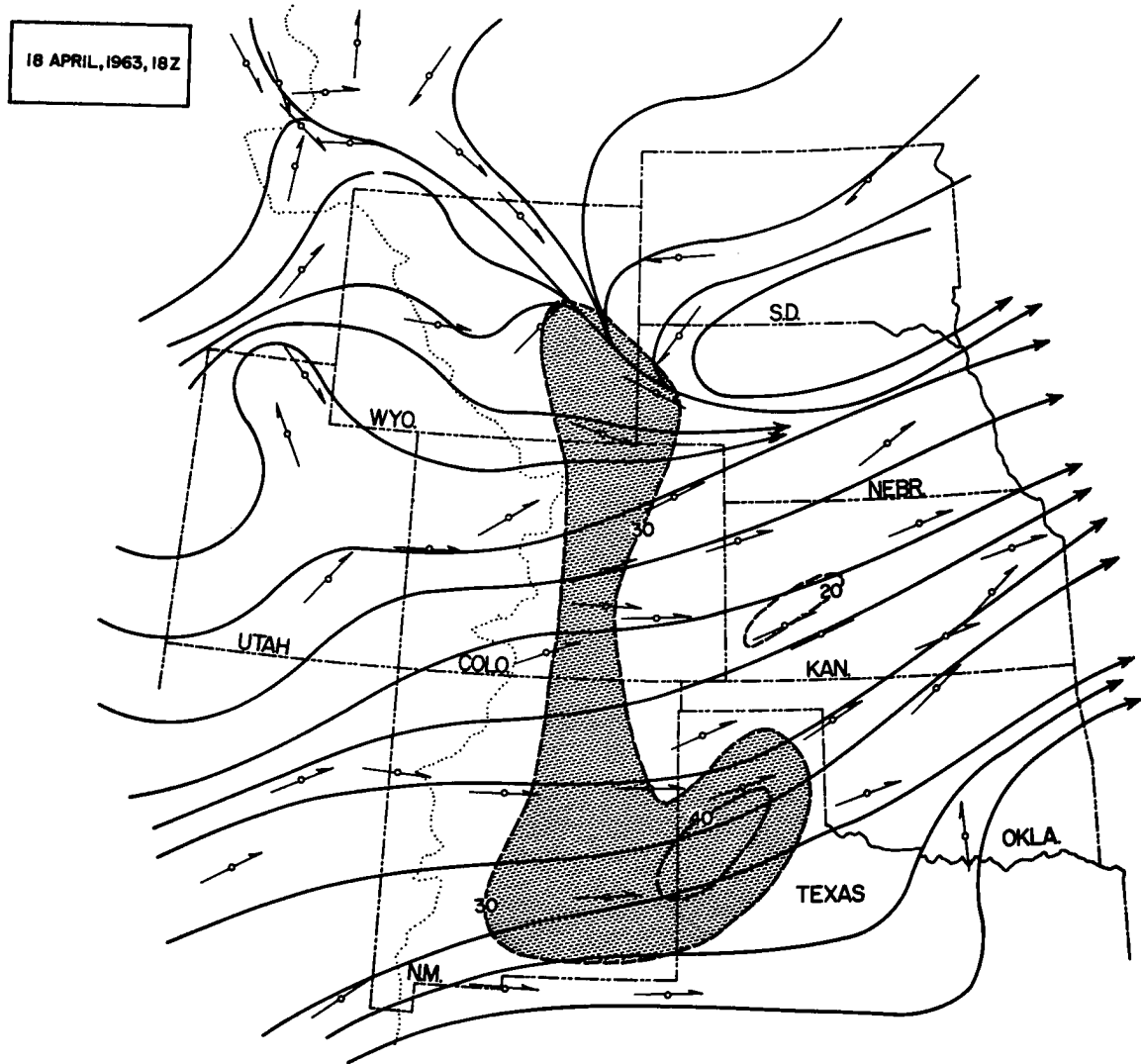


Fig. 2 b: Surface stream lines (solid lines) and peak gusts (during seven-minute interval prior to observation time, knots, dashed lines). Areas with gusts > 30 knots are shaded. Dates and observation times as indicated (after Reiter et al., 1965).

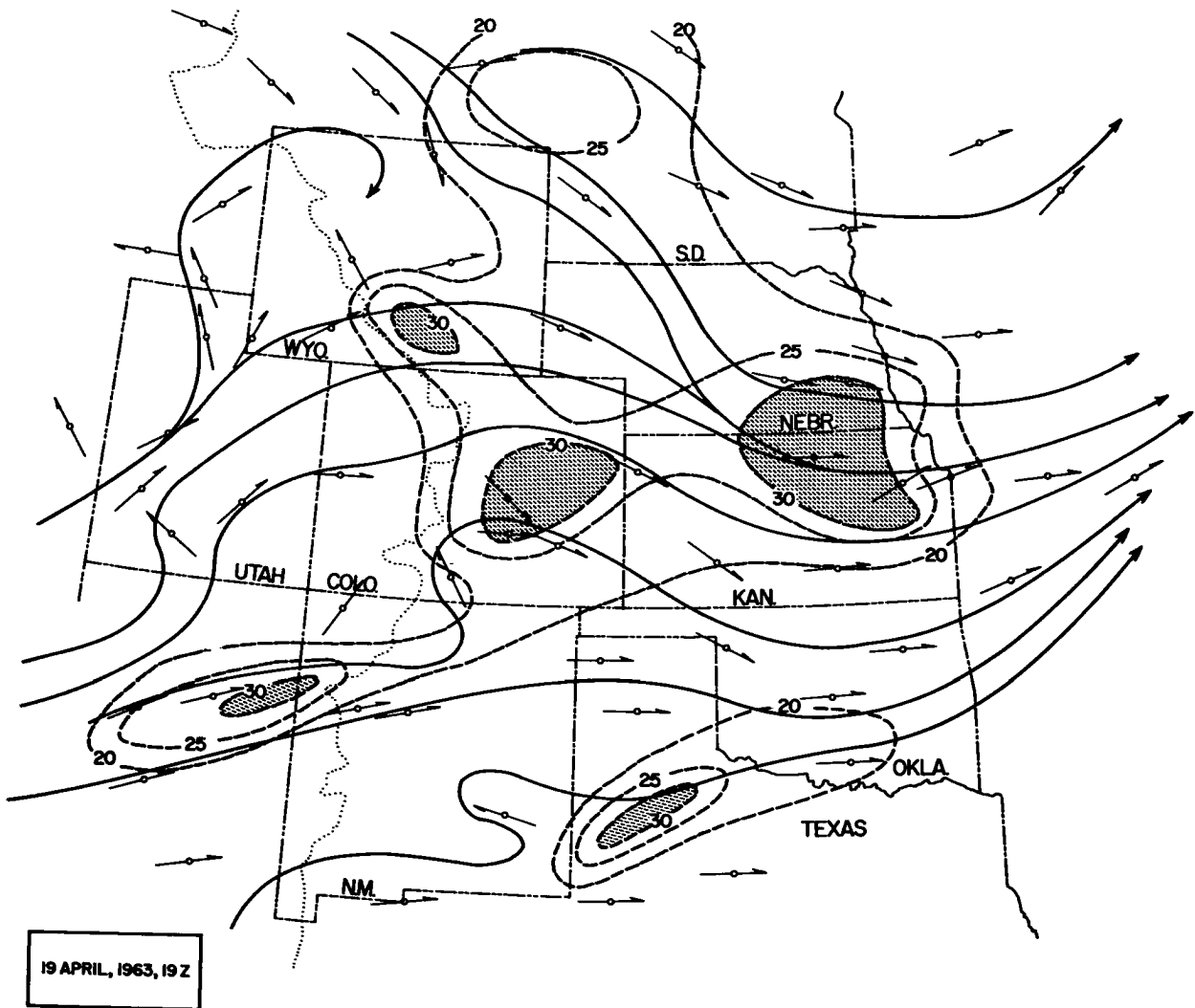


Fig. 2 b: Continued.

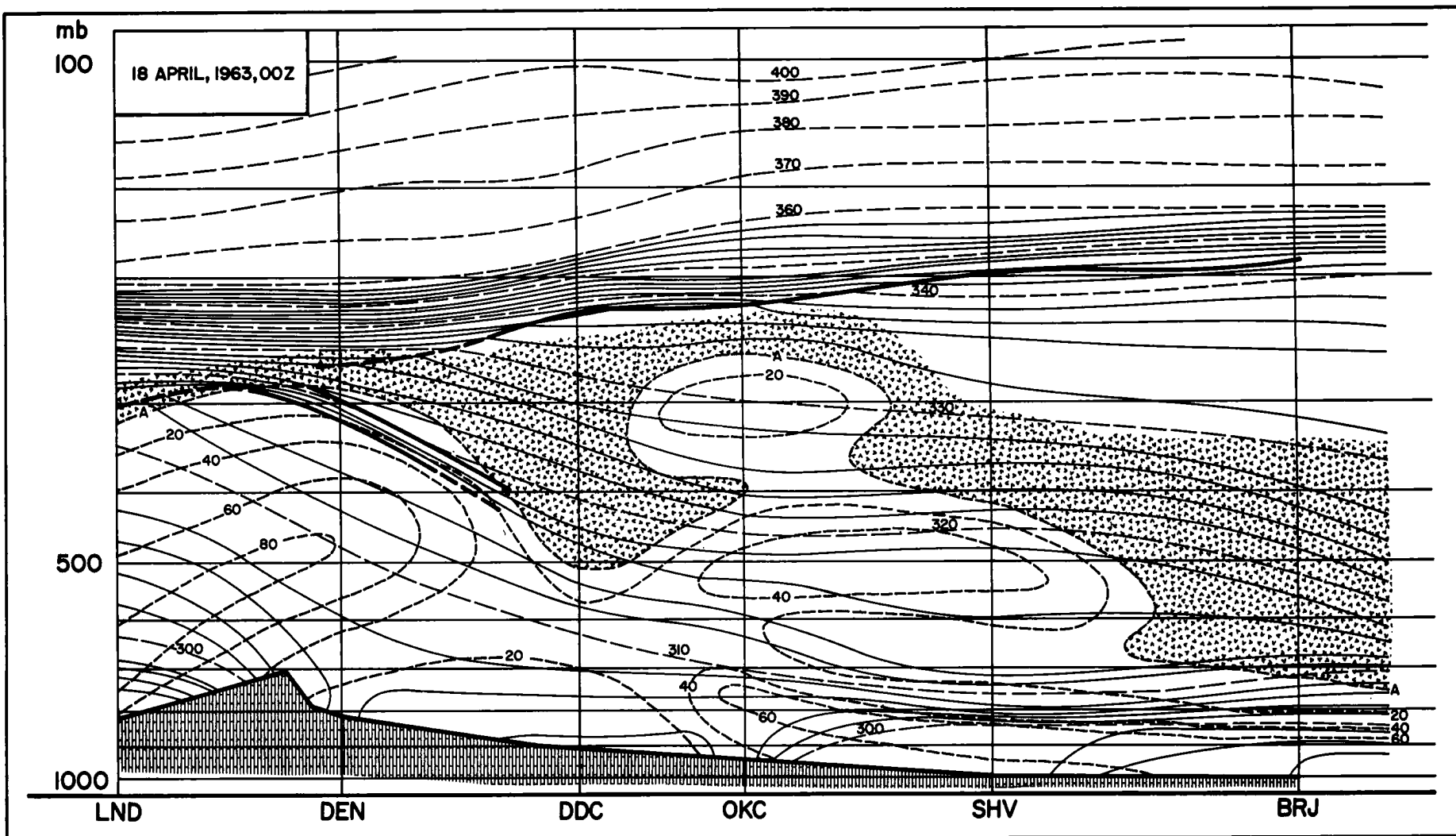


Fig. 3: Cross-sections through the atmosphere for dates and observation times as indicated. (LND = Lander, Wyoming; DEN = Denver, Colorado; DDC = Dodge City, Kansas; OKC = Oklahoma City, Oklahoma; SHV = Shreveport, Louisiana; BRJ = Burrwood, Louisiana.) Potential temperatures: $^{\circ}\text{K}$, solid and long-dashed lines; relative humidities: per cent, short-dashed lines. "A" indicates "motorboating". Stable layers and tropopause are marked by heavy dashed and solid lines. (After Reiter et al., 1965)

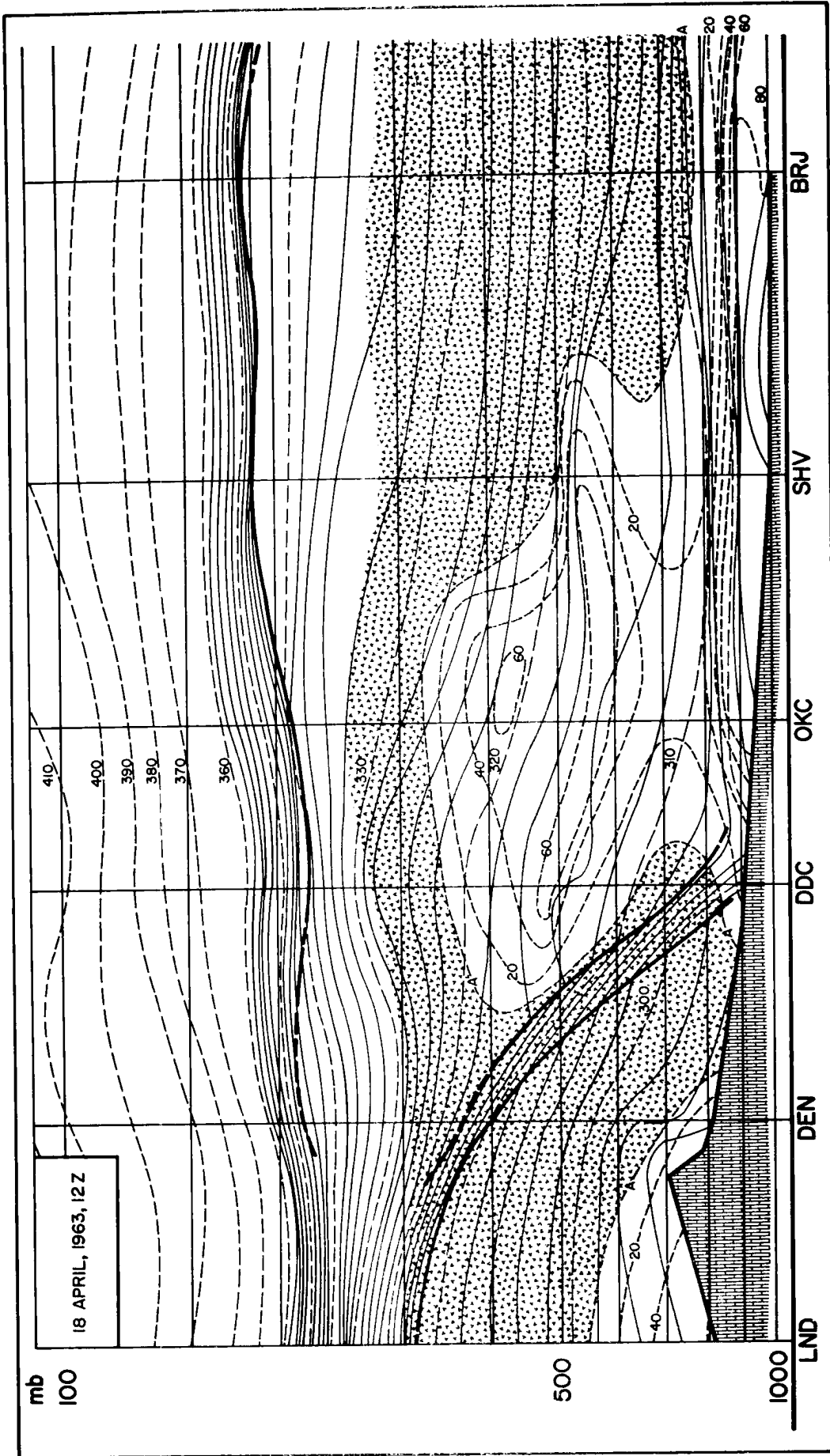


Fig. 3: Continued.

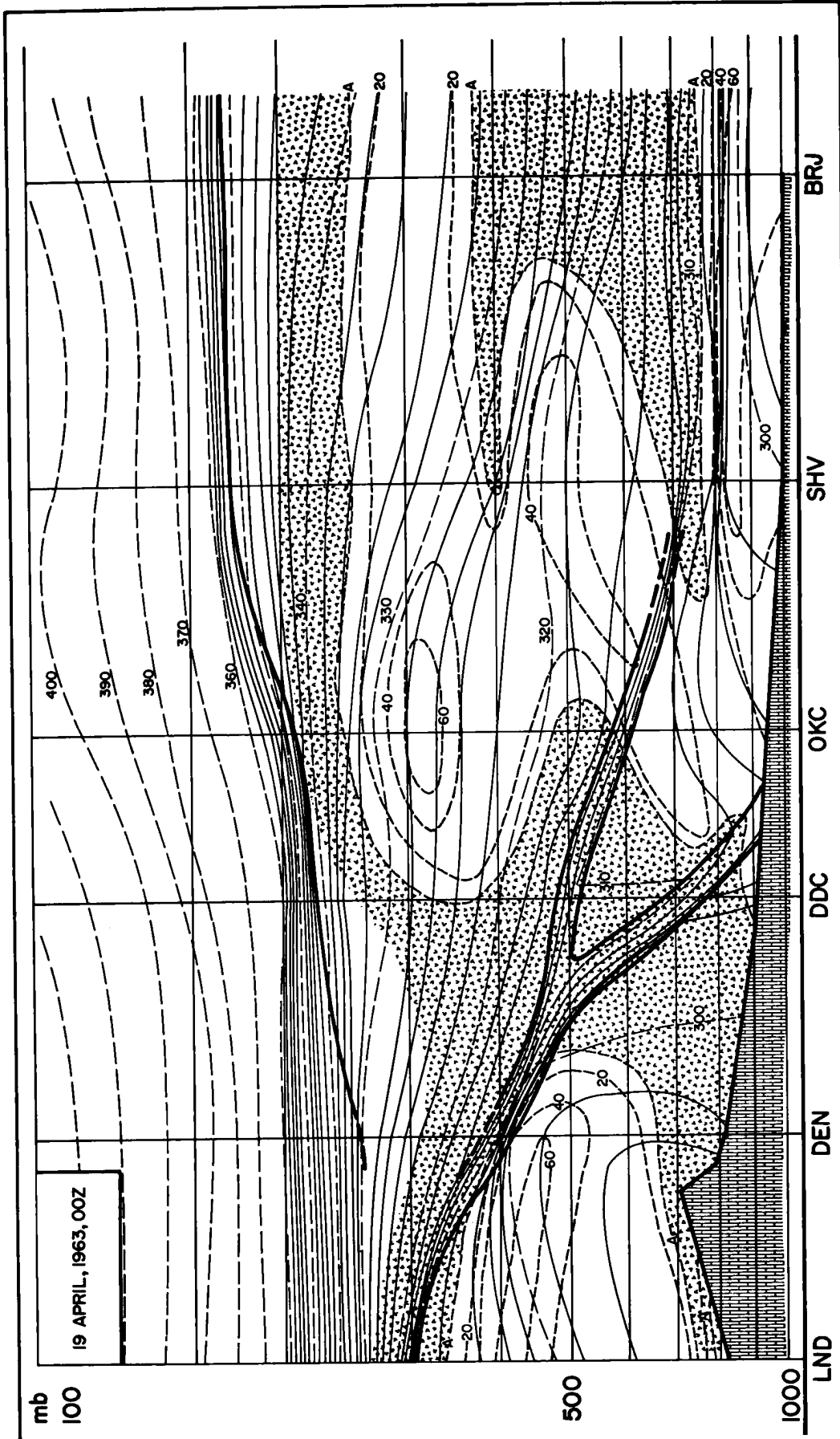


Fig. 3: Continued.

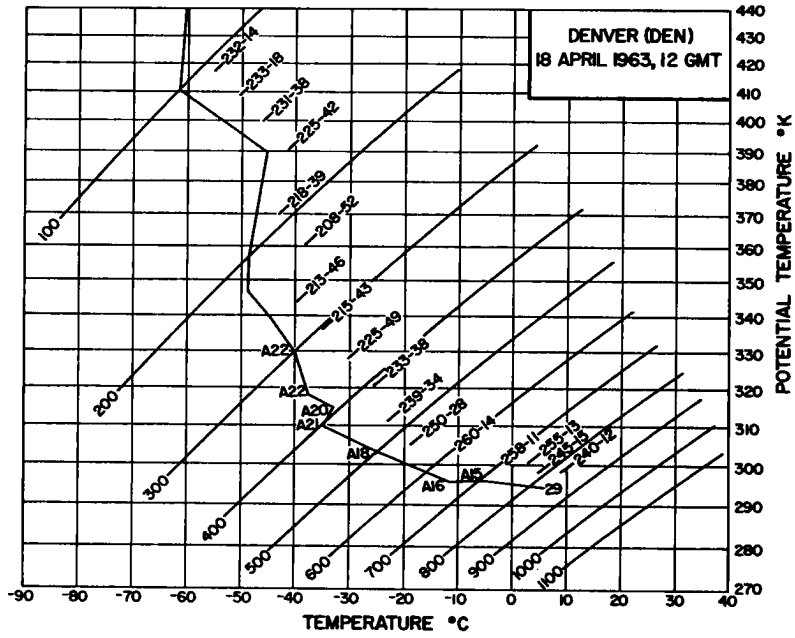


Fig. 4: Temperature sounding, plotted on tephigram, for Denver, Colorado, 18 April 1963, 12 GMT. Values for relative humidity (prefix "A" indicates "motorboating") and for wind direction and speed are entered numerically along the soundings.

Chinook conditions persist in the Denver area during the subsequent observation times, although the depth of the adiabatic mixing layer above the ground varies considerably. It appears deepest on 19 April 00 GMT when it reaches to 422 mb (Fig. 5). This level has been coded erroneously as the tropopause pressure. From Fig. 3 we see, however, that it corresponds to the bottom of the stable layer extending from the stratosphere.

With adiabatic conditions and gusty chinook flow prevailing throughout a deep layer of the troposphere, especially on 19 April 00 GMT, one might expect that radioactive debris will be "tapped" by turbulent erosion processes acting along the bottom of the stable layer. The surface radioactivity data (Fig. 6) do not reveal an increase, however. This should not be surprising, because turbulent mixing would spread the debris--if at all present--over an unusually deep layer, thus reducing any higher concentrations that may have been present in the stable layer. Furthermore, at this time, relatively high values of fallout (Fig. 6) were already present east of the Rocky Mountains. The mixing in the deep adiabatic layer, thus, would have the effect of obscuring any additional input of contaminated air.

III. STRATOSPHERIC-TROPOSPHERIC MASS TRANSPORT:

a. Vertical Splitting of the Stable Layer.

The stable layer shown in Figs. 3, 4, and 5 was well defined in its horizontal extent. Its boundaries are indicated in Figs. 7 and 8 which show isotachs and pressures respectively on the 310 K isentropic surface. Over the cut-off vortex and trough overlying the Great Basin, this isentropic surface is located in the stratosphere. Over, and to the east of, the Continental Divide this level is contained within the stable layer extending from the stratosphere.

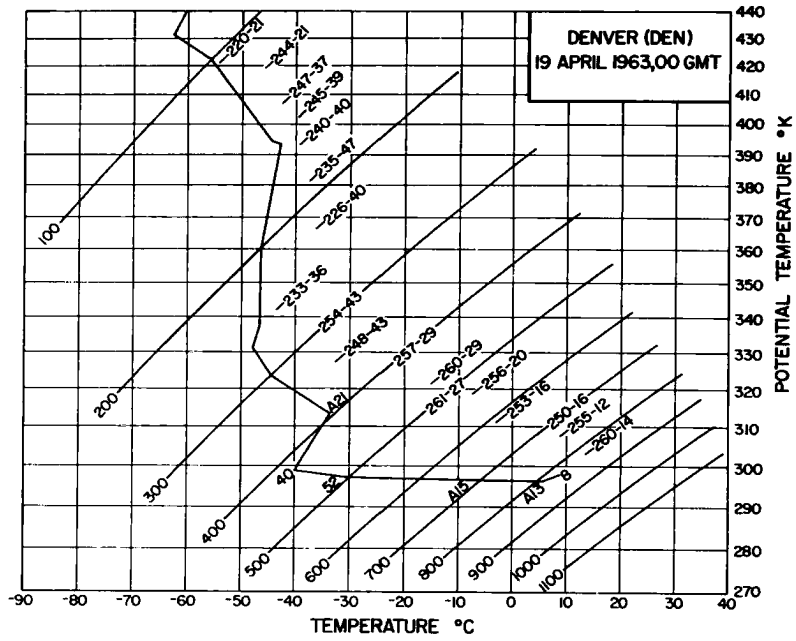


Fig. 5: Same as Fig. 4, except 19 April 1963, 00 GMT.

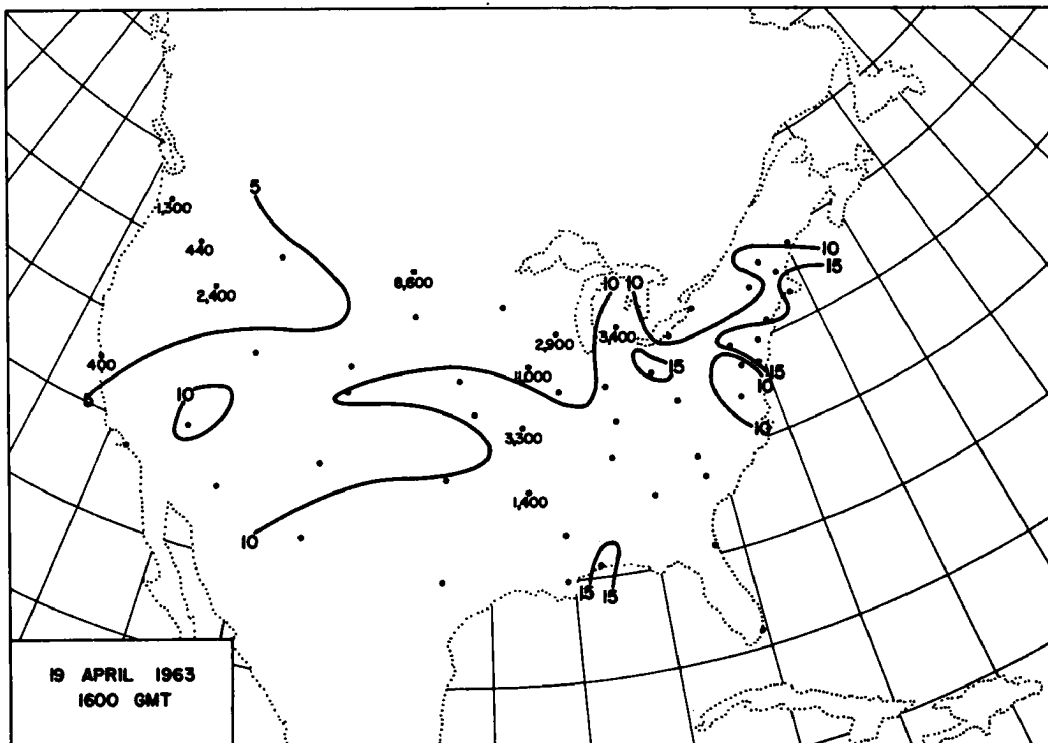


Fig. 6: Isolines of gross beta radioactivity in air (pc/m^3) and numerical values of radioactivity in precipitation (pc/liter), 19 April 1963.

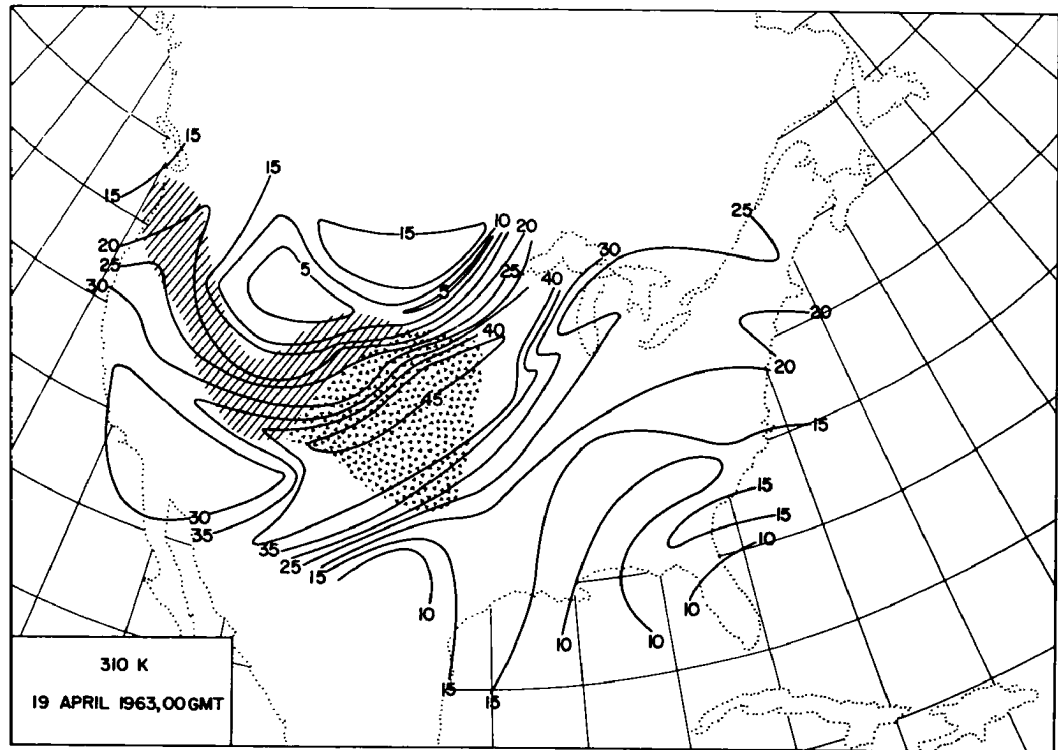


Fig. 7: Isotachs (mps) of 310 K isentropic surface, 19 April 1963, 00 GMT. Areas over which this surface is in the stratosphere indicated by diagonal hatching. Over areas where 310 K surface is within tropospheric stable layer, irregular shading has been applied.

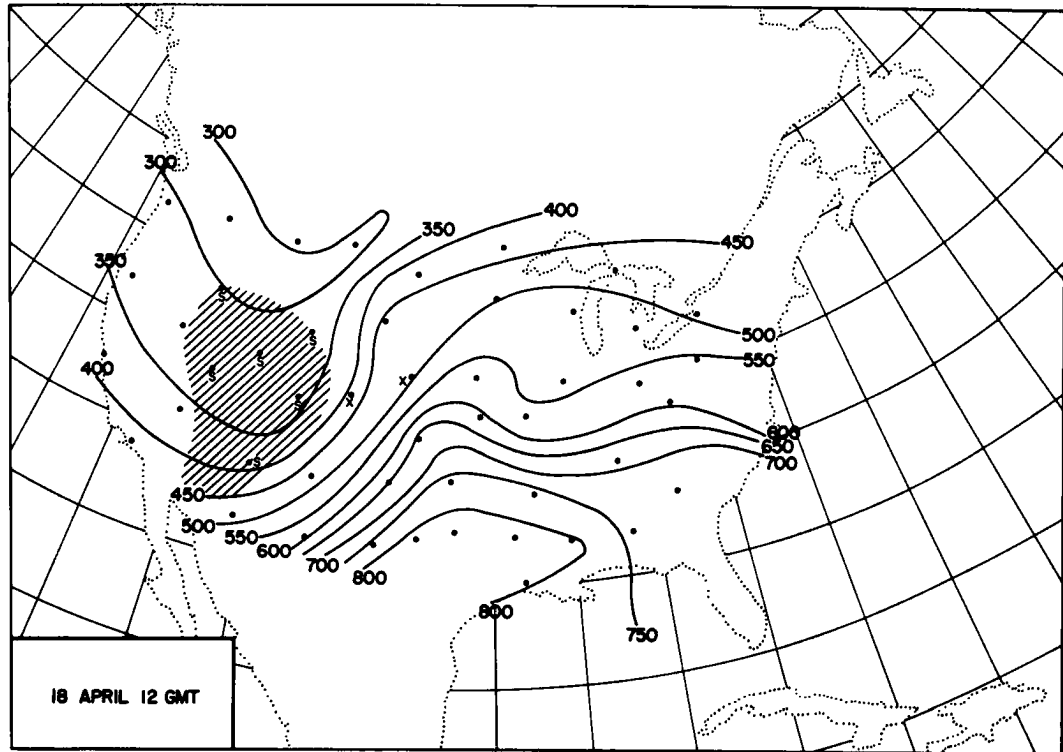


Fig. 8 a: Isobars (mb) of 310 K isentropic surface, 18 April 1963, 12 GMT. Areas over which this surface is in the stratosphere are indicated by diagonal hatching (letter "S" on station locations); over areas where 310 K surface is within tropospheric stable layer, irregular shading has been applied (letter "X" on station locations).

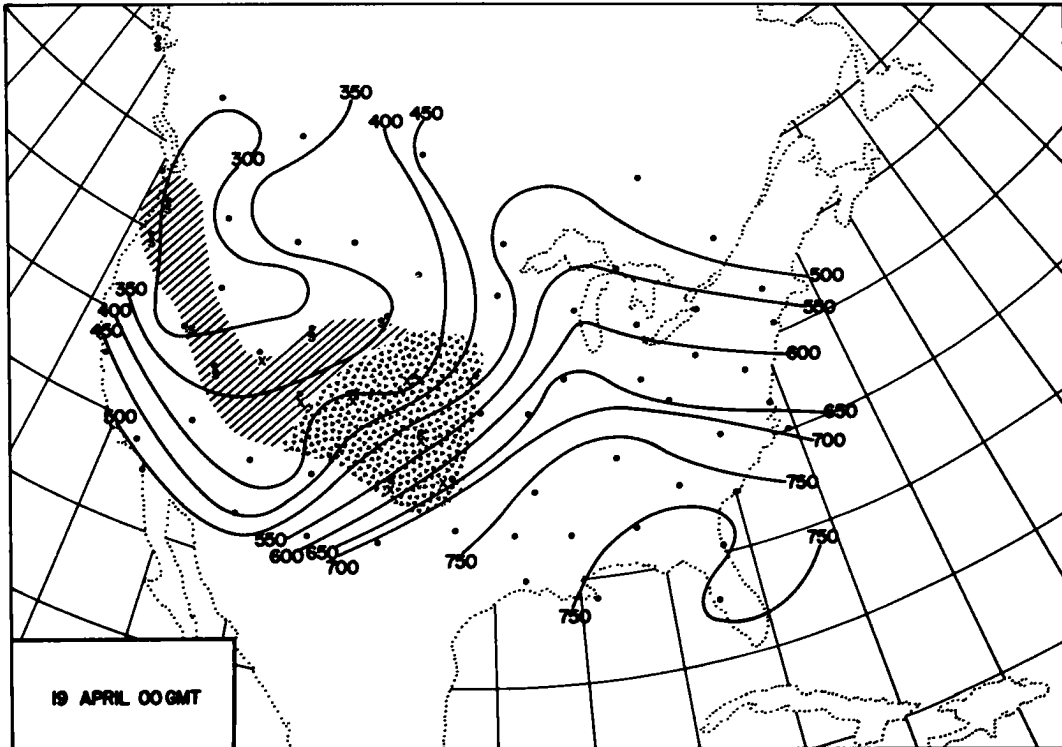


Fig. 8 b: Same as Fig. 8 a, except 19 April 1963, 00 GMT.

The Denver sounding of 19 April 00 GMT (Fig. 5) confines the stable layer between 299 and 313 K. The North Platte (LBF) sounding at the same observation time shows the stable layer between 303 and 317 K (Fig. 9). The Dodge City sounding (Fig. 9) shows two stable layers from 303 to 310.5 K, and 310.5 to 316K, with an adiabatic layer in between that extends from 700 mb to 515 mb. As may be seen from the cross-section in Fig. 3, the stable layer splits to the west of Dodge City (DDC), Kansas. The lower branch of the layer reaches the surface as a weak cold front (Fig. 10). Slightly higher fallout values observed in Lincoln, Nebraska, and Topeka, Kansas, may have been caused by this lower branch of the stable layer. No definite conclusion can be reached, however, since air samples are missing from the previous day at these stations.

Other radiosonde ascents, such as those over Topeka, Omaha, Oklahoma City, and Amarillo, do not show this split in the stable layer.

Fig. 11 shows trajectories traced backwards from 19 April 00 GMT starting within the upper stable layer, as well as within the lower one where it exists separately. Both sets of trajectories indicate that the observed stable layers constitute an intrusion of stratospheric air into the troposphere. From this the question arises as to what may have caused the vertical splitting of the stable layer.

It may be seen from Fig. 2 that relatively strong and gusty winds prevailed east of the Continental Divide, reaching relatively far out into the Great Plains. Fig. 12 shows an analysis of potential temperatures of the surface adiabatic layer on 18 April 21 GMT. Values of 308 K, and slightly larger, are observed east of the mountains in the region where a channel of dry and fast moving (chinook) air is evident from Fig. 2. This flow passes the Dodge City region. It is quite likely that this layer of adiabatic air interlocked locally with the stable layer which was advected from aloft. The energy required for doing so would be minimal and may easily be

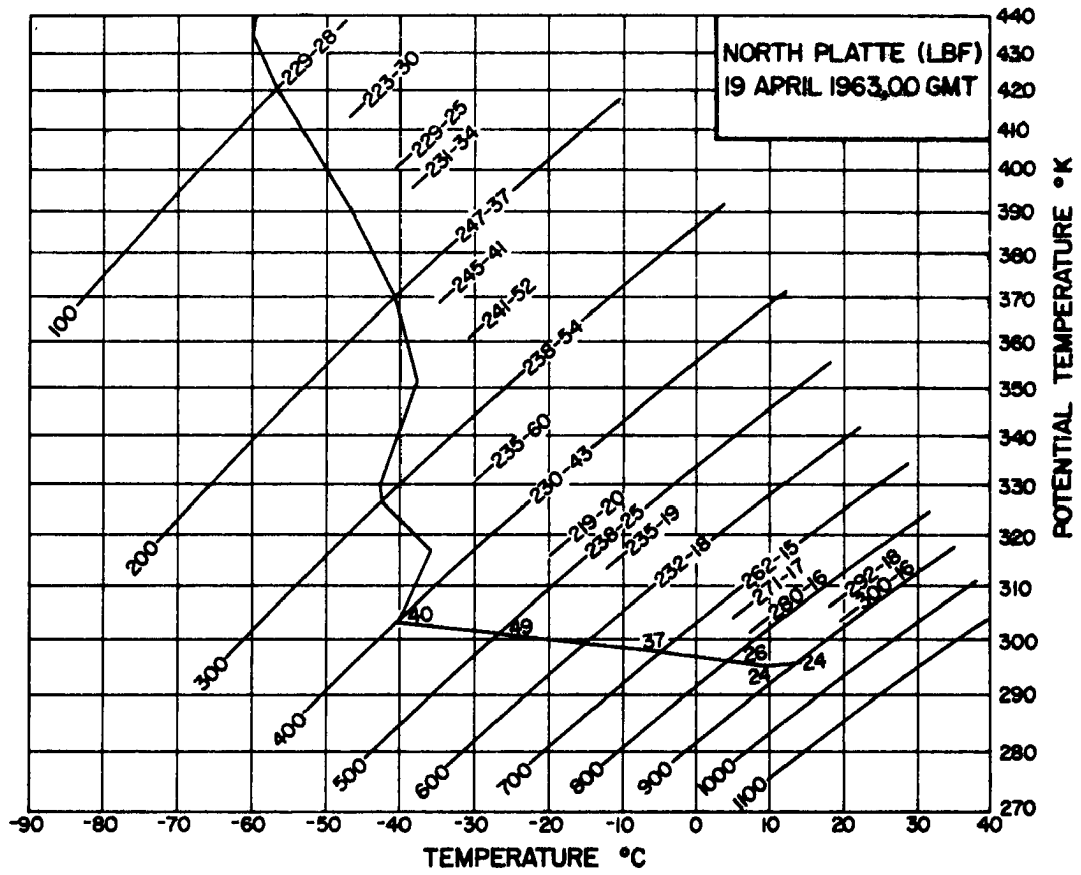


Fig. 9 a: Temperature sounding for North Platte (LBF), 19 April 1963, 00 GMT, plotted on a tephigram. Relative humidities, wind directions, and wind speeds are given numerically along the sounding. Prefix "A" indicates a "motorboating" humidity value.

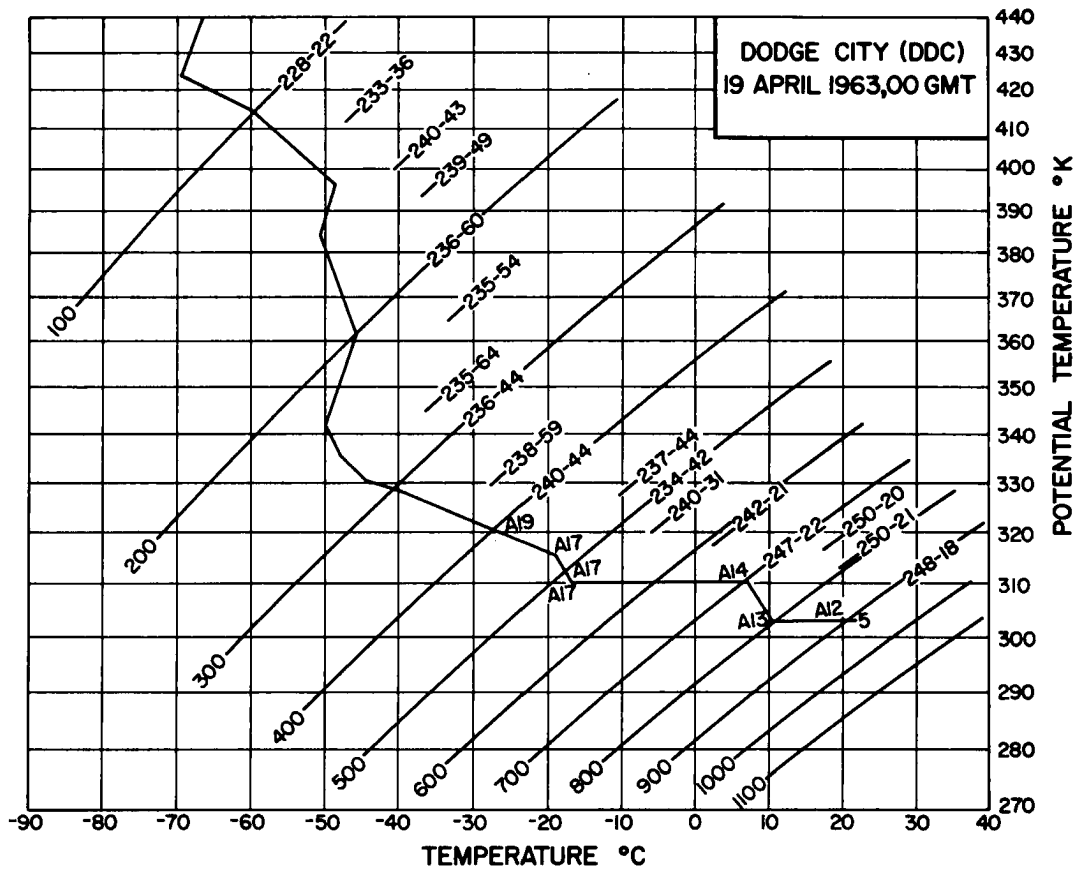


Fig. 9b: Same as Fig. 9 a except sounding for Dodge City (DDC).

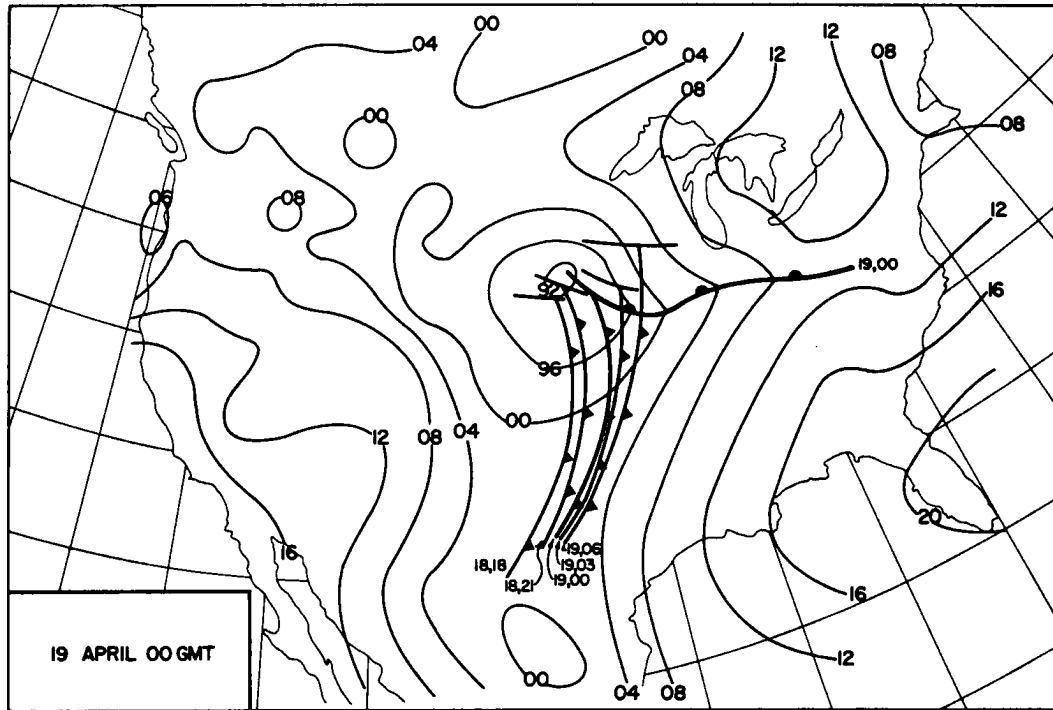


Fig. 10: Surface pressure distribution (last two digits, mb) on 19 April 1963, 00 GMT. Surface frontal positions are plotted for dates and times (GMT) as indicated.

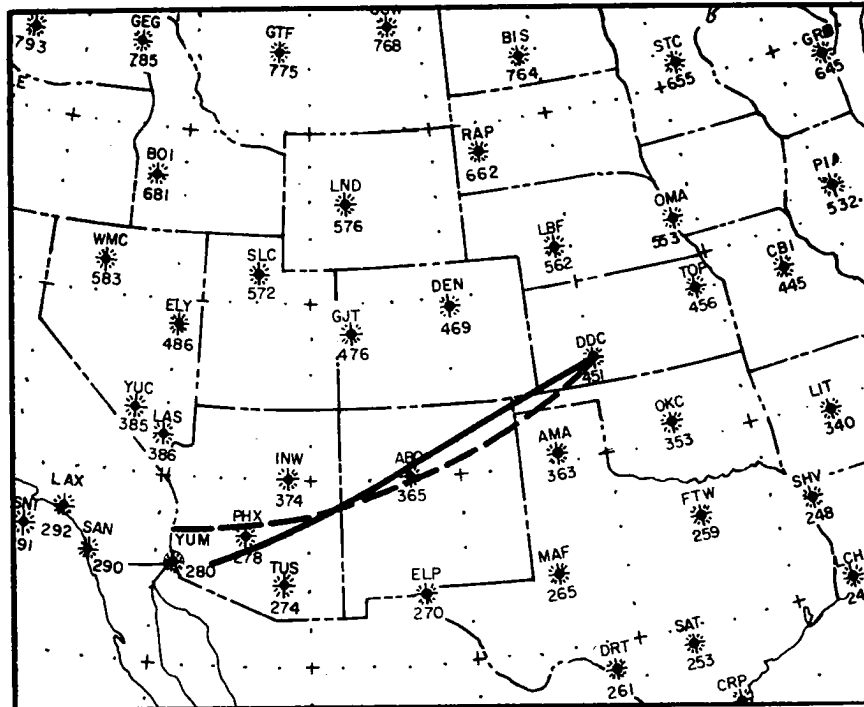


Fig. 11: 12-hour isentropic trajectories between 18 April 1963, 12 GMT and 19 April 00 GMT, ending over Dodge City (DDC). Dashed line: trajectory on 310 K isentropic surface, characteristic of upper stable layer; solid line: trajectory on 305 K isentropic surface, characteristic of lower stable layer.

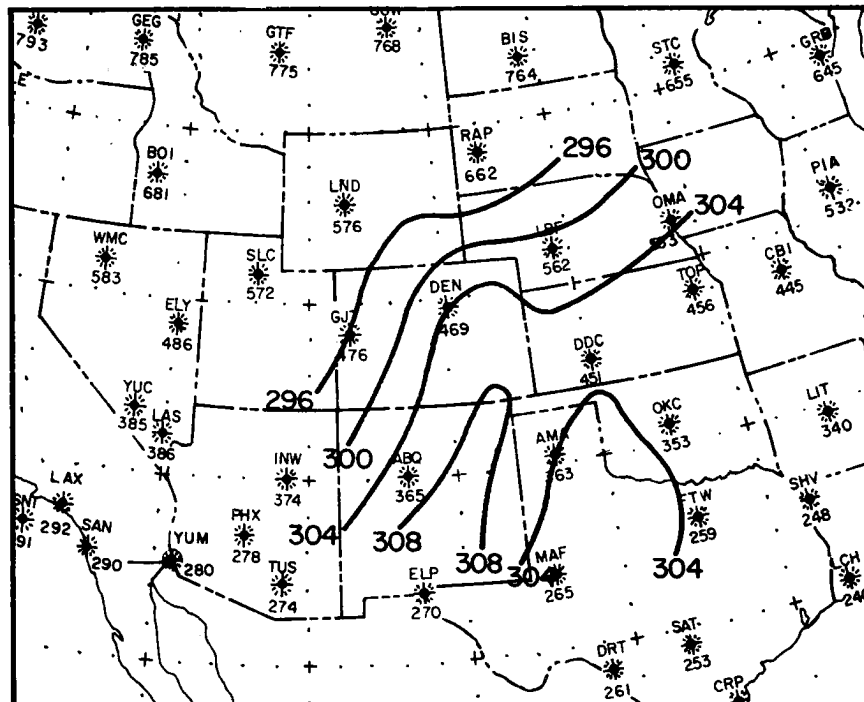


Fig. 12: Potential temperatures (degrees K) within adiabatic surface mixing layer, 18 April 1963, 21 GMT.

supplied from the flow observed in Fig. 2. Motorboating humidity values in the adiabatic layer over Dodge City (Fig. 3) tend to support this conclusion. They are well in line with the large dew point spread at the surface, shown in Fig. 2.

One might reason, therefore, that the small portion of stratospheric air, which appears to be reaching the ground near Dodge City, does so under orographic effects which seem to be reaching relatively far into the plains in the form of dry air descending along the eastern slopes of the Rocky Mountains.

b. Characteristic Features of the Observed Intrusion.

As mentioned earlier the descending stratospheric air traced in this study did not produce a surface fallout increase as noted in other cases. Other than in the meso-scale phenomenon observed near Dodge City, trajectory analysis of the case described here shows that the stratospheric intrusion remains well above the surface layer over the entire United States.

The amount of mass involved in this intrusion was calculated to be approximately 0.25×10^{12} metric tons. Of this the lower stable layer branching downward near Dodge City constituted only a small fraction--less than 10 per cent--of the total intrusion. In previous studies (Danielsen, 1959 a; Mahlman, 1964, 1965 a; Reiter and Mahlman, 1964, 1965) values of about 0.6×10^{12} metric tons were calculated for that portion of the stable layer which reached the earth's surface. This intrusion, therefore, transports less than one-half, and probably less than one-fourth, of the amount of mass from the stratosphere than was observed in the previous investigations.

The trajectories traced within this layer curve cyclonically around the low, while in previous studies of stratospheric intrusions the air motions followed anticyclonic curvature and descended quickly into the lower troposphere.

measurable increases of radioactivity of the ground, although turbulent mixing may have "tapped" the stable layer containing stratospheric air. Because of the December 1962 treaty banning atmospheric testing of nuclear devices, the stratospheric inventory of radioactive debris in April 1963 was already quite low relative to intensities in fresh injections (Mahlman, 1964, 1965 a). Furthermore, this occurred during the spring fallout maximum in 1963, thus minimizing the effect of a fresh intrusion of stratospheric air. The additional effects of turbulent mixing within a deep layer would have diluted any radioactive material that may have "eroded" into this layer from the stratospheric intrusion. Nevertheless, under different circumstances, especially with high radioactivity concentrations present in the lower stratosphere, chinook weather situations east of the Rocky Mountains may contribute towards transport of nuclear debris from the stratosphere to the ground.

REFERENCES

- Briggs, J., and W. T. Roach, 1963: Aircraft observation near jet streams, Quarterly Journal of the Royal Meteorological Society, 89, 225-247.
- Danielsen, E. F., 1959 a: Abstract--a determination of the mass transported from stratosphere to troposphere over North America during a thirty-six hour interval, Mitteilungen des Deutschen Wetterdienstes, 20 (3), 10-11.
- _____, 1959 b: The laminar structure of the atmosphere and its relation to the concept of a tropopause, Archiv für Meteorologie, Geophysik und Bioklimatologie, A 11, 293-332.
- _____, 1964 a: Radioactivity transport from stratosphere to troposphere, Mineral Industries, Pennsylvania State University, 33 (6), 1-7.
- _____, 1964 b: Project Springfield Report, Defense Atomic Support Agency, 97 pp.

Reiter, E. R. and J. D. Mahlman, 1964: Heavy radioactive fallout over the southern United States, November 1962, Technical Paper No. 58, Department of Atmospheric Science, Colorado State University, 21-49.

_____, and J. D. Mahlman, 1965: Heavy radioactive fallout over the southern United States, November 1962, Journal of Geophysical Research, 70 , (to be published).

Staley, D. O. ,1960: Evaluation of potential vorticity changes near the tropopause and the related vertical motions, vertical advection of vorticity, and the transfer of radioactive debris from stratosphere to troposphere, Journal of Meteorology, 17, 591-620.

_____, 1962: On the mechanism of mass and radioactivity transport from stratosphere to troposphere, Journal of the Atmospheric Sciences, 19, 600-608.

RELATION OF TROPOPAUSE - LEVEL INDEX CHANGES
TO RADIOACTIVE FALLOUT FLUCTUATIONS

by

J. D. Mahlman

ABSTRACT

The downward transport of radioactive debris from the stratosphere, in association with tropopause-level cyclogenesis, offers a possible physical explanation for seasonal and shorter-period fallout peaks. In order to examine these possibilities an index designed to measure the relative amount of cyclonic activity in the atmosphere is derived and then compared with seasonal and short-term variations in mean fallout intensity. It is shown from the analyses that the spring fallout peak cannot be explained adequately by an increase of cyclonic activity at this time of year. Shorter-period fallout increases, however, are statistically related to occurrences of cyclogenesis in the upper troposphere.

Seasonal stratospheric-tropospheric mass exchange calculations, determined independently from the fallout and index data, indicate a mean stratospheric residence half-time of one year. Therefore, the proposed cyclogenetic process appears to provide the predominate transport mechanism.

I. INTRODUCTION:

In nearly every year since about 1955 a spring maximum of surface radioactivity resulting from nuclear testing has appeared in the northern hemisphere (Fry, Jew, and Kuroda, 1960; Gustafson, Brar, and Kerrigan, 1961; Peirson, 1963). This spring peak is distinct from the heavy fallout that is observed to follow shortly after periods of extensive testing in the atmosphere. The fallout maxima, which occur soon after these testing periods, are in accordance with the assumption that the mean tropospheric residence time of radioactive debris is of the order of one month. Because the spring peaks often occur many months after the termination of atmospheric nuclear testing, it is necessary to postulate that the stratosphere provides the debris reservoir for these maxima (Fry, Jew, and Kuroda, 1960; Libby and Palmer, 1960).

As a result of the higher static stabilities and lack of precipitation scavenging in the stratosphere, much longer mean particle residence times would be expected in this region than in the troposphere. At present, a plausible estimate of mean residence time is five years for the tropical stratosphere and one year or less for the polar stratosphere (Libby, 1959). This corroborates the assumption that the stratosphere is the probable debris source for these seasonal oscillations in surface fallout intensity.

The problem of explaining the seasonal fallout variations now becomes one of understanding the physical processes which lead to an exchange of mass between the stratosphere and troposphere. Several authors have previously suggested that the transport of mass and radioactive debris downward from the stratosphere is associated with extratropical cyclones (Storebø, 1959; Staley, 1960, 1962, Miyake et al., 1962). Staley (1960) demonstrated that this

type of mass exchange occurs as a discrete intrusion and hence results in the transport of large amounts of contaminated stratospheric air into the troposphere. It has been further hypothesized that the sinking is associated with cyclogenetic processes at tropopause level and leads to the occurrence of individual shorter period surface fallout peaks (Danielsen, 1964 a; Mahlman, 1964 a, b). More recent research (Mahlman, 1964 c; Reiter and Mahlman, 1964) verified this hypothesis and also revealed that the sinking process is characterized by extremely strong vorticity advection and mass convergence near jet stream level.

Because of the apparent dependence of individual fallout maxima upon upper tropospheric cyclones, one may inquire whether the yearly fluctuations in mean fallout are thus a result of seasonal changes in cyclonic activity and whether or not the individual shorter-period peaks may be statistically related to upper cyclonic activity throughout the year. A way to examine this problem would be to develop an index parameter that describes the relative amount of tropopause level cyclonic activity in the middle latitudes, and then compare the seasonal variations of the index with those of the mean fallout intensity.

II. DEVELOPMENT OF THE CYCLONE INDEX:

Some of the initial attempts toward the development of a simple quantitative description of the state of atmospheric flow at a given level were made by Rossby (1939) and by Allen et al. (1940). These efforts to produce numerical indices which would reduce the complexities of atmospheric motions resulted in the well-known zonal index. Utilization of this index to describe atmospheric motions on a global basis has proved to be highly valuable in

many areas of atmospheric research. However, for certain specialized problems, this index fails to provide a sufficiently reliable description of the state of atmospheric motions (Namias, 1950; Riehl, Yeh and LaSeur, 1950). Also, if hand computation is necessary, the time required to calculate a series of zonal index values may be prohibitive.

It has been mentioned earlier that possible correlations between the formation of extratropical cyclones and increases in the surface radioactive fallout might be established by using atmospheric indices. The type of index parameter employed should provide an adequate description of the relative amount of cyclonic activity in the atmosphere. In estimating cyclonic activity, a difficulty arises in the use of the zonal index because the increasing kinetic energy of the current (produced by the release of available potential energy) tends to overshadow any decrease in index resulting from the deformation of the pressure field in a growing cyclonic disturbance. Furthermore, a strong seasonal dependence appears in the zonal index due to the decreasing meridional pressure gradient in the summer months. Because cyclonic disturbances strongly influence the direction of the upper wind field, it appears feasible that the derived index parameter be determined by the deviation of the mean wind vector from westerly flow. It also will be advantageous to restrict the index to a non-dimensional and normalized form. With such a restriction, a purely zonal westerly current will be arbitrarily defined to possess an index of 1.0 and a purely meridional current will be defined to be 0.0 (these index values may be used in the same sense as the "high" and "low index" concepts derived from the original definition of zonal index).

In order to simplify the mathematical approach as much as possible, one may assume a time-independent sinusoidal velocity field at a given height which is everywhere tangent to the isobars and which is projected on a plane earth. The normal distance (y) of a given wave from the x-axis in such a system is then given by

$$y = A \sin \frac{2 \pi x}{L} \quad (1)$$

where A is the amplitude of the wave, and L is the wave length.

The slope of the current at any point in this system is thus

$$\frac{dy}{dx} = \frac{2 \pi A}{L} \cos \frac{2 \pi x}{L} \quad (2)$$

The mean value of a function $\beta (\xi)$ over the interval (a, b) is defined to be

$$\bar{\beta} = \frac{1}{b-a} \int_a^b \beta(\xi) \cdot d\xi \quad (3)$$

By using Eqn. 3 the mean slope of the sinusoidal current over one fourth of a wavelength is given by

$$\overline{\frac{dy}{dx}} = \frac{2 \pi A}{L(nL+L/4-nL)} \int_{nL}^{nL+L/4} \cos \left(\frac{2 \pi x}{L} \right) dx \quad (4a)$$

$$\text{or } \overline{\frac{dy}{dx}} = \frac{4 A}{L} \quad (4b)$$

where $n = 1, 2, 3 \dots$. Due to the assumed symmetry of the current, by integrating over any $nL/4$ wavelengths the mean absolute value of the slope is thus

$$\overline{\left| \frac{dy}{dx} \right|} = \frac{4 A}{L} \quad (5)$$

Also, by definition,

$$\overline{\left| \frac{dy}{dx} \right|} = \tan \overline{|\alpha|} \quad (6)$$

Here, $\overline{|\alpha|}$ is defined to be the absolute value of the mean deviation from a pure west wind ($\alpha = \theta - 270^\circ$ where θ is the wind direction). By substituting Eqn. 6 into Eqn. 5 and solving for $\overline{|\alpha|}$, one obtains

$$\overline{|\alpha|} = \arctan \frac{4 A}{L} \quad (7)$$

which is an expression for the absolute value of the mean deviation from westerly flow of a sinusoidal current of arbitrary amplitude and wavelength.

How, if a cyclone index is defined in terms of the previously specified conditions for zonal ($C = 1.0$) and meridional ($C = 0.0$) flow one may write

$$C = 1 - \frac{\overline{|\alpha|}}{90^\circ} \quad (0^\circ \leq \overline{|\alpha|} \leq 90^\circ) \quad (8)$$

If this derived index is to describe adequately the state of the flow of any given current, the value of $\overline{|\alpha|}$ calculated from the given sinusoidal current must be comparable to the theoretical value obtained from Eqn. 7. The calculated values of $\overline{|\alpha|}$ were obtained from this given sinusoidal current by measuring $\overline{|\alpha|}$ at particular points along a discrete grid interval. This grid distance must necessarily be less than one-half wavelength so that a reliable sample can be obtained. The theoretical value of $\overline{|\alpha|}$ from the given sinusoidal current was then compared with the measured values of $\overline{|\alpha|}$ obtained from the same ideal current. The comparison between the measured and the theoretical values was then analyzed statistically by employing a Student's "t" test. This analysis revealed that the value of $\overline{|\alpha|}$ measured from the given sinusoidal current was significantly lower (at the 95% probability level) than its comparable theoretical value. This resulted from the bias introduced by measuring the slope of the current along the latitude

circle rather than along the wave itself. This difficulty was readily circumvented, however, because the statistical analysis also showed that the measured root-mean-square value of $\overline{|\alpha|}$, $(\overline{|\alpha|^2})^{\frac{1}{2}}$, is an excellent approximation to the theoretical value of $\overline{|\alpha|}$. Thus, one may replace $\overline{|\alpha|}$ in Eqn. 8 by $(\overline{|\alpha|^2})^{\frac{1}{2}}$ to obtain

$$C = 1 - \frac{(\overline{|\alpha|^2})^{\frac{1}{2}}}{90} \quad (9)$$

Recalling that $\alpha = \theta - 270^\circ$, Eqn. 9 may be defined in terms directly applicable to atmospheric measurement so that

$$C = 1 - \frac{1}{90} \left[\frac{\sum_{i=1}^n (\theta - 270^\circ)^2}{n} \right]^{\frac{1}{2}} \quad (10)$$

where n is the number of measurements along the chosen latitude circle. The index C is now in a form in which its measured value (computed by measuring α along a discrete grid interval) compares favorably with the theoretical value of the given ideal current. This is advantageous because a value of C can now be calculated from the data for any current, regardless of its complexity, with reasonable assurance that the calculated value agrees well with the possibly unobtainable theoretical value.

III. APPLICATION OF THE CYCLONE INDEX:

In the present study the possible correlations between the derived cyclone index C near tropopause level and fluctuations of radioactive fallout at the surface were examined. Because the peaks of radioactive debris that results from recent atmospheric tests tend to mask the fallout of older stratospheric debris, one has to investigate such correlations over a period in which no nuclear testing has taken place. Also, this chosen period must

be long enough after the cessation of nuclear testing, so that the influence of tropospheric debris is minimized.

To satisfy these restrictions, the period following the last atmospheric test in December 1962 was chosen for the analysis. This was an especially suitable period because the stratospheric debris intensity was relatively high as a result of heavy testing prior to the test ban.

Since, as noted previously, fallout maxima tend to appear in relation to tropopause-level cyclones, 300 mb was chosen as the most representative level for the calculation. Because the maximum cyclonic intensity generally occurs within the latitude band 40° to 60° N, 50° N was chosen to be an appropriate latitude for the calculation of a series of cyclone index values. Also, since the United States provides the only fallout network which gives values representative over a large area, the index was calculated between 70° W and 180° W longitude, and not around the entire hemisphere.

If Eqn. 10 is applied to the atmosphere under the previously specified conditions, a difficulty arises because the flow direction is frequently non-symmetrical with respect to a given longitude line. In theory this could be avoided by deriving the cyclone index in terms of a more complicated atmospheric current which incorporates the tilting of troughs (Machta, 1949; Arakawa, 1953). Such considerations would, however, make the derivation of C considerably more complex. These difficulties resulting from the asymmetry of the current were in part avoided by measuring a mean θ over the 10 degree latitude interval 45° to 55° N, instead of taking a point value at 50° N.

The cyclone index was calculated at 24 hour intervals for the period January 1963 to December 1964. Computational noise and the higher frequency components were filtered from the time series by using a weighted smoothing technique (Blackman and Tukey, 1958; Holloway, 1958) (Fig. 1). From independent successive calculations

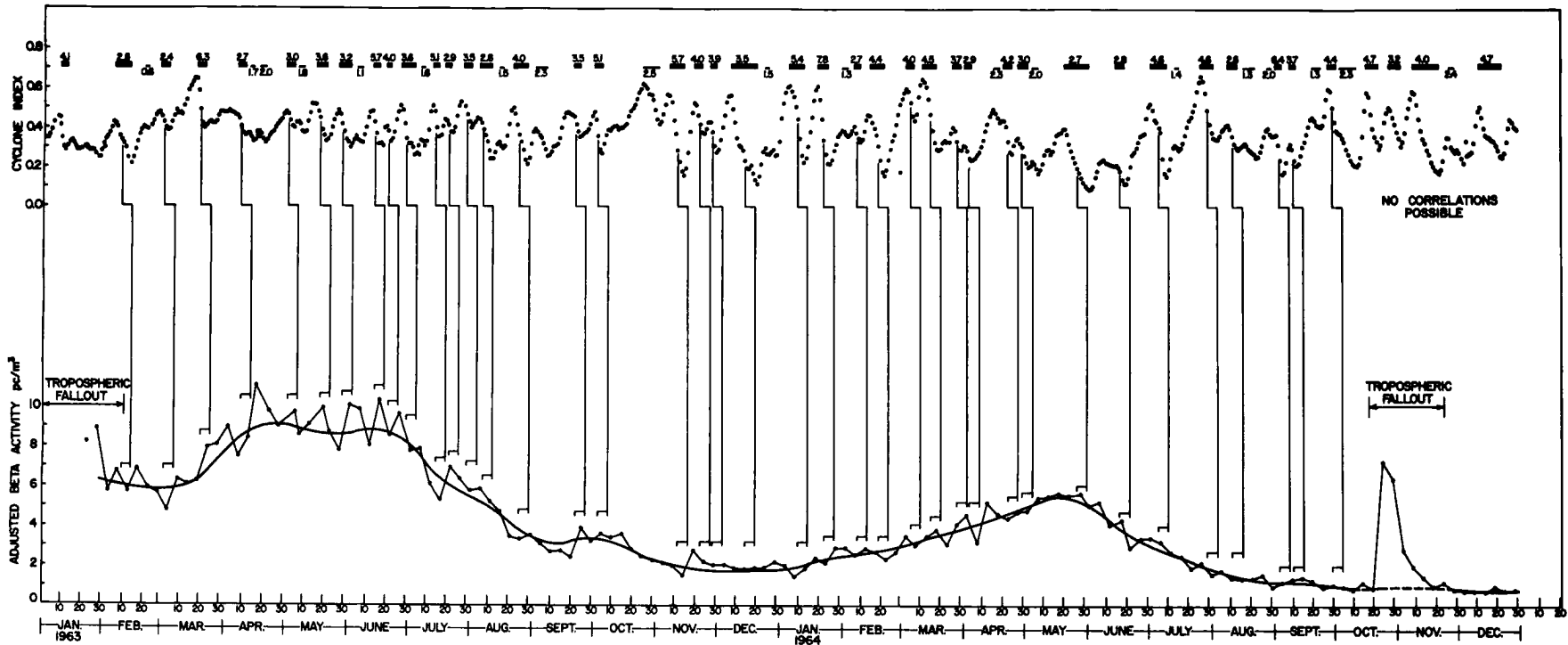


Fig. 1: Time series of comparison between cyclone index and shorter period fallout fluctuations. Upper part of diagram is smoothed cyclone index series. In the lower part: thin connected lines are five day mean age-adjusted gross beta activity; heavy smooth line gives mean monthly fallout values. Vertical lines from cyclone index show the high percentage of fallout increases within five days after rapid cyclone index decreases. Numbers across top of figure are values of $100(C_1 - C_2) / \Delta t$ computed during each cyclone index decrease. Numbers above heavy bars are greater than critical value of 2.5 and numbers below thin bars are below 2.5.

the cyclone index was seen to provide a statistically reliable indication of the relative amount of cyclonic activity in the atmosphere. The index was also checked by calculating separate time series for the first four months of the sample using the 00 GMT and 12 GMT data respectively. The major fluctuations in the two resultant smoothed time series were observed to be identical. The calculated filtered index time series for the indicated period showed a succession of index increases terminated by index drops of equal magnitude (Fig. 1).

IV. RELATION OF THE INDEX SERIES TO THE FALLOUT DISTRIBUTION:

The time distribution of age adjusted fallout in air over the United States was determined by computing area-weighted averages of gross beta activity in picocuries per cubic meter of air from the U. S. Public Health Radiation Surveillance Network Data. Two distinct scales of fallout intensity with respect to time were obtained by calculating 5-day and monthly averages of the mean area-weighted fallout intensity (Fig. 1). This figure shows that an irregular fallout fluctuation of short duration is superimposed upon the seasonal oscillation as determined from the monthly averages. Because of the large number of observations that determine these five-day means and the relatively small variance between the individual measurements, even small fluctuations of fallout intensity become statistically significant. Fig. 1 shows that a very pronounced increase in mean fallout characterized the spring of 1963, and that a spring peak also occurred in 1964. It is also evident from Fig. 1 that the effectiveness of the moratorium was essentially terminated in late October 1964 due to tropospheric debris from the first Chinese nuclear test at that time. The 1964 maximum is in agreement with the observed spring fallout peak in 1960--more than a year after the voluntary test moratorium of 1959 (Gustafson, Brar, and Kerrigan, 1961).

Since radioactive debris in the stratosphere will decrease with time as a result of natural decay, one should express fallout values in terms of intensities adjusted to an arbitrary age. This has the advantage that similar mass transport processes at different times will produce a comparable "measured" radioactive debris intensity in the troposphere. Such an adjustment may also lead to a more accurate determination of the time rate of depletion of the stratospheric-debris inventory as a result of stratospheric-tropospheric exchange mechanisms.

The rate of decay of the 1963 debris was determined by analyzing the time change of the relative contribution of each specific nuclide and taking into account the resultant change in mean half-life of the debris as time progressed (see Table 1). The debris sample was assumed to consist of two portions--an almost non-decaying part (Sr-90 and Cs-137) and a rapidly decaying part. The decay of this mixed sample was determined by assuming no decay of the long-lived portion and decay according to the mean half-life of the other part. This was done for each month so that the rate of decay of a given fallout sample could be obtained by computing the mean half-life from the available data (Fig. 2). The formula stating these physical conditions (valid for slowly decaying debris) is

$$\text{Final Intensity} = I_0 - \frac{30 I_0 (1-Z)}{hl_1 + hl_2} \quad (11)$$

or upon rearranging,

$$\text{Final Intensity} = I_0 \left[1 - \frac{30 (1-Z)}{hl_1 + hl_2} \right] \quad (12)$$

where Z is the percentage of very long-lived debris; hl_1 and hl_2 are the computed mean half-lives of the original and final samples; and I_0 is the original intensity. The measured fallout intensities were then adjusted to an age of 100 days by taking simple ratios from Fig. 2, thus yielding the age adjusted fallout intensities of Fig. 1.

Table 1: Percentage contribution of particular nuclides in total monthly radioactive debris measured in rainfall at Westwood, New Jersey. Half-life of each nuclide in days is given in parentheses.

	PERCENTAGE CONTRIBUTION OF NUCLIDE					
	Sr - 90 (10, 120d)	Sr - 89 (50.5d)	Ce - 144 (285d)	Zr - 95 (65.0d)	Cs - 137 (11, 140d)	Ce - 141 (33.1d)
January 1963	0.9%	26.2%	21.5%	44.8%	1.4%	5.1%
February	1.2	23.8	34.2	34.2	1.6	5.0
March	1.6	18.0	36.8	30.8	2.3	10.7
April	2.0	15.2	49.7	25.8	2.8	4.4
May	2.2	11.4	44.7	28.2	3.2	10.2
June	2.8	10.1	51.6	26.2	4.1	5.0
July	4.0	9.6	55.6	25.6	5.2	
August	3.0	5.5	65.2	20.0	6.4	
September	3.9	4.9	69.4	15.4	6.4	
October	3.9	3.9	72.6	13.2	6.4	
November	3.5	2.1	75.3	12.3	6.8	
December	3.8	1.3	78.8	11.8	4.3	
January 1964	3.8	0.9	80.9	7.1	7.3	

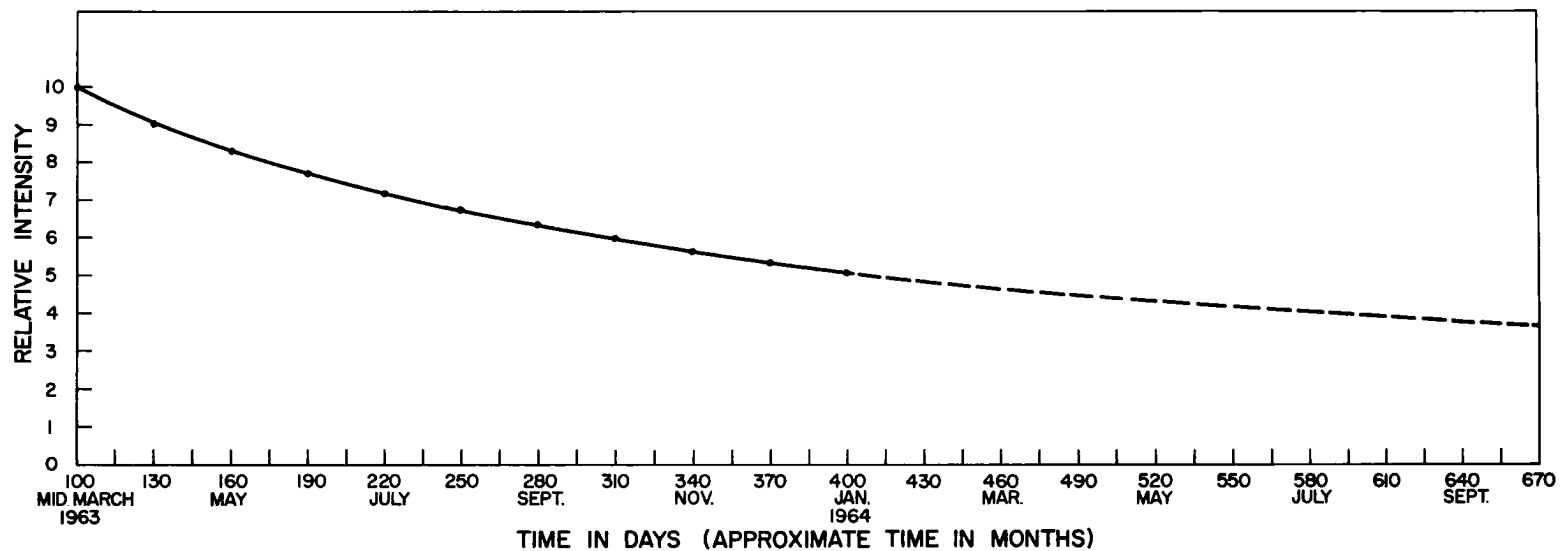


Fig. 2: Natural decay curve for a mixed debris sample computed from relative intensities in Table 1. Source intensity at time 100 days (mid-March 1963) is assumed to be 10 picocuries per cubic meter. Abscissa is in days with the approximate time in months. Black dots represent measured decay; dashed line is extrapolated decay curve.

A comparison of the index time series with that of the mean age-adjusted monthly fallout of Fig. 1 was then attempted. This analysis revealed that no significant relation appeared to exist between these two quantities. Although there were general index breakdowns preceding the April 1963 and May 1964 fallout peaks seen in Fig. 1, equally large break-downs at other times did not produce similar trends in mean fallout distribution. It thus appears that a simple causal relationship cannot be established between the seasonal changes of the index and the spring fallout maximum.

An attempt was then made to construct a comparison between the cyclone index and the mean age-adjusted five day fallout (Fig. 1). In this case a certain relationship between the two time series was noted. Fig. 1 suggests that the shorter period fallout fluctuations--superimposed upon the mean monthly curve--are possibly related to rapid decreases of the cyclone index. It is qualitatively evident from Fig. 1 that a high percentage of fallout increases occur within five days after the center point of the index decrease. Because a fallout increase did not occur within five days after all observed decreases in cyclone index, an attempt was made to differentiate between index decreases with and without subsequent fallout increases. It was determined empirically that the parameter $100 (C_1 - C_2) / \Delta t$ provided a probable method for separating the index decreases associated with fallout from the others (C_1 and C_2 are the initial and final values of cyclone index over the period of decrease and Δt is the time in days over which the decrease occurred) (see Table 2). It was hypothesized from the data given in Table 2 that any value of $100 (C_1 - C_2) / \Delta t$ greater than 2.5 would most likely produce an increase of surface fallout larger than the mean seasonal value within five days after the center point of the index decrease.

Table 2a: Values of $100 (C_1 - C_2) / \Delta t$ computed from index drops in Fig. 1. Calculated values are arranged in chronological sequence. The word "fallout" signifies that a fallout increase occurred within 5 days after the index decrease and a "none" denotes that no subsequent increase was observed.

Dates of Index Drop	$100 (C_1 - C_2) / \Delta t$	Dates of Index Drop	$100 (C_1 - C_2) / \Delta t$
1963 Feb. 5-13	2.6 Fallout	1963 Nov. 27-30	3.9 Fallout
Feb. 20-22	0.6 None	Dec. 7-20	3.5 Fallout
Feb. 28-Mar. 4	2.4 Fallout	1964 Jan. 5-12	5.4 Fallout
Mar. 18-22	6.3 Fallout	Jan. 19-24	7.8 Fallout
Apr. 7-10	2.7 Fallout	Jan. 31-Feb. 3	1.3 None
Apr. 13-15	1.7 None	Feb. 6-9	2.7 Fallout
Apr. 18-21	2.0 None	Feb. 14-21	4.4 Fallout
May 1-5	3.0 Fallout	Mar. 3-7	4.0 Fallout
May 7-10	1.8 Fallout	Mar. 11-19	4.5 Fallout
May 16-21	3.6 Fallout	Mar. 26-29	3.7 Fallout
May 27-June 1	3.2 Fallout	Mar. 31-Apr. 4	2.9 Fallout
June 5-8	1.1 None	Apr. 15-18	2.3 None
June 13-16	5.7 Fallout	Apr. 20-24	4.2 Fallout
June 20-22	4.0 Fallout	Apr. 27-May 2	3.0 Fallout
June 27-July 4	3.6 Fallout	May 4-7	2.0 Fallout
July 7-9	1.6 None	May 27-June 1	2.7 Fallout
July 13-16	5.1 Fallout	June 15-18	2.8 Fallout
July 19-22	2.9 Fallout	July 1-9	4.6 Fallout
July 28-Aug. 1	3.5 Fallout	July 13-15	1.4 None
Aug. 4-11	2.8 None	July 26-Aug. 1	4.6 Fallout
Aug. 15-17	1.5 None	Aug. 8-13	2.6 Fallout
Aug. 22-29	4.0 Fallout	Aug. 16-22	1.3 Fallout
Sept. 2-8	2.3 None	Aug. 28-30	2.0 None
Sept. 20-24	3.5 Fallout	Sept. 1-4	6.4 Fallout
Oct. 1-5	5.1 Fallout	Sept. 8-11	3.7 Fallout
Oct. 25-Nov. 2	2.5 Fallout	Sept. 19-23	1.3 None
Nov. 7-14	5.7 Fallout	Sept. 28-Oct. 10	3.8 Fallout
Nov. 19-24	4.0 Fallout		

Table 2b: Values of $100 (C_1 - C_2) / \Delta t$ computed from index drops in Fig. 1. Calculated values are arranged in ascending order of $100 (C_1 - C_2) / \Delta t$. The word "fallout" signifies that a fallout increase occurred within 5 days after the index decrease and a "none" denotes that no subsequent increase was observed.

Value of $100 (C_1 - C_2) / \Delta t$	Fallout Occurrence	Value of $100 (C_1 - C_2) / \Delta t$	Fallout Occurrence
0.6	None	3.0	Fallout
1.1	None	3.2	Fallout
1.3	None	3.5	Fallout
1.3	None	3.5	Fallout
1.3	Fallout	3.5	Fallout
1.4	None	3.6	Fallout
1.5	None	3.6	Fallout
1.6	None	3.7	Fallout
1.7	None	3.7	Fallout
1.8	None	3.9	Fallout
2.0	None	4.0	Fallout
2.0	None	4.0	Fallout
2.0	Fallout	4.0	Fallout
2.3	None	4.0	Fallout
2.3	None	4.2	Fallout
2.4	Fallout	4.4	Fallout
2.5	None	4.5	Fallout
2.6	Fallout	4.6	Fallout
2.6	Fallout	4.6	Fallout
2.7	Fallout	5.1	Fallout
2.7	Fallout	5.1	Fallout
2.7	Fallout	5.4	Fallout
2.8	Fallout	5.7	Fallout
2.8	Fallout	5.7	Fallout
2.9	Fallout	6.3	Fallout
2.9	Fallout	6.4	Fallout
3.0	Fallout	7.8	Fallout
3.0	Fallout		

The hypothesis that short term fallout increases are statistically related to discrete decreases in the cyclone index, was examined by a test known as the "superposed epoch method" (Panofsky and Brier, 1958). To test the reality of this hypothesis, the (+ or -) sign of the change in fallout was tabulated as a function of lag distance in days from the center point of a critical $(100 (C_1 - C_2) / \Delta t > 2.5)$ decrease in the cyclone index. This was done for 32 occurrences of $100 (C_1 - C_2) / \Delta t > 2.5$ and is given in Fig. 3 in terms of the sum of the deviation of fallout increases from an even distribution of plus and minus values. Fig. 3 shows a marked tendency for a peak of plus values (fallout increases) to occur 4 days after the center point (lag = 0 days) in the index decrease. This is compatible with the physical hypothesis that fallout increases are controlled by cyclogenetic processes at tropopause level. It is also evident from the figure that a pronounced period of fallout decrease occurs about 14-18 days after $t = 0$. The noted decreases of fallout intensity are also consistent with this model because of the quasi-periodic nature of the index changes --evident from the cyclone index time series given in Fig. 1.

The statistical reality of this observation was tested by computing linear correlation coefficients (r) between equal samples from the 32 values of $100 (C_1 - C_2) / \Delta t > 2.5$ as a function of lag from 0 to 18 days. To do this the 32 values were divided into two samples of 16 each. The summation of positive values of fallout change from each sample of 16 was then noted for each day from $t = 0$ -18 days. The cross correlation between these two samples of 16 was then computed by pairing the sum of the positive values of fallout change from the two samples for each day from 0-18 days.

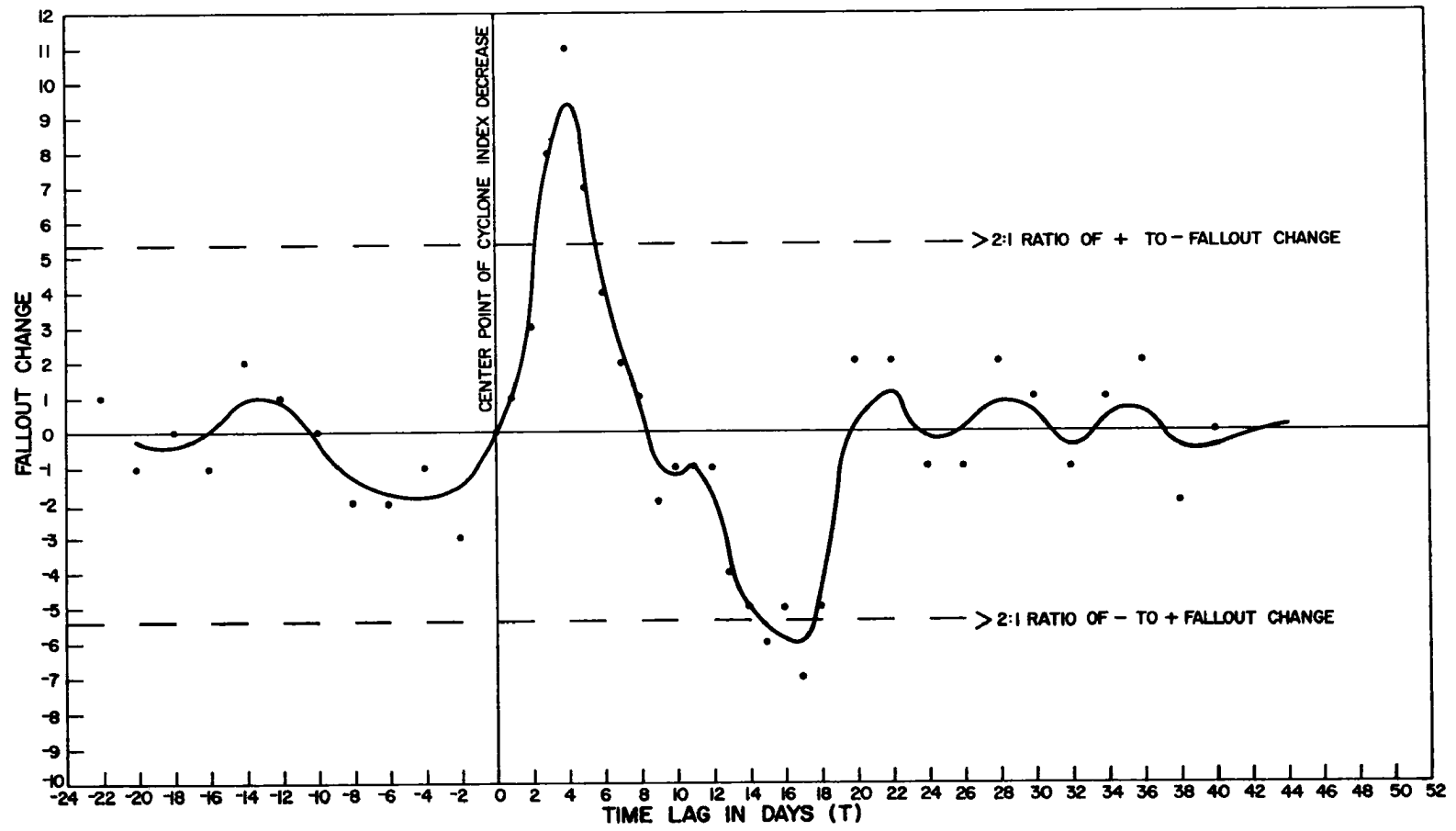


Fig. 3: Time distribution of excess of positive values of fallout change from an even distribution of plus and minus values from sample of 32 occurrences of $100 (C_1 - C_2) / \Delta t > 2.5$ taken from Fig. 1. Time = 0 days was taken to be the center point of the critical cyclone index decreases. Solid line represents smoothing of points by 1-2-1 weighting method.

By choosing samples randomly from the 32 values of $100 (C_1 - C_2) / \Delta t > 2.5$, values of r were obtained by the above procedure. This was repeated five times to give the values

$$r = + 0.695$$

$$r = + 0.545$$

$$r = + 0.551$$

$$r = + 0.686$$

$$r = + 0.583$$

$$r = + 0.61$$

In addition to this, correlations were calculated between the first and last 16 values to determine whether or not the process was in any way different as the debris became progressively more long lived. The value of r from this type of pairing was calculated to be + 0.531. Furthermore, to possibly detect seasonal effects, a value of r was computed by pairing critical occurrences of $100 (C_1 - C_2) / \Delta t$ between October 15-April 15 against those between April 15-October 15. In this case r was found to be + 0.626.

Because of the obvious non-independent nature of the data (see Fig. 1), comparison of these values of r with those given in critical correlation coefficient tables can seriously exaggerate the significance of the results. This difficulty was circumvented by generating values for 0-18 days as before from the same time series but from starting dates selected at random. A machine program was then prepared which computed values of r between all "randomly" generated data sets. This procedure produced a sample of 1764 random values of r for comparison with the values obtained above from the "critical" index decreases. The program output showed that 138 or 7.8% of all values of random r were greater

than + 0.5 and 60 or 3.4% were greater than + 0.60. Thus, even with the use of highly time-dependent data, the hypothesis is verified at a relatively high probability level.

The statistical evidence in favor of this hypothesis implies that a quite reliable surface forecasting model for stratospheric debris could be developed from our knowledge of the types of upper flow patterns which produce descents of mass (and radioactivity) from the stratosphere. Furthermore, the geographic location of these predicted maxima could be estimated from the knowledge of trajectory behavior in these regions of descending motions (Danielsen, 1959 b, 1961, 1964 a, b; Staley, 1960, 1962; Danielsen, Bergman, and Paulson, 1962; Mahlman, 1964 a; Reiter, 1963; Reiter and Mahlman, 1964).

V. SEASONAL MASS EXCHANGE FROM INDEX AND FALLOUT DATA:

In view of the discrete nature of the investigated stratospheric-tropospheric transport mechanism, it is of interest to arrive at independent measurements of seasonal mass transport and stratospheric residence half-times from the data presented in the previous sections. Estimates of this type are especially relevant in terms of the general circulation problem and in view of comparison with previous estimates.

Measurements of surface fallout from Fig. 1 show that the age-adjusted mean gross beta intensity in 1964 is slightly less than 50% of the mean 1963 value. This suggests a stratospheric particle residence half-time of about one year for the period after the voluntary test moratorium of December 1962.

The largest portion of the late 1962 stratospheric debris burden was due to mid- and high latitude weapons testing. As a result, this estimate is limited by these specialized input conditions and by the immensely complicated nature of the entire physical problem.

Because of its inherent statistical nature, a more meaningful determination of residence half-time should be expressed in terms of height, season, and circulation latitude of injection into the stratosphere.

By employing the arguments presented in previous sections, from the index data, it was possible to arrive at quantitative estimates of seasonal transport of mass from the stratosphere into the troposphere--valid only for the injection conditions mentioned in the previous paragraph. This was crudely accomplished by noting the number of critical index decreases from Fig. 1 ($100 (C_1 - C_2) / \Delta t > 2.5$) which occurred within the 1963 and 1964 time periods. There were found to be 22 and 23 such decreases, respectively. In view of previous estimates for individual cases of mass transport from the stratosphere (Danielsen, 1959 a; Mahlman, 1964 a; Reiter and Mahlman, 1964), a value of 0.6×10^{12} metric tons of mass transported per critical index decrease was assumed. Because the index described cyclogenetic activity over only 1/3 of the hemispheric circumference, the number of critical occurrences was multiplied by a factor of three. Also, since the index described only cyclogenesis between 40 and 60° N, a factor of 2 was introduced to take into account the possibility of transport due to this process at other latitudes. This factor of 2 is roughly compatible with measurements of mean latitudinal fallout distribution by other investigators (Libby and Palmer, 1960; Libby, 1959; Martell, 1959; Lockhart et al, 1960). By employing these assumptions a seasonal mass transport value of 80×10^{12} metric tons of air per year is obtained. This is equivalent to about one-sixth of the total mass of the stratosphere for one hemisphere or approximately one-half of the polar stratosphere. The estimated yearly depletion rate of one-half

the mass of the polar stratosphere agrees well with the value inferred previously from the fallout data. Furthermore, the compatibility of these results suggests that the large majority of seasonal mass transport from the stratosphere is directly attributable to the cyclogenetic mechanism proposed here and elsewhere (Danielsen, 1964 a; Mahlman, 1964 a, b, c; Reiter and Mahlman, 1964).

VI. SUMMARY AND CONCLUSIONS:

An index designed to measure the relative amount of cyclonic activity in a given region of the atmosphere was derived in order to compare its variations with changes in surface fallout intensity. Quantitative calculations from the data revealed that a quite pronounced statistical correspondence existed between rapid decreases of the cyclone index and subsequent short-period increases in surface fallout intensity.

Two independent estimates of seasonal exchange of mass between the stratosphere and troposphere were obtained from the fallout and the index data respectively. Both computations indicated a value of mean residence half-time of approximately one year for the period 1963 and 1964.

The investigation thus quantitatively documents the hypothesis that tropopause level cyclogenesis is the predominate mechanism leading to stratospheric-tropospheric mass exchange as proposed earlier (Danielsen, 1964 a; Mahlman, 1964 a, b, c; Reiter and Mahlman, 1964). However, the data do not indicate that these cyclogenetic processes are directly responsible for the spring fallout peaks. This lends support to the assumption that annual fallout (and ozone) variations result from seasonal changes in eddy- and energy exchange processes in the lower stratosphere (Newell, 1964). A complete analysis of such processes, especially with respect to shorter-period variations in the stratosphere, is necessary before a physically consistent fallout transport model can be devised.

ACKNOWLEDGEMENTS

The author is grateful to Prof. Elmar R. Reiter for the extensive encouragement and guidance he gave while the research was in progress. Thanks are due to Mr. William D. Ehrman who provided invaluable technical and computational assistance, and to Mrs. Sandy Olson who typed the manuscript.

The data used for analysis were made available by the National Weather Records Center in Asheville, North Carolina, and by the U. S. Department of Health, Education, and Welfare, Public Health Service Radiation Surveillance Network.

REFERENCES

- Allen, R. A., R. Fletcher, J. Holmboe, J. Namias, and H. C. Willett, 1940: Report on an experiment in five-day weather forecasting, Papers in Physical Oceanography and Meteorology, Massachusetts Institute of Technology and Woods Hole Oceanographic Institution, 8, No. 3, 94 pp.
- Arawaka, H., 1953: Tilted-trough model as an interaction between low- and high latitude disturbances, Journal of Meteorology, 10, 64-66.
- Blackman, R. B. and J. W. Tukey, 1958: Measurement of Power Spectra, New York, Dover Publications, 190 pp.
- Danielsen, E. F., 1959 a: Abstract--A determination of the mass transported from stratosphere to troposphere over North America during a thirty-six hour interval, Mitteilungen des Deutschen Wetterdienstes, 20 (3), 10-11.
- _____, 1959 b: The laminar structure of the atmosphere and its relation to the concept of a tropopause, Archiv für Meteorologie, Geophysik und Bioklimatologie, 11, 293-332.
- _____, 1961: Trajectories: isobaric, isentropic, and actual, Journal of Meteorology, 18, 479-486.
- _____, 1964 a: Radioactivity transport from stratosphere to troposphere, Mineral Industries, Pennsylvania State University, 33 (6), 1-7.
- _____, 1964 b: Project Springfield Report, Defense Atomic Support Agency, 97 pp.
- _____, K. H. Bergman, and C. A. Paulson, 1962: Radioisotopes, potential temperature and potential vorticity--a study of stratospheric-tropospheric exchange processes, Department of Meteorology and Climatology, University of Washington, 54 pp.
- Fry, L. M., F. A. Jew, and P. K. Kuroda, 1960: On the stratospheric fallout of strontium-90: the spring peak of 1960, Journal of Geophysical Research, 65, 2061-2066.
- Gustafson, P. F., S. S. Brar, and M. A. Kerrigan, 1961: Appearance of a spring maximum in nuclear test debris in 1960, Science, 133, 460-461.

- Holloway, J. L., Jr., 1958: Smoothing and filtering of time series and space fields, Advances in Geophysics, Academic Press, New York, 4, 351-389.
- Libby, W. F., 1959: Radioactive fallout particularly from the Russian October series, Science, 45, 151-175.
- _____, and C. E. Palmer, 1960: Stratospheric mixing from radioactive fallout, Journal of Geophysical Research, 65, 3307-3317.
- Lockhart, L. B., Jr., R. L. Patterson, Jr., A. W. Saunders, Jr., and R. W. Black, 1960: Fission product radioactivity in the air along the 80th meridian (west) during 1959, Journal of Meteorology, 65, 3987-3997.
- Machta, L., 1949: Dynamic characteristics of a tilted-trough model, Journal of Meteorology, 6, 261-265.
- Mahlman, J. D., 1964 a: Relation of stratospheric-tropospheric mass exchange mechanisms to surface radioactivity peaks, Technical Paper No. 58, Department of Atmospheric Science, Colorado State University, 1-19.
- _____, 1964 b: On the feasibility of relating seasonal fallout oscillations to hemispheric index patterns, Technical Paper No. 58, Department of Atmospheric Science, Colorado State University, 55-58.
- _____, 1964 c: Relation of upper air hemispheric index patterns to seasonal fallout fluctuations, Radioactive Fallout from Nuclear Tests, Proceedings of the Second Conference held in Germantown, Maryland, November, 1964 (to be published).
- Martell, E. A., 1959: Atmospheric aspects of strontium-90 fallout, Science, 129, 1197-1206.
- Miyake, Y., K. Sarukashi, Y. Katsurage, and T. Kanazawa, 1962: Seasonal variation of radioactive fallout, Journal of Geophysical Research, 67, 189-193.
- Namias, J., 1950: The index cycle and its role in the general circulation, Journal of Meteorology, 7, 130-139.
- Newell, R. E., 1964: Further ozone transport calculations and the spring maximum in ozone amount, Pure and Applied Geophysics, 58, 191-206.

- Panofsky, H. A. and G. W. Brier, 1958: Some Applications of Statistics to Meteorology, College of Mineral Industries, The Pennsylvania State University, 224 pp.
- Peirson, D. H., 1963: Beryllium-7 in air and rain, Journal of Geophysical Research, 68, 3831-3832.
- Reiter, E. R., 1963: A case study of radioactive fallout, Journal of Applied Meteorology, 2, 691-705.
- _____, 1964: Comments on paper by S. Penn and E. A. Martell, "An analysis of the radioactive fallout over North America in late September 1961", Journal of Geophysical Research, 69, 786-788.
- _____, and J. D. Mahlman, 1964: Heavy fallout over the southern United States, November 1962, Technical Paper No. 58, Department of Atmospheric Science, Colorado State University, 21-49.
- Riehl, H., T. C. Yeh, and N. E. LaSeur, 1950: A study of variations of the general circulation, Journal of Meteorology, 6, 181-194.
- Rossby, C. -G. and Collaborators, 1939: Relation between variations in the intensity of the zonal circulation of the atmosphere and the displacements of the semi-permanent centers of action, Journal of Marine Research, 2, 38-55.
- Staley, D. O., 1960: Evaluation of potential-vorticity changes near the tropopause and the related vertical motions, vertical advection of vorticity, and the transfer of radioactive debris from stratosphere to troposphere, Journal of Meteorology, 17, 591-620.
- _____, 1962: On the mechanism of mass and radioactivity transport from stratosphere to troposphere, Journal of the Atmospheric Sciences, 19, 450-467.
- Storebø, P. B., 1959: Orographical and climatological influences on deposition of nuclear-bomb debris, Journal of Meteorology, 16, 600-608.
- U. S. Atomic Energy Commission, 1964: Health and Safety Laboratory, Fallout Program Quarterly Summary Report, July 1, 1964, HASL - 142.

THE BEHAVIOR OF JET STREAMS IN POTENTIAL
FALLOUT SITUATIONS

by
Elmar R. Reiter

ABSTRACT

It is shown from a case study that the splitting of jet streams into several branches, which is frequently observed over the United States on the leading edges of intense jet maxima, may be explained by conservation of potential vorticity within an atmospheric layer moving over an obstacle. Such an obstacle may be a large mountain barrier, such as the Rocky Mountains, or a slow-moving dome of cold air in the lower troposphere, as is typical for cold outbreaks associated with strong jet streams.

I. INTRODUCTION:

In the case of radioactive fallout which occurred during the latter part of November 1962 over the southern United States (Reiter and Mahlman, 1964, 1965), an intrusion of stratospheric air could be traced within a stable layer, sinking through the vertical extent of the troposphere in a matter of two to three days. The flow of contaminated air was associated with a well-developed jet stream.

It has been shown in an earlier study (Reiter and Mahlman, op. cit.) that only part of the stratospheric air reached the ground in an anticyclonic jet branch, while a large portion of air contained within the stable layer continued to travel in the upper troposphere following cyclonically curved trajectories. Such splitting of the jet-stream flow has been observed on other occasions (Reiter and Nania, 1964; Reiter, et al., 1965), and it appears to occur rather regularly on the leading edge of well-pronounced jet maxima over the United States. This "fingery" structure of the exit region of strong jet maxima may elude the observer over other regions of the globe. In these regions the rawinsonde network may not be dense enough--or provide enough accurate information--to reveal such structural details of the upper flow patterns.

It appears than an explanation of this "splitting" of jet streams may--at least in part--be sought in the different behavior of cyclonic and anticyclonic sides of jet streams under flow conditions in which potential vorticity is conserved.

II. TRAJECTORIES OF CONSTANT POTENTIAL VORTICITY:

Bolin (1950) has shown that conservation of potential vorticity in an atmospheric layer which undergoes vertical shrinking (and

horizontal divergence) while crossing a mountain range leads to an anticyclonic deflection of the flow over the mountain. By the same reason, the air flow acquires cyclonic flow characteristics to the lee of the mountain range, where vertical air columns between isentropic surfaces undergo a stretching effect. This leads to the formation of troughs in the lee of mountains.

Bolin's computations were made for a straight non-shearing current impinging on the mountain range. He was able to show that only orographic barriers of considerable lateral extent would produce a significant effect on the jet-stream flow in the upper troposphere.

Reiter (1961, 1963, 1965) argued that varying initial conditions of relative vorticity $q \neq 0$, such as they may be found on the cyclonic and anticyclonic sides of actual jet streams, will lead to varying degrees of deflection as the flow crosses the mountains. Assuming in first approximation a horizontal wind profile across the jet stream, with a vorticity discontinuity in the jet axis, and different--but constant--values of q on either side of the axis, the flow is expected to split when crossing the mountain range. One might argue that the "gap" between the now existing two jet axes is controlled by turbulence effects which will generate a new horizontal wind profile in this region.

The cases of observed jet-stream "splitting" mentioned above occurred over the central and eastern United States, well to the east of the Rocky Mountains. In each case the jet maximum was associated with a "cold dome" near the surface, in which isentropic surfaces are bulging upward. From the point of view of potential vorticity conservation, it should make little difference whether the flow was forced over an orographic barrier, or over an "obstacle"

of cold air, just as long as the latter moved slower than the wind in the layers under consideration.

Indicating initial conditions (before the flow encounters the cold dome) by subscripts "o", we may write for the potential vorticity P

$$P = \frac{q_o + f_o}{\Delta p_o} = \frac{q + f}{\Delta p} \quad (1)$$

where Δp is the thickness of the layer contained between two isentropic surfaces (assuming adiabatic flow), or

$$\frac{V_o K_o + S_o + f_o}{\Delta p_o} = \frac{VK + S + f}{\Delta p} \quad (2)$$

$S = - \frac{\partial V}{\partial n}$ indicates shearing vorticity, K is the curvature of relative streamlines. Upon solving for K we arrive at

$$K = \frac{\Delta p f_o - \Delta p_o f}{\Delta p_o V} + \frac{\Delta p K_o V_o}{\Delta p_o V} + \frac{\Delta p S_o - \Delta p_o S}{\Delta p_o V} \quad (3)$$

From the analytic expression for curvature we may compute the angle ψ of flow deflection from the original direction

$$\begin{aligned} \sin \psi = & \int_{x_1}^{x_2} \left(\frac{\Delta p f_o - \Delta p_o f}{\Delta p_o V} \right) dx + \int_{x_1}^{x_2} \frac{\Delta p K_o V_o}{\Delta p_o V} dx \\ & + \int_{x_1}^{x_2} \left(\frac{\Delta p S_o - \Delta p_o S}{\Delta p_o V} \right) dx \end{aligned} \quad (4)$$

For merging flow conditions, $\frac{\partial \sin \psi}{\partial n} < 0$

For "splitting" flow conditions, $\frac{\partial \sin \psi}{\partial n} > 0$

To simplify the problem we will make the following assumptions:

(1) The thickness of the atmospheric layer contained between two isentropic surfaces does not change in the direction normal to the jet stream:

$$\frac{\partial \Delta p_o}{\partial n} = 0; \quad \frac{\partial \Delta p}{\partial n} = 0$$

(2) $K_o = 0$

(3) $S_o = S$, i. e., the horizontal shears remain constant as the flow crosses the barrier.

Differentiating Eqn. (4) with respect to n , we find that, because of assumption (1), and since $\partial f / \partial n$ as well as $\partial f_o / \partial n$ are very small quantities, contributions from the first and second integral term are negligibly small. The main contribution towards $\frac{\partial \sin \psi}{\partial n}$ comes from the last integral term in Eqn. (4), which may be written as

$$\frac{\partial \sin \psi}{\partial n} = \frac{\partial S}{\partial n} \int_{x_1}^{x_2} \frac{\Delta p - \Delta p_o}{\Delta p_o V} dx + S \frac{\partial}{\partial n} \int_{x_1}^{x_2} \frac{\Delta p - \Delta p_o}{V \Delta p_o} dx \quad (5)$$

After expansion of the second integral term we arrive at

$$\begin{aligned} \frac{\partial \sin \psi}{\partial n} = & \frac{\partial S}{\partial n} \int_{x_1}^{x_2} \frac{\Delta p - \Delta p_o}{\Delta p_o V} dx + \frac{S}{\Delta p_o} \int_{x_1}^{x_2} \frac{1}{V} \frac{\partial (\Delta p - \Delta p_o)}{\partial n} dx \\ & + \frac{S}{\Delta p_o} \int_{x_1}^{x_2} \frac{(\Delta p - \Delta p_o)}{V^2} S dx \end{aligned} \quad (6)$$

The second integral term vanishes because of assumption (1), and the third term reduces to

$$\frac{S^2}{\Delta p} \int_{x_1}^{x_2} \frac{\Delta p - \Delta p_0}{V^2} dx$$

because of assumption (3). Thus the splitting effect may be expressed by

$$\frac{\partial \sin \psi}{\partial n} = \frac{1}{\Delta p_0} \frac{\partial S}{\partial n} \int_{x_1}^{x_2} \frac{\Delta p - \Delta p_0}{V} dx + \frac{S^2}{\Delta p_0} \int_{x_1}^{x_2} \frac{\Delta p - \Delta p_0}{V^2} dx \quad (7)$$

East of the cold dome, $(\Delta p - \Delta p_0) > 0$. Since $\frac{\partial S}{\partial n} > 0$ in crossing the jet axis, $\frac{\partial \sin \psi}{\partial n} > 0$, indicating a splitting tendency caused by the first integral term in equation (7). The second integral term will also give a positive contribution, however negligibly small because $S^2 \ll \partial S / \partial n$, and $V^2 \ll V$. We, therefore, will have to evaluate only the first integral term.

III. THE CASE OF 22 NOVEMBER 1962:

Fig. 1 shows the flow pattern on the 300 K isentropic surface. On 22 November 1962, 12 GMT a well-pronounced splitting of the flow is observed near Columbia, Missouri. In the vicinity of this split, assumption (3) made above is not expected to introduce appreciable errors into our estimates. Also assumption (2) is approximately satisfied.

A cross-section from Green Bay (GRB), Wisconsin, to Oklahoma City (OKC), Oklahoma, for the same observation time is shown in Fig. 2. If we were to consider the layer between 290 and 300 K, assumption (1) is approximately fulfilled between Columbia (CBI), Missouri, and Topeka (TOP), Kansas. Outside this area slight modification on account of $\frac{\partial \Delta p_0}{\partial n} \neq 0$ are to be expected.

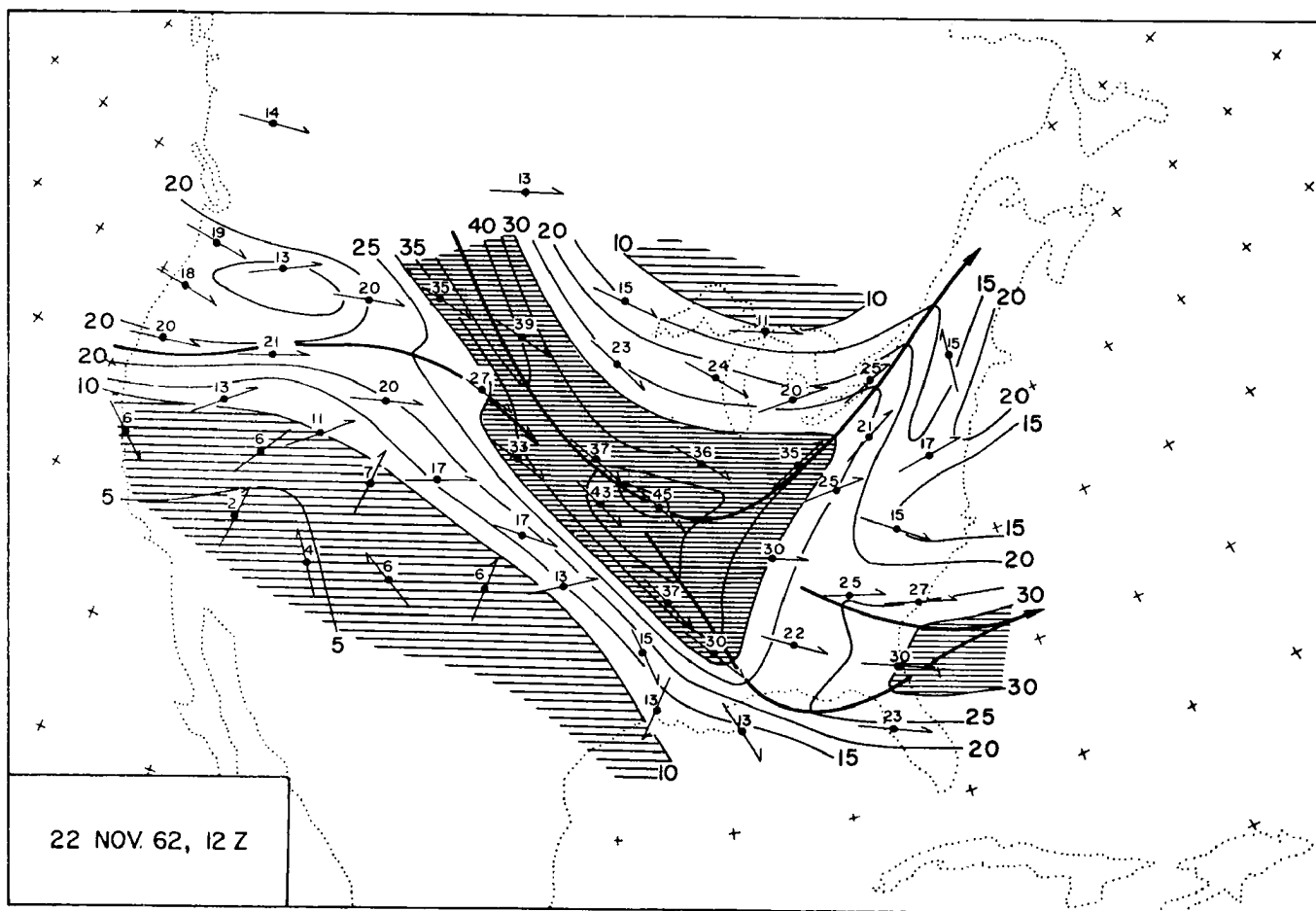


Fig. 1: Isotachs (mps) of isentropic surface 300 K, 22 November 1962, 12 GMT. Regions with speeds less than 10 mps and more than 30 mps are marked by different shading. Jet axes are shown by heavy lines with arrows.

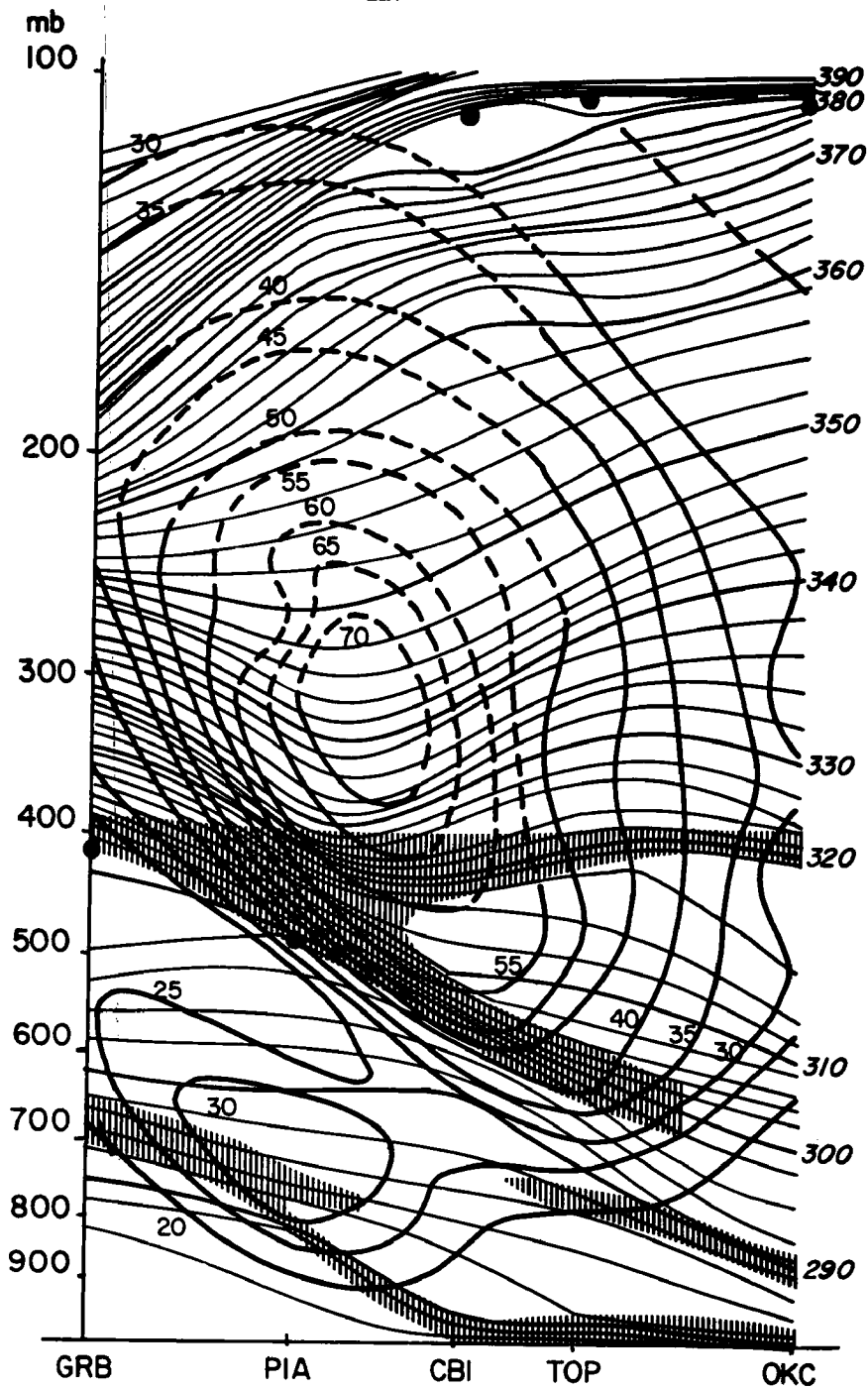


Fig. 2: Cross-section through the atmosphere from Green Bay (GRB), Wisconsin, through Peoria (PIA), Illinois, Columbia (CBI), Missouri, and Topeka (TOP), Kansas, to Oklahoma City (OKC), Oklahoma, 22 November 1962, 12 GMT. Heavy full and broken lines: isotachs (mps, vertical numbers); thin lines: potential temperature ($^{\circ}$ K, slanting numbers). Vertical hatching indicates stable layers. Heavy dots mark the coded tropopause levels.

The integral in Eqn. (5) may be evaluated for 22 November 12 GMT, from the long-section shown in Fig. 3. It extends from Rapid City (RAP), South Dakota, to Nashville (BNA), Tennessee. The following values are obtained

	Omaha - Columbia	Columbia - Nashville
$\Delta p - \Delta p_0$	- 50 mb	135 mb
Δp_0	130 mb	80 mb
$x_2 - x_1$	380 km	580 km
\overline{V}	30 m sec ⁻¹	30 m sec ⁻¹
$\int \frac{\Delta p - \Delta p_0}{\Delta p_0 V} dx$	-4.9 x 10 ³ sec	+ 32.6 x 10 ³ sec

Evaluation of S, and especially of $\frac{\partial S}{\partial n}$, offers some difficulties because according to Fig. 2, there is no discontinuity in horizontal shear at the location of the jet axis. From Figs. 1 and 2, we may estimate the mean horizontal shear, \overline{S} , to be of the order of $\pm 1 \times 10^{-5}$ sec⁻¹, the positive sign holding north of the jet axis, the negative sign south of this axis. Taking Δn as a 5° latitude interval (ca. 560 km), we arrive at $\frac{\Delta \sin \psi}{\Delta n} \approx -1.76 \times 10^{-7}$ or $\Delta \sin \psi \approx -0.1$ over a distance equivalent of 5° latitude, for the section Omaha-Columbia. With a wind direction of approximately 315°, this would mean a change of direction within a 560 km band across the jet axis of about -8°.

For the section between Columbia and Nashville, $\Delta \sin \psi$ over a distance of 560 km across the jet axis amounts to 0.65, that is, winds should back from approximately 315° south of the axis to about 273° north of the axis. This compares well with the wind direction shown in Fig. 1, assuming that the flow pattern, as well as the location and shape of the "cold dome", did not change significantly with time.

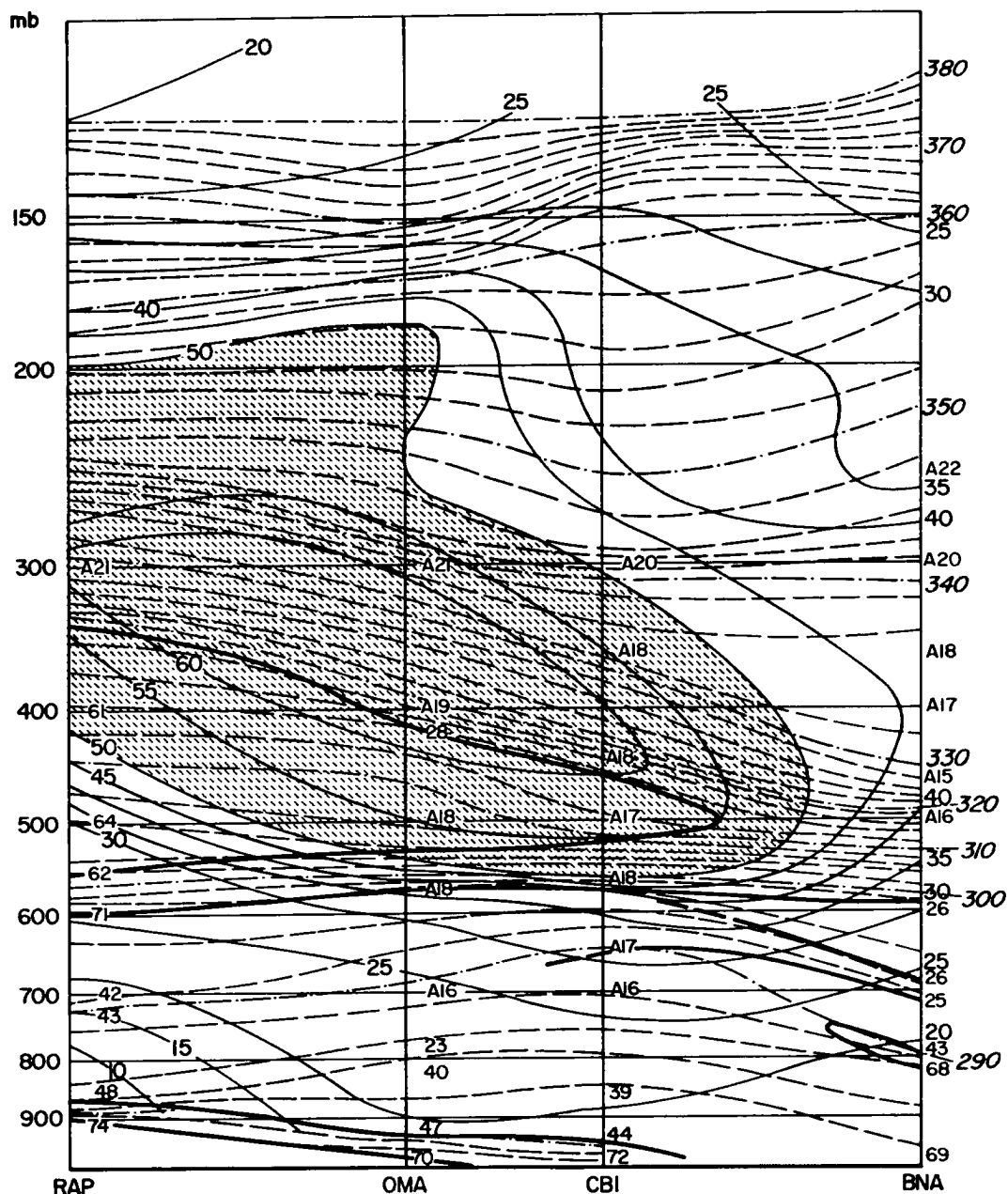


Fig. 3: Section through the atmosphere from Rapid City (RAP), South Dakota, to Omaha (OMA), Nebraska, to Columbia (CBI), Missouri, to Nashville (BNA), Tennessee, 22 November 1962, 12 GMT. Full lines: isotachs (mps, vertical numbers, regions > 50 mps are shaded); thin dashed and dashed-dotted lines: potential temperatures ($^{\circ}$ K, slanting numbers). Heavy full and dashed lines indicate tropopause and boundaries of stable layers. Values of relative humidities are indicated numerically along sounding (prefix "A" denotes "motorboating").

IV. CONCLUSIONS:

The foregoing estimates indicate that the presence of relatively small cyclonic and anticyclonic mean shears on either side of the jet axis suffice to produce pronounced streamline divergence, if the flow is forced over a "cold dome" under conservation of potential vorticity. Thus it appears that this conservation principle may help to explain the splitting of jet streams.

According to Mahlman (1964, 1965 a, b) cases of radioactive fallout are associated with cyclogenesis of certain intensity at tropopause level. Such cases are usually connected with the southward migration of cold anticyclones (cold domes), into which stratospheric air intrusions of stable layers are caught. The radioactive debris then is carried to the ground in these anticyclones. The foregoing case study suggests that the presence of such a cold anticyclone enhances the splitting of flow contained within the stable layer of contaminated air. Thus, the anticyclone produces the dynamic conditions in the upper flow pattern, under which a part of this flow is separated from the jet stream and becomes part of the anticyclonic circulation, in which it sinks into the lower troposphere.

REFERENCES

- Bolin, B. , 1950: On the influence of the earth's orography on the general character of the westerlies, Tellus, 2, 184-195.
- Mahlman, J. D. , 1964: Relation of stratospheric-tropospheric mass exchange mechanisms to surface radioactivity peaks, Technical Paper No. 58, Department of Atmospheric Science, Colorado State University, 1-19.
- _____, 1965 a: Relation of stratospheric-tropospheric mass exchange mechanisms to surface radioactivity peaks, Archiv für Meteorologie, Geophysik und Bioklimatologie, A 17, (to be published).
- _____, 1965 b: Relation of tropopause-level index changes to radioactive fallout fluctuations, Technical Paper No. 70, Department of Atmospheric Science, Colorado State University, 84-109.

Reiter, E. R. , 1961: Meteorologie der Strahlstrome (Jet Streams),
Vienna, Springer, 473 pp.

_____, 1963: Jet Stream Meteorology, Chicago, University of
Chicago Press, 513 pp.

_____, 1965: **Tropospheric** circulation and jet streams,
World Survey of Climatology, Vol. III, Amsterdam, Elsevier,
(to be published).

_____, and J. D. Mahlman, 1964: Heavy radioactive fallout
over the southern United States, November 1962, Technical
Paper No. 58, Department of Atmospheric Science, Colorado
State University, 21-49.

_____, and J. D. Mahlman, 1965: Heavy radioactive fallout
over the southern United States, November 1962, Journal of
Geophysical Research, 70, (to be published).

_____, and A. Nania, 1964: Jet stream structure and clear-air
turbulence (CAT), Journal of Applied Meteorology, 3, 247-260.

_____, D. W. Beran, J. D. Mahlman, and G. W. Wooldridge, 1965:
Effect of large mountain ranges on atmospheric flow patterns as seen
from TIROS satellites, Technical Paper No. 69, Department of
Atmospheric Science, Colorado State University, (to be published).

DEVELOPMENT OF COMPUTER PROGRAMS FOR
COMPUTATION OF MONTGOMERY STREAM FUNCTIONS
AND PLOTTING OF THERMODYNAMIC DIAGRAMS

by

J. D. Mahlman and W. Kamm

ABSTRACT

Machine procedures are developed for computation of isentropic analysis parameters and for plotting of tephigrams, both in terms of derived basic equations. Computation flow charts and program copies are included from both programs.

I. INTRODUCTION:

In detailed analyses of atmospheric structure it is generally necessary that three-dimensional motions of the air be known to a high degree of reliability. It was demonstrated by Danielsen (1959) that this three-dimensional character of the flow may be adequately represented on isentropic surfaces provided that great care is taken in the computation of the Montgomery stream function (M).

Especially the height of the chosen isentropic (θ) surface (Z_θ) must be determined accurately, and also the temperature (T_θ) and pressure (P_θ) on the θ -surface must satisfy Poisson's equation ($\theta = T (1000/P)^{R/c_p}$). By following this procedure one arrives at an expression for M (see section II). It is possible to compute M from this expression by hand with the aid of a plotted thermodynamic diagram but the calculation is very laborious and time consuming. To avoid this difficulty a computer program was written and tested which determines M and other desirable meteorological parameters on a given θ surface from the initial radiosonde data cards (see flow chart 1 and program 1). This program has also been expanded to plot mechanically the thermodynamic diagrams (tephigrams) from these data cards (see flow chart 2 and program 2). It is thus possible to generate data for isentropic analysis in a completely objective manner.

II. MATHEMATICAL DEVELOPMENT:

For an isentropic representation the stream function on this surface is given by

$$M = c_p T_\theta + g Z_\theta \quad (1)$$

where c_p is the specific heat of air at constant p and g is the acceleration of gravity (980.6 cm sec⁻²).

If the height of the θ surface (Z_θ) is expressed as the height of a nearby isobaric level (Z_p) plus the height difference between the θ and p surfaces, Eqn. 1 may be written as

$$M = c_p T_\theta + gZ_p + g(Z_\theta - Z_p). \quad (2)$$

By integrating the hydrostatic equation to find the height difference between the p and θ surfaces, one obtains

$$Z_\theta - Z_p = \frac{-R\bar{T}}{g} \ln \left(\frac{P_\theta}{P_p} \right) \quad (3)$$

where \bar{T} is the mean temperature of the layer under consideration. Combining Eqns. 2 and 3,

$$M = c_p T_\theta + gZ_p + R\bar{T} \ln \left(\frac{P_p}{P_\theta} \right) \quad (4)$$

However, as noted in the previous section, to minimize computational errors P_θ and T_θ should not be determined independently from the radiosonde data. This may be circumvented by solving Poisson's equation for P_θ to obtain

$$P_\theta = 1000 \left(\frac{T_\theta}{\theta} \right)^{c_p/R} \quad (5)$$

where R is the gas constant for dry air. By substitution of Eqn. 5 into Eqn. 4 one obtains:

$$M = c_p T_\theta + gZ_p + R\bar{T} \ln \left[\frac{P_p}{1000} \left(\frac{\theta}{T_\theta} \right)^{c_p/R} \right] \quad (6)$$

This expression for M is now in a form which can be readily computed by machine methods from the original radiosonde cards. Other significant parameters which can be easily obtained from the input data are the height of the θ surface (Z_θ) and the static stability ($-\partial\theta/\partial p$).

III. EXPLANATION OF THE MONTGOMERY STREAM FUNCTION PROGRAM:

The input cards used in this program were purchased from the National Weather Records Center at Asheville, North Carolina. In order to insure sufficiently accurate input data it was necessary to combine two different formats, the 645 WBAN RAOBS CONST PRESSURE and 505 RAOB SIGNIFICANT LEVELS. These are contained in the Climatic Center, USAF, Air Weather Service, (MATS), NWRC, Office of Climatology, U. S. Weather Bureau Reference Manuals. This program was extensively tested and operated on an IBM 1620 computer processing only card input and output capabilities. To avoid the difficulties presented by the limited input capabilities and mixed formats, it was necessary to insert a blank card between each input station to be read into the computer.

After the data are read into the machine, they are arranged in order of descending pressure so that at any given pressure, a corresponding temperature and height is also defined at that level. At this point the machine is instructed to compute the potential temperature ($\theta = T (1000 / p)^{R/c_p}$) for all pressure levels. At pressures lower than 800 mb the data were checked for superadiabatic lapse rates in the soundings by noting the sign of the static stability ($-\partial\theta/\partial p$). If this parameter becomes negative ($-\partial\theta/\partial p > 0$) the machine prints out the discrepancy and continues without modifying the calculation in any way. The calculation of M in a region which possesses a very unstable lapse rate is not seriously affected because under dry adiabatic conditions $\partial M/\partial Z = 0$. Thus the only serious difficulty which arises is the indeterminacy in finding the pressure or height of the θ surface of interest. By noting the lapse-rate discrepancy in the machine print-out, the analyst is aided in his evaluation of the topography of the isentropic surface.

In proceeding to calculate the Montgomery stream function at an isentropic surface of interest, it is necessary to find the temperature at this level (T_θ) by linear interpolation from the input data. This is obtained by employing the formula

$$T_\theta = T_b + (T_t - T_b) \left(\frac{\theta - \theta_b}{\theta_t - \theta_b} \right) \quad (7)$$

where the subscripts t and b indicate values of T and θ from the nearest input data above and below the θ level of interest.

The pressure (P_θ) at this θ level is then calculated from Eqn. 5 and the standard pressure values are scanned to find the nearest value of P_p larger than P_θ . The parameter Z_p in Eqn. 6 is now defined from the data at level P_p . To determine all parameters necessary to calculate from Eqn. 6, an expression for \bar{T} between P_p and P_θ must be found in terms of the input data. This is accomplished by summing the weighted (linear) mean temperatures between all data points from P_p to P_θ as given in the formula

$$\begin{aligned} \bar{T} &= \sum_{i=1}^N \left[\left(\frac{T_i + T_{i+1}}{2} \right) \left(\frac{P_i - P_{i+1}}{P_p - P_\theta} \right) \right] \\ \bar{T} &= \frac{1}{2(P_p - P_\theta)} \sum_{i=1}^N \left[(T_i + T_{i+1}) (P_i - P_{i+1}) \right] \end{aligned} \quad (8)$$

where $T_1 = T_\theta$, $T_N = T_p$, $P_1 = P_\theta$, and $P_N = P_p$. The direction of summation is determined by the sign of $P_p - P_\theta$.

The calculation of M is now performed from Eqn. 6 with the three terms on the right hand side of the equation (abbreviated as M_1 , M_2 and M_3), and their sum (M) being printed out separately.

At this point the wind direction and speed are linearly interpolated from the winds on the nearest standard pressure levels above and below the chosen isentropic surface. In the 645 WBAN RAOBS CONST PRESSURE format the standard pressures are given every 50 mb. This type of interpolation is justified in view of the closeness of standard pressures to any given isentropic level. The wind speed at the chosen θ surface is computed from the formula

$$FF_{\theta} = FF_b + (FF_t - FF_b) \left(\frac{P_b - P_{\theta}}{50} \right) \quad (9)$$

Computation of the wind direction is considerably more complicated because of the difficulty in interpolation when the two wind reports are on opposite sides of the $0^{\circ} = 360^{\circ}$ direction. This problem is circumvented by a series of tests in the program which act to eliminate the "discontinuity" at the $0^{\circ} \equiv 360^{\circ}$ point.

The static stability ($-\partial\theta/\partial p$) is evaluated from the expression

$$-\frac{\partial\theta}{\partial p} = \frac{\theta_t - \theta_b}{P_b - P_t} \quad (10)$$

After all these computations have been completed for a specific level, a new θ level is defined, and the entire calculation is then performed at this new level. The whole procedure is then continuously recycled until the calculations at all θ surfaces of interest have been completed. The machine then reads in a new station and the entire process is repeated until completion.

IV. EXPLANATION OF THE PLOTTING PROGRAM:

The program for plotting tephigrams is designed for the same type of input data utilized in the Montgomery stream function program. Its purpose is to mechanically plot radiosonde soundings on tephigrams in the same manner that has been traditionally done

by hand. The use of this program proved to be of great advantage because of the large increases in speed and accuracy of plotting.

This program was tested and run on an IBM 1620 computer coupled with a California Computer Products x-y continuous-roll plotter. It is designed to plot soundings to the same scale as the University of Chicago Pressure-Altitude Tephigram Chart No. 3. As before, the input data are arranged by the machine in order of descending pressure.

Because this plotter is only capable of linear representation, it is necessary to convert the tephigram coordinates to meet this specification. The tephigram is an area-conserving thermodynamic diagram which is linear in the centigrade temperature (T) and the entropy (ϕ). The entropy, however, is expressed on the diagram in terms of the potential temperature and does not appear explicitly as a coordinate. The differential relationship between entropy and potential temperature is given by

$$d\phi = c_p d \ln \theta \quad . \quad (12)$$

On this tephigram, the zero entropy point is defined to be at the intersection of the $T = -90$ C and $\theta = 230$ K lines. Under this condition, upon integration the entropy is given by

$$\phi = c_p \ln (\theta / 230) \quad . \quad (13)$$

However, in the input data the only thermodynamic variables given are T and P. Thus from Poisson's equation

$$\phi = c_p \left[\ln \left(\frac{T + 273.16}{230} \right) - \chi \ln \left(\frac{P}{1000} \right) \right] \quad (14)$$

where $\chi = 0.2857$, and T is given in centigrade. In terms of the computer plotter a scale factor must be introduced so that the

tephigram specifications are satisfied. This gives

$$y(\text{sounding}) = \text{scale factor} \left[\ln \left(\frac{T + 273.16}{230} \right) - 0.2857 \ln \left(\frac{P}{1000} \right) \right] \quad (15)$$

From the linear equation above and comparisons with the actual tephigram, the scale factor gives equation (15) the following form:

$$y(\text{sounding}) = \frac{595}{50 \ln \frac{500}{230}} \left[\ln \left(\frac{T + 273.16}{230} \right) - 0.2857 \ln \left(\frac{P}{1000} \right) \right] \quad (16)$$

This now defines completely the y coordinate.

The x coordinate (T) on the tephigram is linear and thus is easily determined by measurement to be

$$x = 0.0709 T. \quad (17)$$

This now completely specifies the sounding. It is then plotted as a continuous line which is linear between data points. When a humidity reading is available at a given point a small x is plotted (see sample sounding, Fig. 1). To save time the pressure, height, temperature, and humidity values are printed out by the machine and attached to the sounding at a later time. It is equally simple to instruct the plotter to write out these values, but with the present machine this is very time consuming.

This program has produced tephigram soundings which are considerably more accurate than those obtained by hand-plotting. A disadvantage arises if certain computations necessitate the use of a tephigram underlay with the machine-plotted sounding. In principle this problem could be circumvented by using computer plotting paper which contains printed tephigram coordinates. It is, of course, possible to adapt this approach to any other thermodynamic diagram and to a computer plotter of almost any specification.

ACKNOWLEDGEMENT

This publication was prepared and funded jointly with the Department of Commerce, U. S. Weather Bureau, Contract No. Cwb - 10879.

REFERENCE

Danielsen, E. F., 1959: The laminar structure of the atmosphere and its relation to the concept of a tropopause, Archiv für Meteorologie, Geophysik und Bioklimatologie, A 11, 293-332.

SYMBOL CORRESPONDENCE TABLE

TEXT	PROGRAM	DESCRIPTION
----	ISTA	Station
----	IYR	Year
----	IMØ	Month
----	IDA	Day
----	IHR	Hour
dd	DD	Wind speed
ff	FF	Wind direction
Z	HGT	Height
T	T	Temperature
P	P	Pressure
θ	TH	Potential temperature
θ	TH1	Isentropic level of computation
P_p	PP	Standard level closest to TH1
M	F	Montgomery stream function = $M_1 + M_2 + M_3$
M_1	F1	$c_p T_\theta$
M_2	F2	gZ_p
M_3	F3	$RT \ln \left[\frac{P_p}{1000} \left(\frac{\theta}{T_\theta} \right)^{c_p/R} \right]$
\overline{T}	TBAR	Average temperature of the layer between P_p and P_θ
Z_p	HGT (M)	Height at P_p
$\frac{-\partial\theta}{\partial P}$	STAB	Static stability
----	HUM	Relative humidity

The following symbols, when added to a previously defined symbol, indicate the following:

T = value above TH1

B = value below TH1

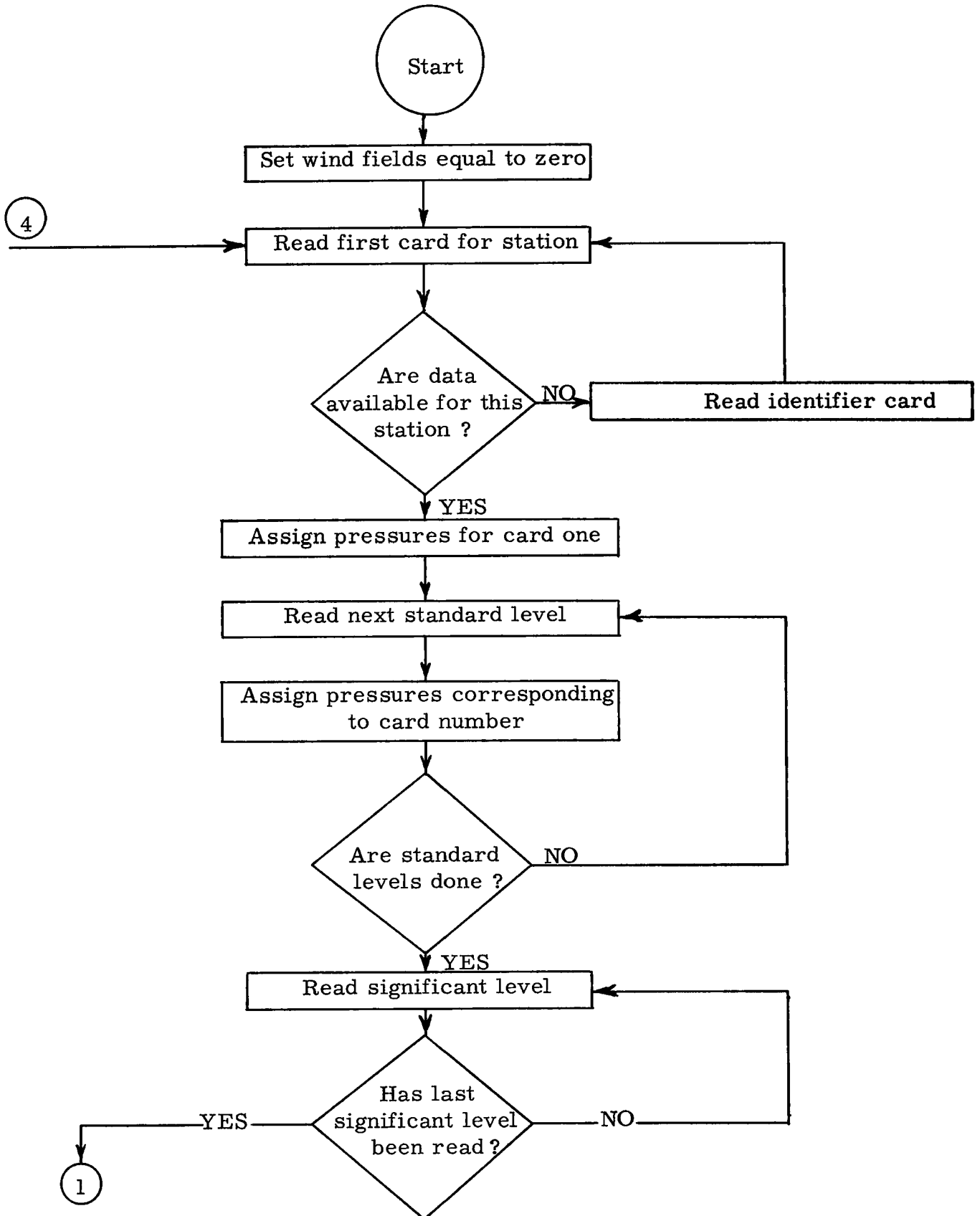
TH = value at the surface TH1

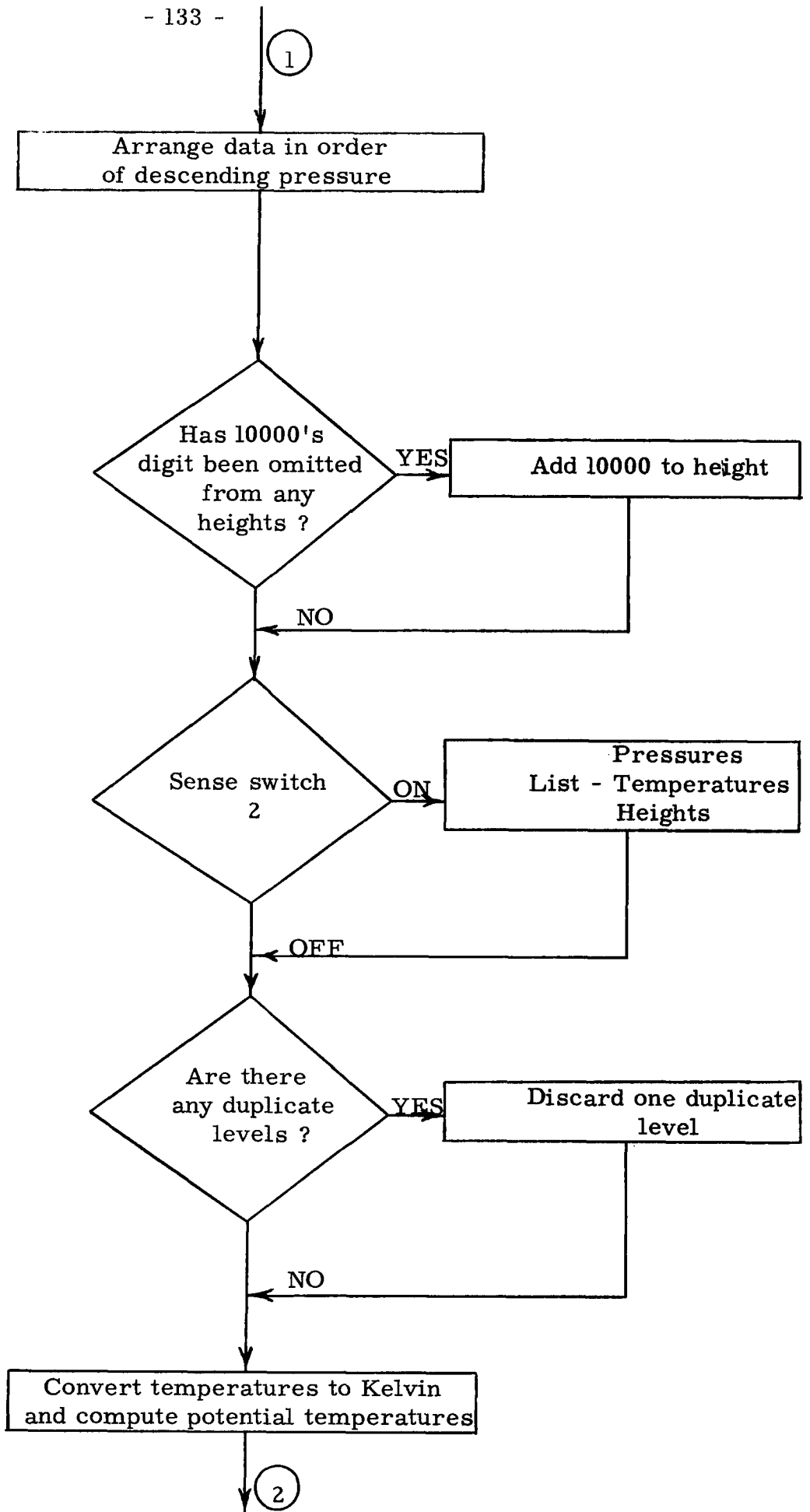
i. e., TB = temperature at the nearest level below TH1

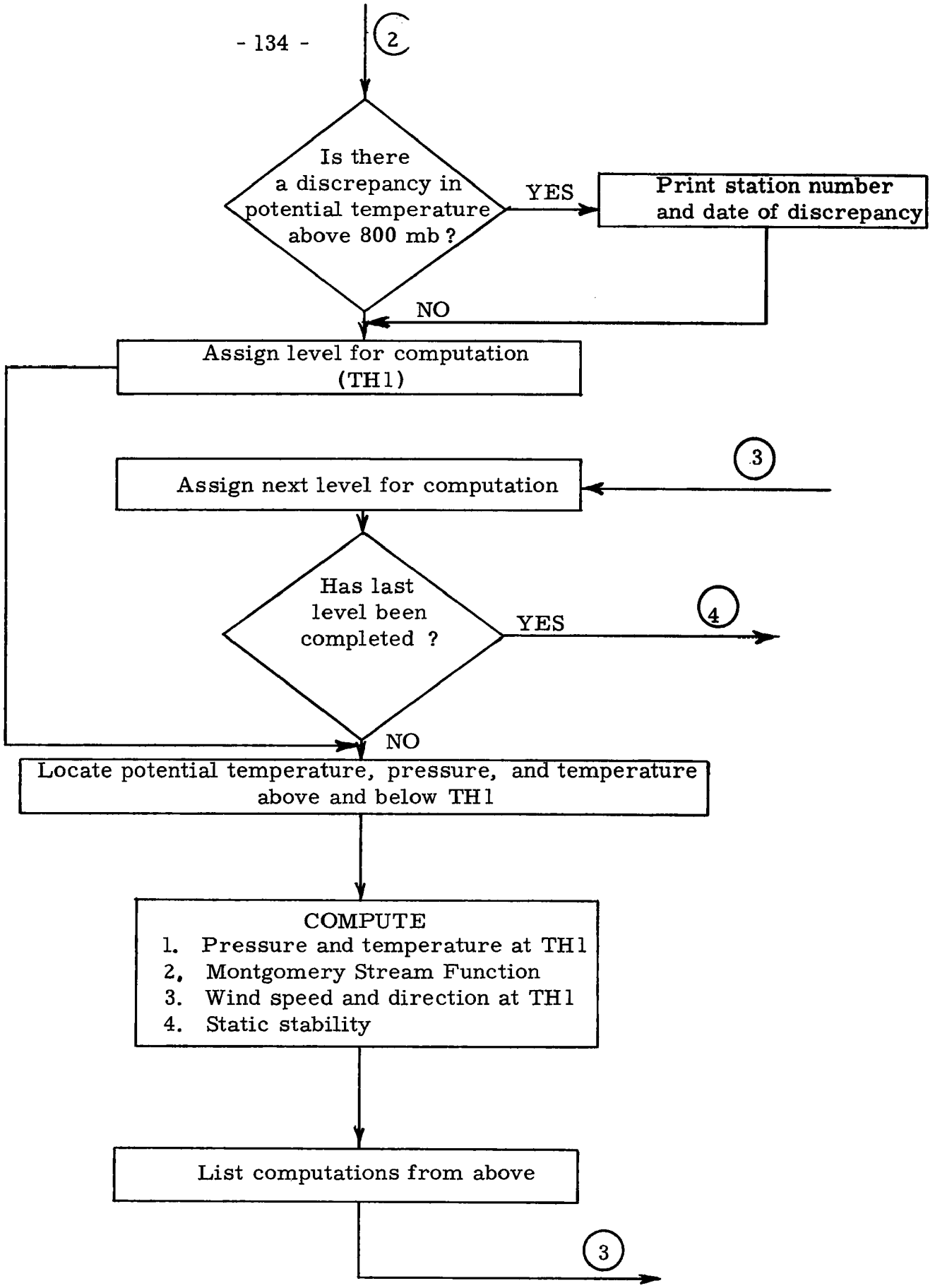
PPT = nearest standard level above TH1

DDTH = wind direction at TH1

FLOW CHART 1 - MONTGOMERY STREAM FUNCTIONS







NOTE: Program will terminate when all data has been completed, rather than from a normal exit.

MONTGOMERY STREAM FUNCTION PROGRAM

```
C      COMPUTE MONTGOMERY STREAM FUNCTIONS WITH WINDS NUMBER ONE 1620
      DIMENSION T(50),P(50),HGT(50),          TH(50),FP(50),FT(50),FHGT(50)
      1,DD(50),FF(50),FDD(50),FFF(50)
C      ZERO OUT WIND FIELDS
      DC 711 I=1,50
      DC(I)=0
711   FF(I)=0
C      READ FIRST STANDARD LEVEL
904   READ 900,ISTA,IYR,IMU,IDA,IHR,JJ,(HGT(I),T(I),DD(I),FF(I),I=1,3),N
      1C
900   FORMAT(15,4I2,I1,15X,3(F4.0,F4.1,2X,F3.0,F2.0),I1)
      KK1=-1
      KSTA=ISTA
      J=0
      NN=0
C      CHECK FOR MISSING STATION DATA
      IF(NC)914,914,905
914   READ 916,JUNK
916   FORMAT(I2)
      GC TC 904
C      ASSIGN PRESSURES FOR CARD ONE
905   P(1)=1000.
      DC 924 I=2,3
924   P(I)=P(I-1)-50.
      IF (NC-5)901,901,902
902   N=4
      GC TC 903
901   N=NC-1
903   J=J+4
      K=J+3
C      READ REMAINDER OF STANDARD LEVEL CARDS
906   READ 907,JJ,(HGT(I),T(I),DD(I),FF(I),I=J,K)
907   FORMAT(13X,I1,4(F4.0,F4.1,2X,I3,I2))
C      ASSIGN PRESSURES FOR CARD TWO THROUGH FIVE
      GC TC (908,909,910,911      ),JJ
908   P(J)=850.
      GC TC 912
909   P(J)=650.
      GC TC 912
910   P(J)=450.
912   M=J+1
      MM=K
      DC 913 I=M,MM
913   P(I)=P(I-1)-50.
      GC TC 9112
911   P(J)=250.
      J=J+1
      P(J)=200.
      J=J+1
      P(J)=175.
      J=J+1
      P(J)=150.
C      STANDARD LEVELS HAVE BEEN READ IN
      K=J
9112  NN=NN+1
      IF(NN-N)903,925,925
925   I=K+1
C      READ SIGNIFICANT LEVELS
915   READ 917,ISTA,P(I),T(I),HGT(I)
917   FORMAT(15,13X,F4.0,F4.1,3X,F5.0)
```

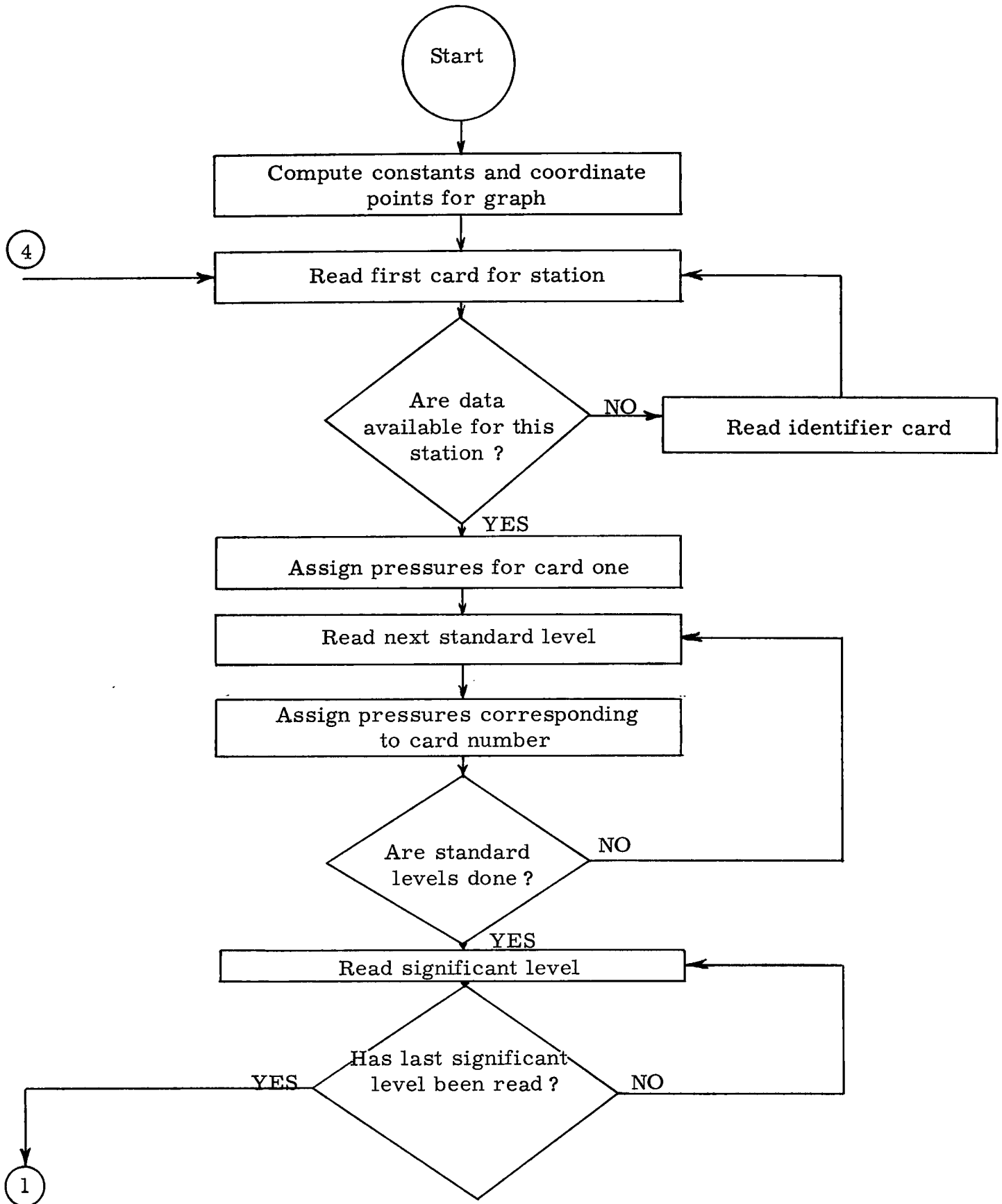
```
      IF (ISTA)918,918,919
919  I=I+1
      GC TC 915
918  N=I-1
      J=1
923  I=1
C    ARRANGE DATA IN ORDER OF DECENDING PRESSURE
      K=1
      DUMP=P(I)
      DC 920 I=2,N
922  IF(DUMP-P(I))921,920,920
921  DUMP=P(I)
      K=I
920  CCNTINUE
      FFF(J)=FF(K)
      FCD(J)=CD(K)
      FP(J)=DUMP
      FT(J)=T(K)
      FHGT(J)=FHGT(K)
      P(K)=0.0
      J=J+1
      IF(J=N)923,923,926
926  CCNTINUE
      DC 927 I=1,N
      CD(I)=FCD(I)
      FF(I)=FFF(I)
      T(I)=FT(I)
      FHGT(I)=FHGT(I)
927  P(I)=FP(I)
      I=2
C    CHECK FOR HEIGHTS WITH 10000 DIGIT DROPPED
779  IF(HGT(I)-HGT(I-1))778,777,777
777  I=I+1
      IF(I=N)779,781,781
778  II=I
      DC 782 K=II,N
782  HGT(K)=HGT(K)+10000.
781  CCNTINUE
C    IF SS2 PUNCH DATA FOR CHECK ON ORDER
      IF(SENSE SWITCH 2)831,832
831  PUNCH 950,(P(I),I=1,N)
950  FORMAT(16F5.0)
      PUNCH 951,(T(I),I=1,N)
951  FORMAT(16F5.1)
      PUNCH 952,(HGT(I),I=1,N)
952  FORMAT(13F6.0)
832  I=1
C    CHECK FOR DUPLICATE DATA AND DISCARD ONE
704  IF(P(I)-P(I+1))701,702,701
701  I=I+1
      IF(I=N)704,703,703
702  K=I+1
      N=N-1
      DC 705 I=K,N
      P(I)=P(I+1)
      CD(I)=CD(I+1)
      FF(I)=FF(I+1)
      T(I)=T(I+1)
705  FHGT(I)=FHGT(I+1)
      I=K
```

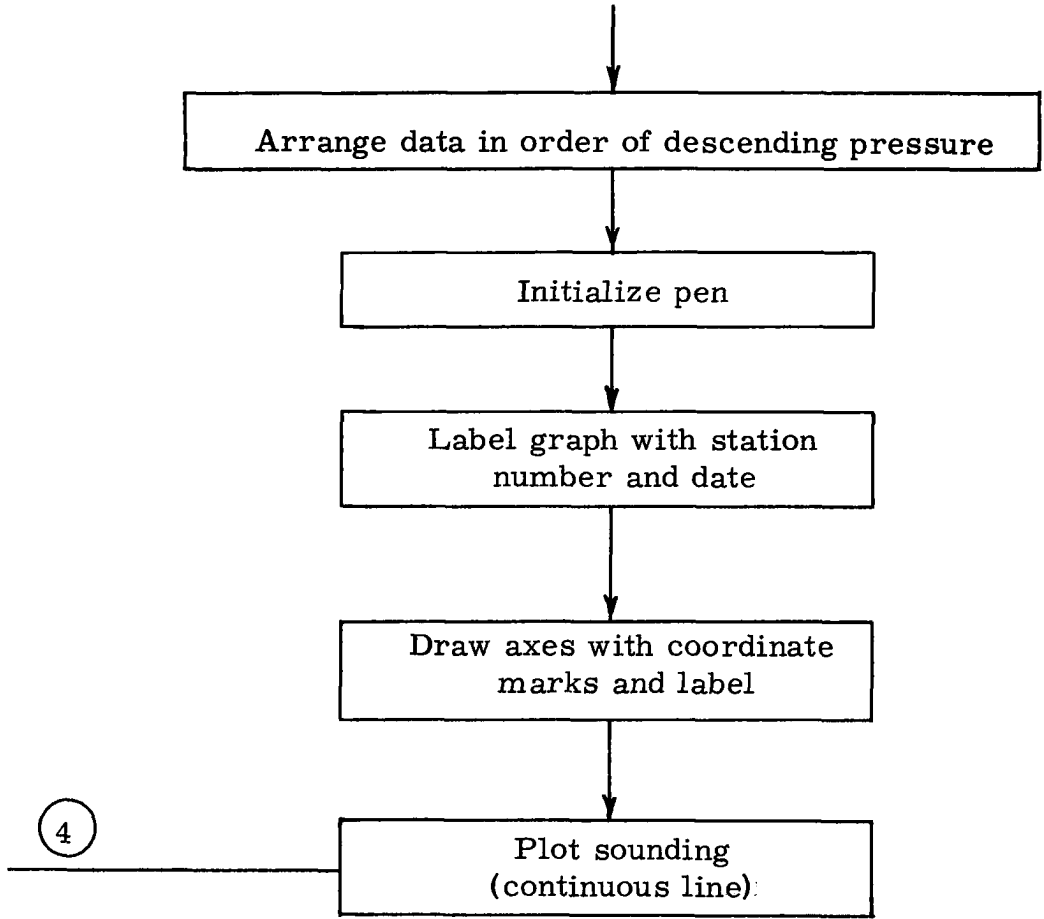
```
GC TC 704
703 CCNTINUE
C   CCNVERT TEMPERATURES AND COMPUTE POTENTIAL TEMPERATURES
DC 30 I=1,N
T(I)=T(I)+273.2
30 TH(I)=T(I)*(1000./P(I))**.2857
I=1
C   CHECK FOR DISCREPANCIES IN POTENTIAL TEMPPERATURES ABOVE 800 MD
802 IF(P(I)-800.)800,800,801
801 I=I+1
GC TC 802
800 KI=I+1
DC 803 I=KI,N
IF(TH(I)-TH(I-1))805,803,803
803 CCNTINUE
GC TC 804
805 PUNCH 806,KSTA,IYR,IMO,IDA,IHR
806 FORMAT(62HTHERE IS A DISCREPANCY IN THE THETA VALUES FOR STATION N
LUMBER I5,4I2)
C   ASSIGN POTENTIAL TEMPERATURES FOR COMPUTATION
804 TH1=290.
GC TC 40
210 IF(TH1-320.)211,212,212
211 TH1=TH1+5.
GC TC 40
212 IF(TH1-350.)213,904,904
213 TH1=TH1+10.
40 I=1
FFTH=0.0
DCTH=0.0
C   SEARCH LIST FOR VALUES ABOVE AND BELOW LEVEL BEING COMPUTED
220 IF(TH(I)-TH1)50,60,70
50 GC TC 80
60 TTH=T(I)
GC TC 90
70 THB=TH(I)
TB=T(I)
PPB=P(I)
IF(I-1)210,210,71
71 THT=TH(I-1)
TT=T(I-1)
PPT=P(I-1)
GC TC 100
80 I=I+1
GC TC 220
C   COMPUTE PRESSURE AND TEMPERATURE AT LEVEL OF INTEREST
C   FIND NEAREST STANDARD LEVEL
100 TTH=TB+(TT-TB)*((TH1-THB)/(THT-THB))
90 PTH=1000.*((TTH/TH1)**3.5001
IPP=PTH/100.
AAA=IPP*100
DIF=PTH-AAA
IF(DIF-50.)400,400,410
400 PP=AAA+50.
GC TC 132
410 PP=AAA+100.
132 I=1
130 IF(ABSF(PP-P(I))-0.1)120,120,110
110 I=I+1
IF(I-N)130,131,131
```

```
131 CONTINUE
120 J=I
    AA=0.0
160 IF(PTH-P(J+1))162,161,161
161 CCC=P(J+1)
    P(J+1)=PTH
162 AA=AA+ (T(J)+T(J+1))*(P(J)-P(J+1))
    IF(PTH-P(J+1))150,140,140
150 J=J+1
    GC TC 160
140 TBAR=(1.0/(2.0*(PP-PTH)))*AA
C   COMPUTE MONTGOMERY STREAM FUNCTION IN THREE SEGMENTS
    P(J+1)=CCC
    Z=10.**6
    F1=10.046*TTH*Z
    F2=9.806*HGT(I)*10000.
    M=I
    F3=2.8704*Z*TBAR*LOGF(PP/PTH)
    PP=PP-50.
    I1=M
    I=1
812 IF(ABSF(PP-P(I))-0.01)811,811,809
809 I=I+1
    IF(I-N)812,812,500
500 IF(SENSE SWITCH 1)501,823
C   ERROR ONE-DATA LIST EXCEEDED,CANNOT COMPUTE WIND
501 PUNCH 502
502 FORMAT(7HERROR 1)
    GC TC 823
811 I2=I
    IF(FF(I1))505,505,808
808 IF(FF(I2))505,505,807
505 IF(SENSE SWITCH 1)503,823
C   ERROR TWO-WIND SPEED IS NEGATIVE
503 PUNCH 504
504 FORMAT(7HERROR 2)
    GC TC 823
C   INTERPOLATE WIND DIRECTION AND WIND SPEED
807 FFTH=FF(I1)+((FF(I2)-FF(I1))*((P(I1)-PTH)/50.))
    DD1=DD(I2)-DD(I1)
    IF(DD1-180.)818,816,816
816 DD1=DD1-360.
    GC TC 819
818 IF(DD1+180.)817,819,819
817 DD1=DD1+360.
819 DDTH=DD(I1)+DD1*((P(I1)-PTH)/50.)
    IF(DCTH)821,823,822
821 DDTH=DDTH+360.
    GC TC 823
822 IF(DCTH-360.)823,824,824
824 DDTH=DDTH-360.
823 CONTINUE
C   COMPUTE STABILITY FACTOR
    PP=PP+50.
    STAB=(THT-THB)/(PPB-PPT)
    F=F1+F2+F3
    ISTA=KSTA
C   PUNCH RESULTS AND PROCEED TO NEXT LEVEL
    PUNCH 10,IYR,IMC,IDA,IHR,ISTA,N,F1,F2,F3,F
10  FORMAT(4I2,1X,I5,1X,I2,2X,4E15.5)
```

```
      KK1=KK1+1
      IF(KK1)678,678,737
678 PUNCH 190,(TH(I),I=1,N)
190 FORMAT(10F8.2)
      PUNCH 677,(P(I),I=1,N)
677 FORMAT(13F6.0)
737 PUNCH 739,FFTH,CDTH
739 FORMAT(12HWIND SPEED =F5.1,4X,16HWIND DIRECTION =F7.1)
738 PUNCH 741,TBAR,THB,THT,TB,TT
741 FORMAT(5HTBAR=F6.1,3X,4HTHT=F6.1,3X,4HTHB=F6.1,3X,3HTT=F6.1,3X,3HT
1B=F6.1)
      PUNCH 734,PTH,HGT(M),TH1,PP,STAB
734 FORMAT(4HPTH=F7.1,3X,4HHGT=F8.0,3X,4HTH1=F7.1,3X,3HPP=F7.1,6H STAB
1=F6.3)
      GC TC 210
      END
```

FLOW CHART 2
MACHINE PLOTTING OF THERMODYNAMIC DIAGRAMS





TEPHIGRAM SOUNDING PROGRAM

```
C   PROGRAM PLOT SOUNDINGS
    DIMENSION P(50),T(50),FP(50),FT(50)
    DIMENSION TM(6),TTM(17)
C   CALCULATE TIC MARK VALUES
    CC=595./(50.*LOGF(50./23.))
    TM1=20.0
    DC 17 I=1,6
    TM(I)=.0709*TM1
17  TM1=TM1-20.
    TTM1=400.
    DC 18 I=1,17
    TTM(I)=LOGF(TTM1/230.)*CC
18  TTM1=TTM1-10.0
    L=C
    FK=2./7.
C   READ FIRST STANDARD LEVEL
40  READ 900,ISTA,IYR,IMO,IDA,IHR,JJ,(T(I),I=1,3),NC
    KK1=1
    KSTA=ISTA
900 FORMAT(I5,4I2,I1,15X,3(4X,F4.1,7X),I1)
    J=C
    NN=0
C   CHECK FOR MISSING STATION DATA
    IF(NC)914,914,905
914 READ 916,JUNK
916 FORMAT(I2)
    GC TC 40
C   ASSIGN PRESSURES FOR CARD ONE
905 P(1)=1000.
    DC 924 I=2,3
924 P(I)=P(I-1)-50.
    IF (NC-5)901,901,902
902 N=4
    GC TC 903
901 N=NC-1
903 J=J+4
    K=J+3
C   READ REMAINDER OF STANDARD LEVEL CARDS
906 READ 907,JJ,(T(I),I=J,K)
907 FORMAT(13X,I1,4(4X,F4.1,7X))
C   ASSIGN PRESSURES FOR CARD TWO THROUGH FIVE
    GC TC (908,909,910,911),JJ
908 P(J)=850.
    GC TC 912
909 P(J)=650.
    GC TC 912
910 P(J)=450.
912 M=J+1
    MM=K
    DC 913 I=M,MM
913 P(I)=P(I-1)-50.
    GC TC 9112
911 P(J)=250.
    J=J+1
    P(J)=200.
    J=J+1
    P(J)=175.
    J=J+1
    P(J)=150.
C   STANDARD LEVELS HAVE BEEN READ IN
```

```
      K=J
9112 NN=NN+1
      IF(NN-N)903,925,925
925 I=K+1
C    READ SIGNIFICANT LEVELS
915 READ 917,ISTA,P(I),T(I)
917 FORMAT(15,13X,F4.0,F4.1)
      IF(ISTA)918,918,919
919 I=I+1
      GO TO 915
918 N=I-1
      J=1
923 I=1
      K=1
C    ARRANGE DATA IN ORDER OF DECENDING PRESSURE
      DUMP=P(I)
      DO 920 I=2,N
922 IF(DUMP-P(I))921,920,920
921 DUMP=P(I)
      K=I
920 CCONTINUE
      FP(J)=DUMP
      FT(J)=T(K)
      P(K)=0.0
      J=J+1
      IF(J-N)923,923,926
926 CONTINUE
      DO 927 I=1,N
      T(I)=FT(I)
927 P(I)=FP(I)
      L=L+1
C    ZERO PEN
      Z=PLCTF(11111.)
      Y=0.0
      X=0.0
      Z=PLCTF(Y)
      Z=PLCTF(60000.)
      Y=-.3
      X=0.0
      Z=PLCTF(Y)
      Z=PLCTF(50000.)
C    LABEL GRAPH WITH DATE AND STATION
      CALL CHAR(5,.1,0,KSTA,IYR,IMO,IDA,IHR)
11  FORMAT(15,1X,4I2)
      Z=PLCTF(60000.)
C    DRAW X AXIS WITH TIC MARKS
      Y=0.0
      X=.0709*40.
      Z=PLCTF(Y)
      Z=PLCTF(50000.)
      DO 13 I=1,6
        Y=0.0
        X=TM(I)
        Z=PLCTF(Y)
        Y=.1
        X=TM(I)
        Z=PLCTF(Y)
        Y=0.0
        X=TM(I)
        Z=PLCTF(Y)
```

```
13 CCNTINUE
  Y=0.0
  X=.0709*(-90.)
  Z=PLCTF(Y)
  Z=PLCTF(60000.)
C   DRAW Y AXIS WITH TIC MARKS
  Y=LCGF(400./230.)*CC
  X=.0709*(-90.)
  Z=PLCTF(Y)
  Z=PLCTF(50000.)
  DC 14 I=1,17
  Y=TTM(I)
  X=.0709*(-90.)
  Z=PLCTF(Y)
  Y=TTM(I)
  X=.0709*(-90.)-.1
  Z=PLCTF(Y)
  Y=TTM(I)
  X=.0709*(-90.)
  Z=PLCTF(Y)
14 CCNTINUE
  Y=LCGF(1.0)*CC
  X=.0709*(-90.)
  Z=PLCTF(Y)
  Z=PLCTF(60000.)
C   PLCT SCUNDING
  Y=(LCGF((T(1)+273.16)/230.))-FK*LOGF(P(1)/1000.))*CC
  X=.0709*T(1)
  Z=PLCTF(Y)
  Z=PLCTF(50000.)
  DC 30 I=2,N
  Y=(LCGF((T(I)+273.16)/230.))-FK*LOGF(P(I)/1000.))*CC
  X=.0709*T(I)
30 Z=PLCTF(Y)
  Z=PLCTF(60000.)
C   CCNTINUE TO NEXT SET OF DATA
  GC TC (50,50,70),L
50 Y=9.5
  X=0.0
  Z=PLCTF(Y)
  GC TC 40
70 Y=-19.0
  X=10.0
  Z=PLCTF(Y)
  L=0
  GC TC 40
  END
```

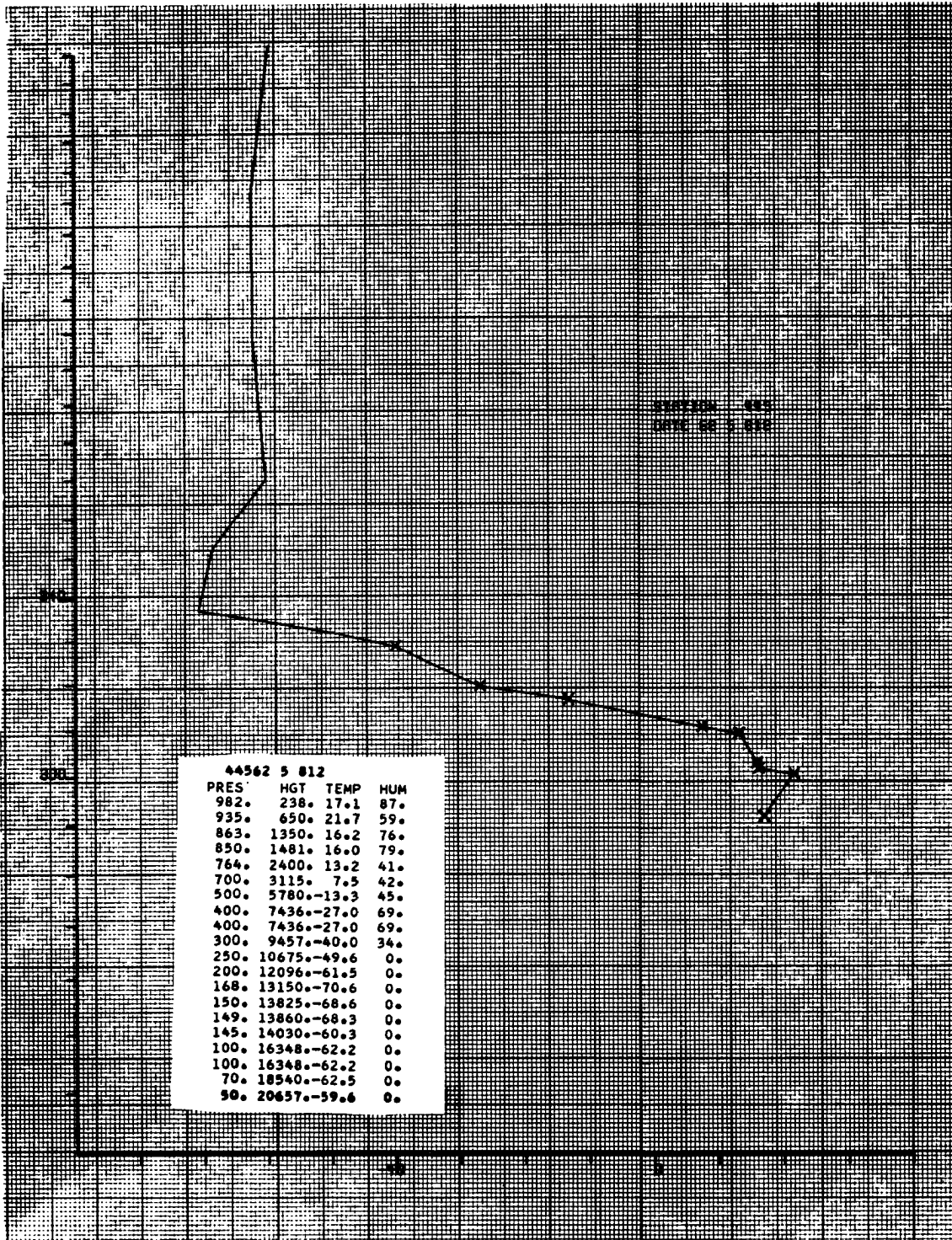


Fig. 1: Example of sounding plotted to the scale of a tephigram (Columbia, Missouri, 8 May 1962, 12 GMT). Sounding points with humidity reports are indicated by "X." The ordinates of diagram are temperature ($^{\circ}\text{C}$) and potential temperature ($^{\circ}\text{K}$).